HYDROCHEMISTRY, RADON IN GROUNDWATER AND ITS EXHALATION FROM ROCKS AROUND MIKA, N.E NIGERIA.

BY

Allen Sati, DANIEL, B.Tech. Applied Geology (ATBU) 2008

(M.Sc/SCIE/1774/2011-2012)

A THESIS SUBMITTED TO THE SCHOOL OF POSTGRADUATE STUDIES, AHMADU BELLO UNIVERSITY, ZARIA

IN PARTIAL FULFILLMENT OF THE REQUIREMENTS FOR THE AWARD OF MASTERS DEGREE IN APPLIED GEOLOGY (HYDROGEOLOGY)

DEPARTMENT OF GEOLOGY
FACULTY OF SCIENCE
AHMADU BELLO UNIVERSITY, ZARIA
NIGERIA

APRIL, 2016

Declaration

I declare that the work in this thesis entitled "Hydrochemistry, Radon in Groundwater and its Exhalation from Rocks around Mika, N.E Nigeria" has been carried-out by me in the Department of Geology under the supervision of Dr. Abdullahi Suleiman Arabi and Prof. Idris Isa Funtua. The information derived from literature has been duly acknowledged in the text and a list of references provided. No part of this thesis was previously presented for another degree or diploma at this or any other institution.

Allen, Daniel Sati

Date

Certification

This thesis entitled "Hydrochemistry, Radon in Groundwater and its Exhalation from Rocks around Mika, N.E Nigeria" by Allen, Daniel Sati meets the regulations governing the award of Masters Degree in Applied Hydrogeology of the Ahmadu Bello University, and is approved for its contribution to knowledge and literary presentation.

_____ _____

Dr. A.S. Arabi Date
Chairman, Supervisory Committee

_____ _____

Prof. I.I. Funtua Date
Member, Supervisory Committee

_____ _____

Dr. H. Hamza Date
Head of Department

_____ _____

Prof. Bala Kabir Date
Dean, School of Postgraduate Studies

Acknowledgement

I wish to express my profound and unreserved gratitude to my creator and Almighty Father in Heaven for His ever-sufficient grace, mercies, divine favour and guidance throughout my life and all I have achieved thus far. May His name be praised forever and ever.

My gratitude also goes to my supervisors; Dr. A.S. Arabi and Prof. I.I. Funtua, who despite their tight schedules, still make-out time to thoroughly check, correct, support, guide and advise me when I needed it most. Thank you and God bless you abundantly.

I will like to appreciate my lecturers in the Department of Geology; Prof. K. Schoeneich, Dr. H. Hamza, Prof. U. Dambatta, Prof. P. Ogunleye, Dr. A. Ibrahim, Dr. A.E. Ikpokonte, Prof. S. Alagbe, Dr. M.L. Garba, Dr. T. Najime, Dr. I. Hamidu, and to all other lecturers and members of staff of the Department of Geology not mentioned but whom have contributed in one way or the other, knowingly or unknowingly, towards adding knowledge to me. I say a very big THANK YOU and may God increase you also.

To my parents, Mr. and Mrs. Daniel Sati and my siblings; Engr. Daniel Lawrence, Engr. Daniel Calvin, Mr. Daniel James, Mrs. Afiniki Peter Ngai, Mrs. Blessing Barnabas Wanapia, my in-laws (Females and Males), my nephews and nieces. Thank you so much for your moral and financial support throughout the course of my programme. I promise never to disappoint you.

My friends and classmates; Mr. M.P. Segun, Mr. S. Adamu, Mr. T. Abubakar, Miss N. Vanessa, Mr. G. Bala, Mr. I. Ephraim, Mr. A. Usman and others not mentioned, thank you for your support and company, I really appreciated it. May God Almighty help us in all our endeavors.

I will like to specially appreciate my friend, elder brother and classmate, Late Mr. Abdullahi Mohammed (of blessed memory), you improved my practical groundwater geophysical survey skills but left us without notice, only to wake up on morning with the news of you sudden demise. May God grant you eternal rest, till we meet to part no more, Amin.

Abstract

In Nigeria, groundwater is the most widely utilized source of freshwater for consumption and other domestic uses, as well as for irrigational purposes but its quality still remains a major issue. This study was undertaken to evaluate radon in groundwater, its emanation/exhalation from rocks, associated radiological hazards and present the hydrochemical status of the groundwater, around Mika uranium mineralization, Northeastern, Nigeria. Previous study of the problem of natural radioactivity in drinking water from wells drilled in rock types rich in uranium has shown tendency to have high radon concentrations. Radon (^{222}Rn) was widely reported as contributing the largest component of human exposures to natural radiation and it is the second major cause of lung cancer, after cigarette smoking. Seventeen (17) groundwater samples and fifteen (15) rock samples were collected. Radon in groundwater and exhalation from rock measurements were carried-out using the DURRIDGE RAD7 electronic radon detector. Radium, thorium and potassium concentrations were determined using the 76x76mm NaI (Tl) detector, optically coupled to a photomultiplier (PMT) and chemical properties of the groundwater was determined using Atomic Absorption Spectrometry (AAS), Flame photometry and Titrimetric methods. Radon concentrations in groundwater vary from 2350 to 46,200 Bqm^{-3} with an average of 29,400 Bqm^{-3} against the U.S.EPA maximum contaminant level (MCL) of 11.1 Bq/l (11,100 Bqm^{-3}) for States without monitoring policy and enhanced indoor air policy. Radon exhalation from rock ranged from 39.7 to 262 Bqm^{-3} with an average of 137 Bqm^{-3}. The emanation coefficient ranged between 0.7 to 5.1 with an average of 2.17 and an exhalation rate range of between 0.73 to 4.83 $mBqkg^{-1}h^{-1}$, an average of 2.52 $mBqkg^{-1}h^{-1}$. The potential dose due to degassing of radon from groundwater, show an annual absorbed dose range of 37.06 to 728.48 $mSvy^{-1}$ with an average of 463.59 $mSvy^{-1}$, an annual effective dose range of 88.94 to 1748.35 $mSvy^{-1}$ with an average of 1112.62 $mSvy^{-1}$ and annual dose due to ingestion of ^{222}Rn ranged from 0.05 to 0.92 $mSvy^{-1}$ with

an average of 0.59 $mSvy^{-1}$ which is within ICRP recommended reference level of 1 $mSvy^{-1}$ but far above WHO recommended level of 0.1 $mSvy^{-1}$. Radium, thorium and potassium activity concentrations ranged from 15.33 to 63.38 $Bqkg^{-1}$(an average of 35.72 $Bqkg^{-1}$), 41.51 to 333.64 $Bqkg^{-1}$ (an average of 161.86 $Bqkg^{-1}$) and 161.73 to 2166.56 $Bqkg^{-1}$ (an average of 1153.25 $Bqkg^{-1}$), respectively. The reported world average for ^{226}Ra, ^{232}Th and ^{40}K is 35, 30 and 400 $Bqkg^{-1}$, respectively. Dose rates due to gamma radiation from combined contributions from ^{226}Ra, ^{232}Th and ^{40}K, ranged from 79.50 to 270 $nGyh^{-1}$, with an average of 164.02 $nGyh^{-1}$ (higher than the world median value of 60 $nGyh^{-1}$). Annual effective dose ranged from 0.24 to 0.83 $mSvy^{-1}$ with an average of 0.50 $mSvy^{-1}$. Radium equivalent of the rock samples ranged from 163.97 to 603.46 $Bqkg^{-1}$ with an average value of 355.99 $Bqkg^{-1}$, this value is lower than the world accepted upper limit of 370 $Bqkg^{-1}$. External hazard index ranged from 0.44 to 1.63 with an average value of 0.96, close to the world accepted upper limit of 1 (unity). The water types identified are; HCO_3-Na (82%), Na-SO_4 (12%) and Ca-Cl (6%). Based on Wilcox's classification, with respect to percent sodium (%Na), 11.8% of the groundwater samples were considered good for irrigation, 52.9% were permissible, 29.4% were doubtful while 5.9% were unsuitable for irrigation purposes.

TABLE OF CONTENT

Title Page i

Declaration ii

Certification iii

Acknowledgement iv

Abstract v

Table of Content vii

List of Figures xiii

List of Tables xv

List of Plates xvi

List of Appendices xvii

CHAPTER ONE

INTRODUCTION

1.1 Background of study 1

1.2 Justification 5

1.3 Aim and Objectives of Study 6

1.4 Study Area 7

1.4.1 Location, Extent and Accessibility 7

1.4.2 Relief and Drainage 8

1.4.3 Climate and Vegetation 9

1.4.4 People and Land-use 10

1.5 Radioactivity 11

1.5.1 Sources of Radiation 17

1.5.1.1 Naturally Occurring Radionuclides 17

1.5.1.2 Artificially Produced Sources 19

1.5.2 Radioactivity Pathways 20

1.5.3 Radiation Surveys 20

1.5.3.1 Ionization Chambers 21

1.5.3.2 Proportional Counters 21

1.5.3.3 Geiger – Müller Counters 22

1.5.3.4 Scintillation Detectors 22

1.5.4 Radiation Dose23

1.5.4.1 Count Rates 23

1.5.4.2 The Roentgen (R) 24

1.5.4.3 The Rad 24

1.5.4.4 The Rem or Sievert 25

1.5.5 Maximum Permissible Dose 25

CHAPTER TWO

2.1 Review of Regional Geology and Hydrogeology of Nigeria 27

2.1.1 Geology 27

2.1.2 Hydrogeology 30

2.2 Review of Previous Work on Radon 31

CHAPTER THREE

MATERIALS AND METHODS

3.1 Introduction 38

3.1.1 Desk Studies 38

3.1.2 Fieldwork 38

3.1.2.1 Field Observations 38

3.1.2.2 Water Sampling/ In-situ Measurements 39

3.1.2.3 Water Level measurement/Thickness of Dry Zone 40

3.1.2.4 Rock Sampling 41

3.1.3 Insitu/Laboratory Analysis 41

3.1.3.1 Radon in Water Analysis 41

3.1.4 Radon Exhalation Rate measurement 43

3.1.5 Radon Emanation Coefficient Measurement 45

3.1.6 Sample Preparation for NaI (TI) Gamma Spectrometry Measurement 46

3.1.6.1 Rock Sample Collection 46

3.1.6.2 Rock Sample Preparation 46

3.1.6.3 Evaluation of Radioactivity of Samples 46

3.1.6.4 Calibration and Efficiency Determinations 47

3.1.6.5 Standards 47

3.1.6.6 Background 47

3.1.7 Dose Rates Calculations 48

3.1.7.1 Radon Dose Calculation 48

3.1.7.2 Dose Rates due to γ Radiation 50

3.1.7.3 Annual Effective Dose Rate due to γ Radiation 51

3.1.7.4 Radium equivalent (Ra_{eq}) Determination 51

3.1.7.5 External Hazard Index (H_{ex}) 52

3.1.8 Cations and Anions in Groundwater Analysis 52

3.1.8.1 Methodology and Procedures for Water Analysis 53

3.2 Sodium Absorption Ratio (SAR) Determination 57

3.3 Percent Sodium (%Na) Determination 57

3.4 Soil Permeability Index (PI) Determination 58

3.5 Chloro Alkaline Index (CAI) Determination 58

CHAPTER FOUR

RESULTS

4.1 Lithologic Mapping 60

4.2 Groundwater Configuration 62

4.3 Radon in Groundwater 63

4.4 Radon Emission from Rock Materials 66

4.4.1 Radon Exhalation Rates and Emanation Coefficients 69

4.5 Gamma Radiation measurements and Dose Rates 71

4.5.1 Dose Rates due to Gamma Radiations 74

4.6 Hydrochemistry of the Study Area 77

4.6.1 Correlation Matrix 79

4.6.2 Water Types 80

4.6.3 Graphical Presentation of Hydrochemical Data 80

4.6.3.1 Piper Diagram 81

4.6.3.2 Durov Plot 82

4.6.3.3 Shoeller Diagram 83

4.6.4 Assessment of Groundwater Quality for Irrigation Purposes 85

CHAPTER FIVE

DISCUSSIONS

5.1 Geologic of the Study Area 86

5.2 Groundwater Configuration within the Study Area 87

5.3 Radon Concentration in Groundwater 88

5.4 Radon Emmission from Rock Materials 91

5.4.1 Radon Exhalation Rates and Emanation Coefficients of the Rocks 91

5.5 Gamma Radiations within the Study Area 92

5.5.1 Dose Rates due to Gamma Radiations within the Study Area 93

5.5.2 Annual Effective Dose Rates 93

5.5.3 Radium Equivalent Activity Index (Ra_{eq}) of the rocks 94

5.5.4 External Hazard Index (H_{ex}) of the rocks 94

5.6 Hydrochemistry of the Study Area 95

5.6.1 Total Dissolved Solids (TDS) 95

5.6.2 Hydrogen-Exponential (pH) 96

5.6.3 Conductivity and Salinity 97

5.6.4 Major Cations and Anions Distribution 97

5.6.4.1 Cations 97

5.6.4.2 Anions 100

5.6.4.3 Correlation Matrix 102

5.6.5 Water Type/Specie 102

5.6.6 Assessment of Groundwater Quality for Irrigation Purposes 103

5.6.6.1 Sodium Absorption Ratio (SAR) 103

5.6.6.2 Percent Sodium (%Na) 103

5.6.6.3 Soil Permeability Index (PI) 103

5.6.6.4 Chloro-Alkaline Index (CAI) 104

CHAPTER SIX

SUMMARY, CONCLUSION AND RECOMMENDATIONS

6.1 Summary and Conclusion 105

6.2 Recommendations 107

REFERENCES 109

APPENDICES 117

LIST OF FIGURES

Figure 1: Uranium decay series. 2

Figure 2: Illustration of radon emanating from soil or rock grains into pore spaces. 4

Figure 3: Topographic map of the study area. 8

Figure 4: Digital Elevation Map of the study area. 9

Figure 5: Geologic and Orogenic Map of part of West Africa illustrating the position of the Nigerian Pan African terrain. 28

Figure 6: Geologic map of Nigeria showing basement and sedimentary terrains. 30

Figure 7: "HACH Model" Multi-parameter Conductivity/pH meter. 39

Figure 8: Alpha Spectrometer RAD7 Electronic Radon Detector. 42

Figure 9: Typical set-up of RAD7 electronic radon detector. 43

Figure 10: Schematic demonstration of Radon emanation, transport and subsequent exhalation from soil. 44

Figure 11: A Varian AA240FS Atomic Absorbtion Spectrometer. 53

Figure 12: Lithologic Map of the Study Area. 61

Figure 13: Groundwater flow direction map of the study area. 63

Figure 14: Radon (in water) contour map of the study area. 65

Figure 15: Radon contour map super-imposed on the Lithologic map of the study area. 65

Figure 16: ^{226}Ra concentration contour super-imposed on ^{222}Rn concentration in Groundwater. 66

Figure 17: Contour Map of ^{222}Rn exhalation from rocks. 68

Figure 18: ^{222}Rn exhalation contour super-imposed on Lithologic map of the study area. 68

Figure 19: ^{222}Rn exhalation rate map super-imposed on Lithologic map of the area. 69

Figure 20: ^{222}Rn Emanation Coefficient Map of the rocks within the study area. 71

Figure 21: ^{226}Ra Concentration Contour Map of the study area. 73

Figure 22: ^{232}Th Concentration Contour Map of the study area. 73

Figure 23: ^{40}K Concentration Contour Map of the study area. 74

Figure 24: Gamma Radiation Dose rates of the rocks within the study area. 76

Figure 25: Radium Equivalent Activity Index (Ra_{eq}) of the rocks of the study area. 76

Figure 26: A plot of Ra_{eq} vs. H_{ex}. 77

Figure 27: Piper Diagram of groundwater of Mika Area and Environs. 81

Figure 28: Durov plot of groundwater of Mika area and environs. 82

Figure 29: Schoeller Plot of the Study Area. 83

LIST OF TABLES

Table 1: Spectral Energy Windows used in the Analysis 47

Table 2: Energy Calibration for Quantitative Spectral Analysis 48

Table 3: Human Exposure to Radiation 49

Table 4: Measured Radon and Thoron Concentrations, Calculated Radon Annual Absorbed Dose, Annual Effective Dose and Annual effective dose due Ingestion by Drinking. 64

Table 5: Radon Exhalation Results Measured on Rock Samples 67

Table 6: Calculated Radon Emanation Coefficient and Exhalation Rate 70

Table 7: Gamma Spectrometry Analysis Results 72

Table 8: Calculated γ – Radiation Dose Rates, Annual Effective Dose Rate, Radium Equivalent and External Hazards. 75

Table 9: Groundwater Physical and Chemical Analysis results. 78

Table 10: Statistical Summary of Physico-chemical Analysis Results. 79

Table 11: Correlation Matrix.79

Table 12: Calculated values of Sodium Adsorption Ratio (SAR), Percent sodium (%Na), Permeability Index (PI) and Chloro-Alkaline Indices (CAI). 84

Table 13: Summarized classification of groundwater for irrigation in the study area. 85

Table 14: Classification based on TDS Values (Davis and Dewiest, 1966). 96

Table 15: Classified irrigation water based on TDS as follows (Wilcox, 1955). 96

LIST OF PLATES

Plate I: Photograph showing Vegetation type within the study area (Taken during the dry season). 10

Plate II: Measuring groundwater level at Madaki Open-Well. 40

Plate III: Part of the shear zone that cuts through the porphyritic granite, northeastern part of the study area. 60

Plate IV: Medium-Grained Granite section of the shear zone, southwestern part of the study area. 62

LIST OF APPENDICES

Appendix 1.

Table 16: Groundwater Elevation and Thickness of Dry Zone (Depth to WT). 120

Appendix 2a.

Table 17: Specific Activity Concentration (Bq/kg). 121

Appendix 2b.

Table 18: Radon Concentration in Water across the Globe. 122

Appendix 2c.

Table 19: Radon Concentration in Outdoor Air. 123

Table 20: Radionuclides (World Average vs. Present Work). 123

Appendix 3.

Figure 30: ^{222}Rn and ^{220}Rn concentration graph of Zing town (borehole). 124

Figure 31: ^{222}Rn and ^{220}Rn concentration graph in of Abuja Village (borehole). 124

Figure 32: ^{222}Rn and ^{220}Rn concentration graph of Monkin town (borehole). 124

Figure 33: ^{222}Rn and ^{220}Rn concentration graph of Kakulu town (borehole). 124

Figure 34: ^{222}Rn and ^{220}Rn concentration graph of Kan-Iyaka village (hand-dug well). 125

Figure 35: ^{222}Rn and ^{220}Rn concentration graph of Mika town (borehole). 125

Figure 36: ^{222}Rn and ^{220}Rn concentration graph of Wuro-yaya community (borehole). 125

Figure 37: ^{222}Rn and ^{220}Rn concentration graph of Manzalang Village (borehole). 125

Figure 38: ^{222}Rn and ^{220}Rn concentration graph of Kwoji community (borehole). 126

Figure 39: ^{222}Rn and ^{220}Rn concentration graph of Mararaban Yorro (borehole). 126

Figure 40: ^{222}Rn and ^{220}Rn concentration graph of Bakinya Village (borehole). 126

Figure 41: ^{222}Rn and ^{220}Rn concentration graph of Dilla Village (borehole). 126

Figure 42: ^{222}Rn and ^{220}Rn concentration graph of Kpantisawa town (borehole). 127

Figure 43: ^{222}Rn and ^{220}Rn concentration graph of Nyaja Village (borehole). 127

Figure 44: ^{222}Rn and ^{220}Rn concentration graph of Tapenla Village (hand-dug well). 127

Figure 45: ^{222}Rn and ^{220}Rn concentration graph of Kassa town (borehole). 127

Figure 46: ^{222}Rn and ^{220}Rn concentration graph of Boduga Community (borehole). 128

`Chapter One

INTRODUCTION

1.5 Background of study

Water and its management will continue to be a major issue with definite and profound impact on our lives and that of our planet (Herschy, 1999). It is the most important natural resources without which life would be non-existent (Adebo and Adetoyinbo, 2009). Availability of safe and reliable sources of water is an essential pre-requisite for sustainable development. Deserts are not habitable because of lack of water (Asonye, *et al.*, 2007).

Freshwater quality and availability remain one of the most critical environmental and sustainability issues of the twenty-first century (UNEP, 2002). Of all sources of freshwater on the earth, groundwater constitutes over 90% of the world's readily available freshwater resources (Boswinkel, 2000). Hence, the need to constantly evaluate the quality of groundwater most especially in areas where the interaction between the geology and groundwater pose an eminent health risk to human settlements.

When the earth was formed, billions of years ago, there were probably many radioactive elements included in the mix of material that became the earth. Three, of interest, have survived to this day, namely; uranium-235, uranium-238, and thorium-232. Each has a half-life measured in billions of years, and each stands at the top of a natural radioactive decay chain (Durridge RAD7 manual, 2014).

Uranium exists as three isotopes: ^{238}U, ^{235}U and ^{234}U. The first two isotopes have their own decay series while the third one is an intermediate product of ^{238}U decay series (Fig.1). Uranium-238 is not abundant but occurs as a trace element in most rocks (average concentration in earth crust is 2 ppm (Mason and Moore, 1984)). As shown in Fig.1, ^{238}U has a half-life of 4.5 billion years, which gives a continuous radium and radon production. When ^{222}Rn decays, the so-called

"short-lived radon daughters" are formed. These are ^{218}Po, ^{214}Pb, ^{214}Bi and ^{214}Po, metal atoms with metallic properties that adsorb to dust and other particles in the air.

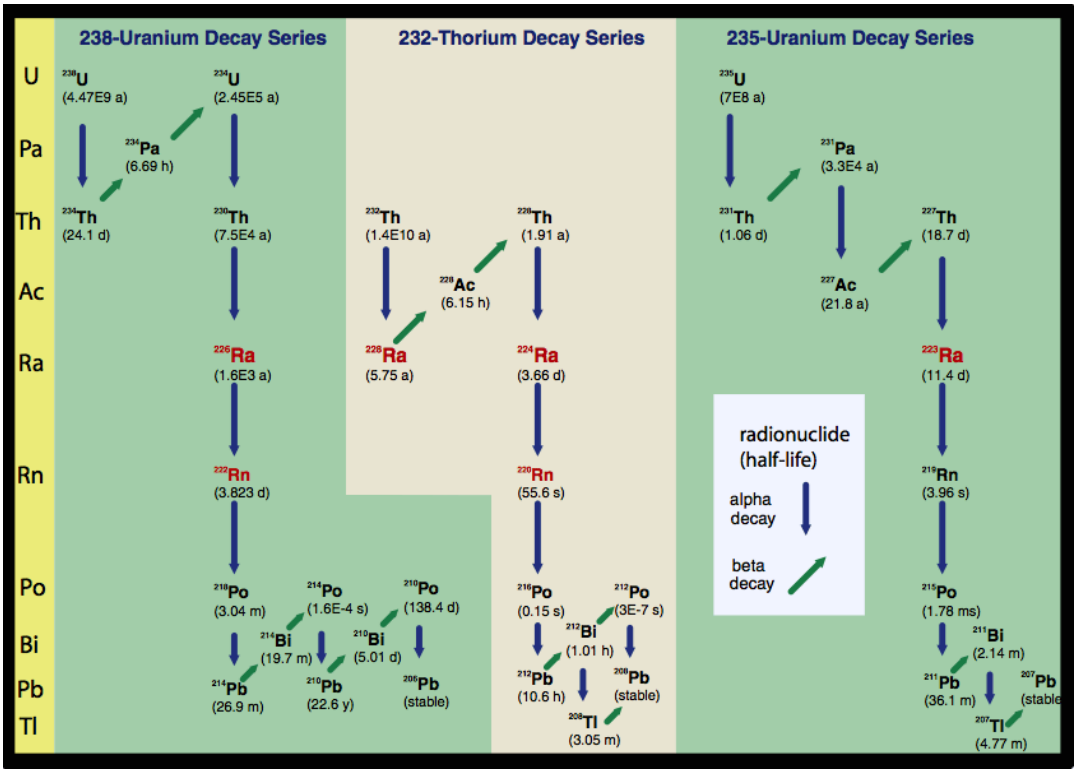


Fig.1: Uranium decay series (elements.geoscienceworld.org).

In reducing environments, uranium occurs as U(IV), and is practically immobile due to the extreme insolubilities of uraninite (UO_2) and coffinite ($USiO_4$). Under these conditions, the uranium concentration in water is less than 10^{-13}M, but under oxidizing condition, ion form complexes (e.g., $UO_2(HPO_4)_2^{2-}$, UO_2^{2+}, $UO_2(CO_3)_2^{2-}$ or $UO_2(CO_3)_3^{4-}$) that are highly stable (Langmuir, 1978; Molinari and Snodgrass, 1990). The uranyl ion (UO_2^{2+}) and its complexes have a high solubility; under certain environmental conditions uranium can be transported long distance in groundwater. Between pH 5 and pH 8.5, uranyl minerals limit the uranium concentration to ~10^{-9}M (Langmuir, 1978), but concentrations are often lower. Uranium is reduced by either organic material, i.e. carbonaceous or bituminous shales or lignites (Molinari

and Snodgrass, 1990), reduced by Fe (producing Fe oxides), reduced by sulphide (Gabelman, 1977) or adsorbed onto mineral surfaces or organic matter. Phosphate rocks are also enriched in uranium, due to co-precipitation of U with Ca^{2+} (Molinari and Snodgrass, 1990). The uranium concentration in natural waters is primarily controlled by sorption (Langmuir, 1978; Wanty, et al., 1991). Langmuir, (1978) used enrichment factors ($[U]_{sorbent}/[U]_{solution}$) to describe the strength of adsorption. These were as high as $1.1x10^6 – 2.7x10^6$ for adsorption onto amorphous Fe oxides, and quite low for adsorption onto clay minerals (2 – 15). Uranium sorption can be inhibited by carbonate complexation of the uranyl ion (Ames, *et al*., 1983).

In igneous rocks, uranium concentration increases with degree of differentiation, very low U concentrations occur in ultrabasics (0.014 ppm) and higher in granites (2 – 15 ppm) and pegmatites (Rogers and Adam, 1969). Uranium does not easily fit into the lattice of rock-forming minerals; a major share is deposited as separate minerals or at grain boundaries during cooling of magma. This is the explanation for the high uranium concentrations in pegmatites, which are formed from residual hydrothermal solutions (Edsfeldt, 2001).

Radon is a radioactive noble gas which is formed through decay of radium. It occurs as three different isotopes in nature, ^{219}Rn, ^{220}Rn and ^{222}Rn. ^{222}Rn with a half-life of 3.82 days is the most important, this is because, other isotopes are very short-lived (^{220}Rn: 55.6 sec; ^{219}Rn: 3.96 sec), and will not be transported very far before they decay. ^{222}Rn is formed through decay of ^{226}Ra in the decay chain of ^{238}U.

Radon gas is produced within the grains in the rocks and soils. Radon atoms that escape from soil or rock grains into the pore space are said to emanate (Fig. 2). The radon emanation coefficient is the percentage of the produced radon atoms that escapes into pore space. Radon exhalation rate describes the amount of radon passing through a surface per unit time (Edsfeldt, 2001).

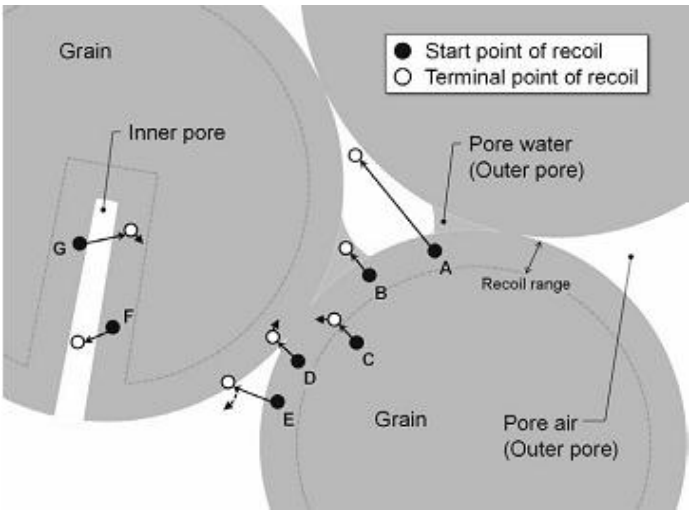


Fig 2: Illustration of radon emanating from soil or rock grains into pore spaces (adopted from Edsfeldt, 2001).

Groundwater is favoured as a source of drinking water in many countries. Water coming from the subsurface is often thought to be cleaner and easier to treat as compared to surface water and as a result of which many wells have been either dug or drilled. However, besides the risk of being contaminated by anthropogenic pollution, groundwater naturally contains several chemical components, which can lead to different kinds of health problems (Skeppstrom and Olofsson, 2007).

If radon and radon daughters are ingested or inhaled and decay inside the human lungs, the radiation has the potential to split water molecules and produce free radicals (e.g. OH). The free radicals are very reactive and may damage the DNA of the cells in the lungs, thus causing cancer (Edsfeldt, 2001). When an individual spends time in an atmosphere that contains radon and its progeny, the part of the body that receives the highest dose of ionizing radiation is the bronchial epithelium, although the extra thoracic airways and the skin may also receive appreciable doses. In addition, other organs, including the kidney and the bone marrow, may receive low doses. If an individual drinks water in which radon is dissolved, the stomach will also be exposed to it (Kendall and Smith, 2002). Darby, *et al.*, (1995) examined the evidence for increased radon-

related mortality from cancer other than lung cancer and reported that no strong evidence was found that radon was causing cancers other than lung cancer. However, WHO (2009) reported that further investigations are focusing on this issue.

^{222}Rn was reported as contributing the largest component of human exposure to natural radiation (UNSCEAR, 2000). Concentration measurements of ^{222}Rn and its progeny for the determination of radiation doses to occupationally exposed individuals and members of the public living in proximity to supervised radiation area are standard practice. The International Commission on Radiological Protection (ICRP, 1991) recommendations for limits to ionizing radiation from man-made sources are 20 mSv.yr^{-1}, effective dose for occupationally exposed workers and 1 mSv.yr^{-1} for members of the public; this does not include medical as a patient or natural background.

1.2. Justification

An aero-radiometric map of part of northeastern Nigeria (Monkin-Sheet 216) showed high radiometric values indicating abnormal occurrences of natural occurring radioactive materials (Airborne spectrometry survey map of contours of total count, selected anomalies and anomalous zones) (GSN, 1975). A study by Funtua, (1992) on the geology and geochemistry of uranium mineralization in Mika and its environs (part of Sheet 216) reported high anomalous uranium concentrations in rocks and identified Mika as the main uranium mineralized area. Arabi, (2012) conducted a study on the radioactivity and chemistry of groundwater from uranium mineralized areas around Gubrunde in which he was able to delineate areas with high uranium amplitudes (>4 μrh^{-1}) within the Upper Benue. Mika and environs are part of the delineated areas.

Skeppstrom and Oloffson, (2007) presented an overview of the problem of natural radioactivity in drinking water from drilled wells in Sweden. The report indicated that in some areas of Sweden where municipal water is not available, wells are drilled in bedrock to extract water for

drinking purposes and other uses. It revealed that groundwater from wells drilled in rock types rich in uranium (e.g. granites) has shown tendency to have both high radon and uranium concentrations. However, high concentrations of radon exceeding the Swedish regulatory limit of 1000 Bq/l have also been reported in bedrock containing low concentrations of uranium (<2 ppm). This might indicate the possible movement of the water from (e.g. pegmatite) at several meters depth, which often goes undetected on geological maps.

Claims of high uranium anomaly proved by radiometric survey, Funtua, (1992) and Arabi, (2012) within the study area, aside the economic dimensions to which might be beneficial to the host communities, human lives are at risk due to decay tendencies of uranium, resulting to daughter products (e.g. Radon-222 and its progeny) which might negatively affect human existence in the area. Hence, the need to study and evaluate the general groundwater quality with respect to radon gas, the health hazards it poses and as well, other groundwater evaluation parameters within Mika Uranium mineralized area and environs. This report will establish baseline data, create awareness and help the government in-order to be proactive so as to forestall future endemic outbreak of lung cancer, stomach cancer and other radon gas related ailments which may endanger lives and well-being of the inhabitants in communities under study.

1.3. Aim and Objectives of Study

The aim of this work is to study the hydrochemistry of groundwater with emphasis on radon gas and radon exhalation/emanation from rocks around Mika and environs. The objectives are as follows;

1. To evaluate the groundwater for radon-222 concentration.

2. To determine the exhalation rates as well as the emanation coefficients of radon-222 from rocks surrounding the communities where the groundwater was evaluated.
3. To establish a relationship (if any) between groundwater water flow direction and radon concentration.
4. To calculate and evaluate various radiation doses due to naturally occurring radionuclides (^{222}Rn, ^{226}Ra, ^{232}Th and ^{40}K).
5. To present a general hydrochemical study of the groundwater with emphasis on major cations and anions, so that the quality of the groundwater for drinking and other domestic uses as well as for irrigational purposes, can be established.

1.4. Study Area

1.4.1 Location, Extent and Accessibility

The study was conducted in Mika and environs, under Zing and Yorro Local Government Areas of Taraba State, Nigeria. The study area is part of Monkin Sheet 216 and part of Dong Sheet 195. It lies between latitudes $08^{o}48^{'}$ to $09^{o}4^{'}$N and longitudes $11^{o}30^{'}$ to $11^{o}48^{'}$E. It is located within the northern part of the Adamawa massif and covers an area of about 1004 km^2.

It can be accessed through intra/interstate roads of Jalingo – Zing road and Mayo-Belwa – Zing road respectively. Footpaths and many rural road networks also link the study area from nearby communities (Fig. 3).

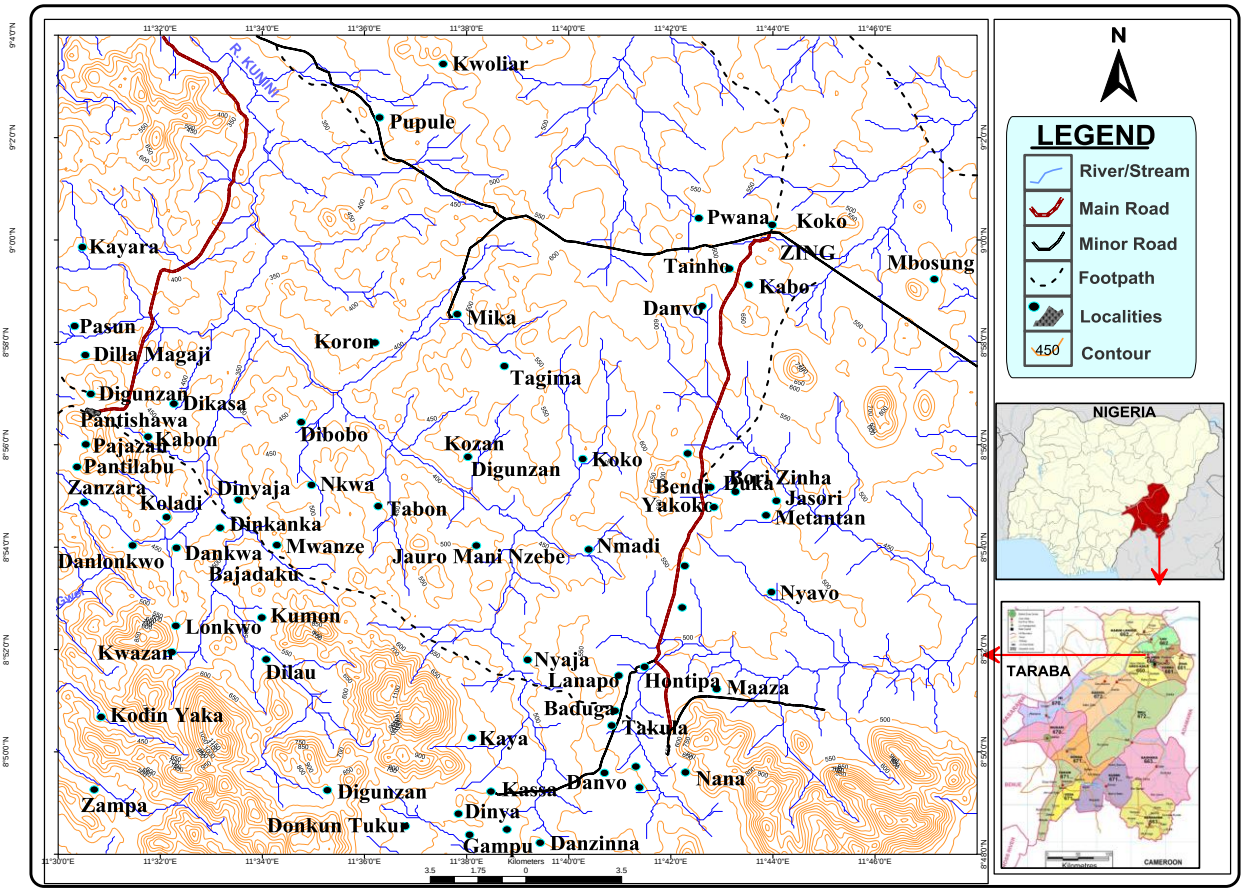


Fig 3: Topographic map of the study area

1.4.2 Relief and Drainage.

The relief configuration of the study area can be categorized into two zones, highlands mountain range and lowlands (Fig. 4). The highlands occupy the southern region stretching from west to south in chains of mountain with elevation ranging from 1800 – 2400 meters high, forming the Adamawa massif ranges. The lowland which occupies about 60% of the region forms most of the human settlements. The area is drained by River Kunini and smaller tributaries that make up the watersheds within the study area.

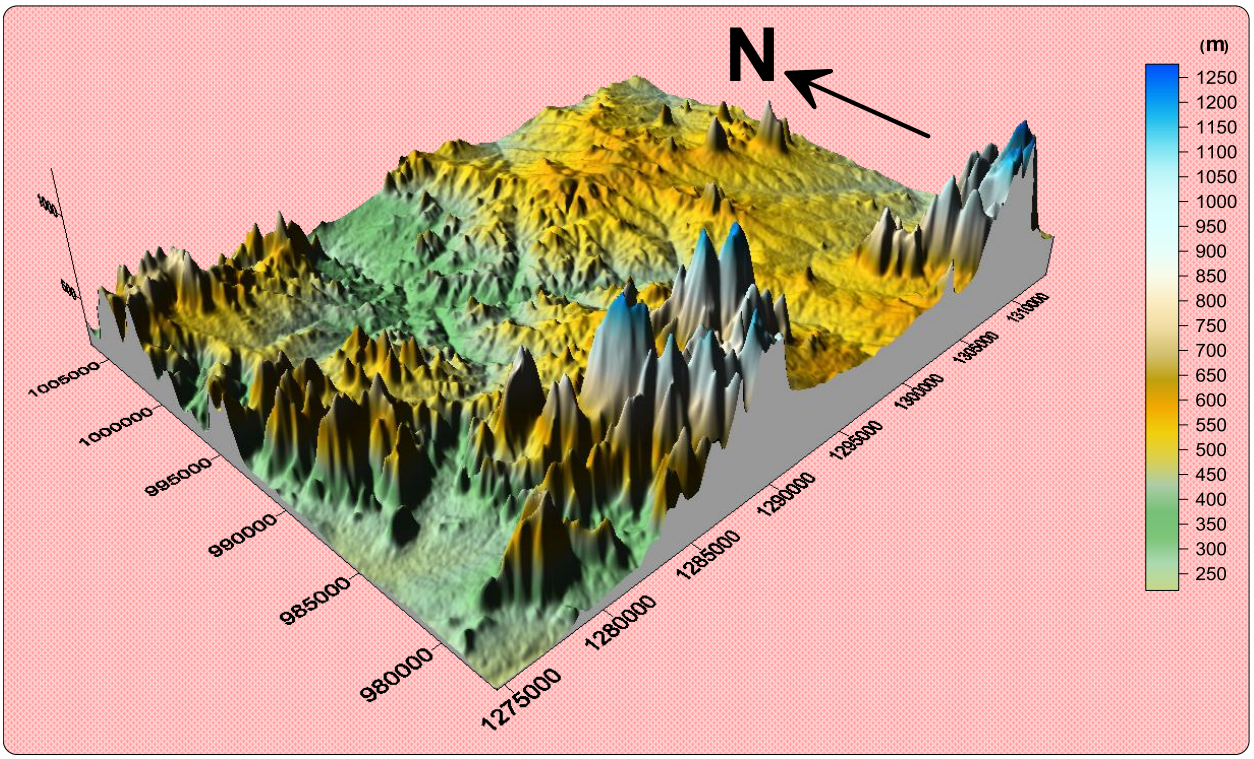


Fig 4: Digital Elevation Map of the study area.

1.4.3 Climate and Vegetation.

The climate of the area is typically a tropical climate marked by dry and rainy seasons. The mean annual rainfall of the area ranges from 819 – 1761mm. It is spread over seven months (April to October). The onset of the rains is April, with low amount but increases gradually reaching a maximum in August, the amount drops gradually with cessation in October (Ray and Yusuf, 2011). Mean monthly temperature ranges between 20^{o}C – 25^{o}C while the relative humidity is lowest (26%) in March and reaches 98% in August (Oruonye, 2014). The study area is within the savannah grassland belt, particularly in the guinea Savannah sub-region, characterized by scattered, deciduous tall trees with broad leaves and tall grasses (Plate 1).



Plate I: Photograph showing tall trees and grasses with broad leaves within the study area (taken during the dry season).

1.4.4 People and Land-use

Mika and environs, predominantly accommodates the Mumuye ethnic tribe in Taraba State. Their unique tribal marks and a large opening on the ear, mostly seen on elderly women, makes them stand-out from other tribes within and outside the State. Other tribes like the Fulani, mostly engaged in cattle rearing, are found settled around the Mumuye communities. Mumuye people are predominantly farmers, producing crops like yam, cassava, maize and beans. They also engage in civil service, public service, small scale livestock, hunting as well as petty trading. Bush burning is a common practice during the dry season (mostly for hunting purposes, (e.g.), Bush rats and Squirrels), even though, this practice affects the environment negatively as it increases the rate of erosion during the rainy season.

1.5 Radioactivity

Radioactivity is the emission of radiation originating from a nuclear reaction or as a result of the spontaneous decay of unstable atomic nuclei. The term radioactive decay refers to the process whereby unstable atomic nuclei decay with the loss of energy by the emission of elementary particles (e.g., alpha particles, beta particles, neutrons, and gamma – photons) directly from the nucleus or the atomic electron shells (e.g., Auger electrons and X-ray photons) within which the nucleus resides (L'Annungiata, 2012).

Radioactivity was discovered in the 1896 by Henri Becquerel (L'Annungiata, 2007; 2012). At the beginning of 1896, on the very day that news reached Paris of the discovery of X-rays, Henri Becquerel thought of carrying out research to see whether or not natural phosphorescent materials emitted similar rays. He placed samples of uranium sulphate on to photographic plate, which were enclosed in black paper or aluminium sheet to protect the plates from exposure to light. After developing the photographic plates, he discovered that the uranium salts emitted rays that could pass through the black paper and even a metal sheet or thin glass positioned between the uranium salts and the photographic plates. Becquerel reported his findings to the French Academy of Sciences in February and March of 1896 (Becquerel, 1896a, b). At first, he thought the rays were as a result of phosphorescence, that is, excitation of the crystals by sunlight forcing the crystals to give off their own rays. However, Henri Becquerel carried-out further tests demonstrating that the rays emanating from the uranium salts were independent of any external source of the excitation including light, electricity, or heat, and the intensity of the rays did not diminish appreciably with time (L'Annungiata, 2012). In a speech delivered during his Nobel lecture on December 11, 1903, he remarked thus; "we were thus faced with a spontaneous phenomenon of a new order" (Becquerel, 1903).

Becquerel provided evidence that all uranium salts emitted the same radiation and that this was a property of the uranium atom particularly since uranium metal give off much more intense radiation than the salts of that element. The new radiation produced ionization, and the intensity of the radioactivity could be measured by this ionization. Not only did these rays produce ionization, but he was able to demonstrate that a large portion of these rays, could be deflected by a magnetic field and were charged particles of the property similar to cathode rays (L'Annungiata, 2012). J.J. Thomson discovered in 1897 that cathode rays were electrons (Thomson, 1897) and years later, Ernest Rutherford named the electron originating from nuclear decay as beta particles (Rutherford, 1903).

Following Becquerel's discovery of spontaneous radiation from uranium, Marie Curie studied the mysterious rays emitted by uranium and discovered that not only uranium gave off the mysterious rays discovered by Becquerel, but thorium did as well. She and her husband (Pierre Curie) observed that the intensity of the spontaneous rays emitted by uranium or thorium increased as the amount of uranium or thorium increased. They concluded that these rays were a property of the atoms of uranium and thorium; thus, they decided to coin these substances as "radioactive" (L'Annungiata, 2007 & 2012). The emanation of such spontaneous rays from atoms would now be referred to as "radioactivity" (Curie, 1905).

Ernest Rutherford in 1899, named two types of nuclear radiation as "alpha" and "beta", which he characterized on the basis of their relative penetrative power in matter, that is, alpha radiation would be more easily absorbed by matter than beta radiation. In harmony with this nomenclature, Rutherford assigned the term "gamma" rays to the yet more penetrating radiation (Rutherford, 1903). From the previous discovery that radium gives out three distinctive types of radiation (Villard, 1900a, b), Rutherford named and characterized the three types of nuclear radiation on the basis of their penetrating power in matter as follows;

The Alpha Particles: These are very easily absorbed by thin layers of matter, and which give rise to the greater portion of the ionization of the gas observed under the usual experimental conditions. The alpha particle, structurally equivalent to the nucleus of a helium atom and denoted by the Greek letter **α**, consists of two protons and two neutrons. Alpha particles are emitted as decay product of many radionuclides predominantly of atomic number greater than 83 (L'Annungiata, 2012).

Alpha particles are emitted by radionuclide with distinct energies that range between 4 and 10 MeV; and half-lives of the nuclide will vary over a wide range of thim from 10^{10} years to microseconds. Radionuclides emitting alpha particle of low energy decay with long half-life, whereas those emitting alpha particles of high energy have short half-lives (L'Annungiata, 2007). Alpha particles posses a double positive charge due to the two protons present. This permits ionization to occur within a given substance by the formation of ion pairs due to coulombic attraction between a traversing alpha particle and atomic electrons of the atoms within the material the alpha particle traverse. The two neutrons of alpha particle give it additional mass, which further facilitates ionization by coulombic interaction or even direct collision of the alpha particle with atomic electrons (L'Annungiata, 2012).

The Beta Particles: These consist of negatively charged particles projected with high velocity, and which are similar in all respect to cathode rays produced in a vacuum tube (L'Annungiata, 2012). Beta particles are electrons with greater penetrating power than alpha particles but owing to a lesser ability to ionize, they are not as damaging to living cells as are alpha particles (Solomon, 2005).

Beta decay may be defined as any nuclear decay process whereby the mass number (A) of the nucleus remains the same and the atomic number (Z) changes. There are

three main types of beta decay, namely; negatron (β^-), emission which involves the emission of a negative beta particle or negative electron from the nucleus; positron (β^+), emission whereby a positive beta particle or positively charged electron is emitted; and Electron capture (EC), which does not result in the emission of any beta particle (L'Annungiata, 2012).

Some beta emitters occur in nature, mostly among the heavy elements of the uranium, thorium and actinium groups, commonly found in association with crystalline rocks. Thorium, for instance, is a practical constituent of some minerals, notably thorite and monazite (a mixed rare earth and thorium phosphate). The actinide elements are the fourteen chemical elements that follow actinium in group IIIB of the periodic table, all of which are radioactive, because their nuclei are so large that they are unstable and release great amount of energy when they undergo spontaneous fission. Generally, the heavy elements of the uranium, thorium and actinium groups have an excess of neutrons and hence decay by the emission of electrons (Solomon, 2005).

Gamma Radiation: The discovery of a highly penetrating radiation that was nondeviable in an external magnetic field, which is now known as gamma radiation was discovered by Paul Villard at the Ecole Normal in Paris in 1900. The discovery was reported to the French Academy of Sciences (Villard, 1900a, b).

Radionuclide decay processes often leave the product nuclide in an excited energy state. The product nuclide in such an excited state either falls directly to the ground state or descends in steps to lower energy state through dissipation of energy as gamma radiation. A nuclide in an excited energy state is referred to as a nuclear isomer, and the transition (or decay) from higher to a lower energy state is referred to as isomeric transition (L'Annungiata, 2012).

Gamma radiation undergoes many diverse interactions with matter at different energy ranges. Low-energy gamma radiation may be totally absorbed by an atomic electron that is then emitted. The ejected electron is known as a photoelectron, and the process is known as the photoelectric effect (Solomon, 2005).

Gamma radiation can also interact with an atomic electron, sharing its energy and giving rise to the Compton Effect, in which the original gamma radiation is scattered away with reduced energy and the electron is ejected. This electron is known as a Compton electron. Gamma radiation of sufficiently high energy can also interact with the electric field of the positively charged nucleus producing an electron and a positron. This phenomenon is known as pair production (Solomon, 2005).

When a beam of gamma radiation passes through matter, its intensity after emergence has diminished, principally as a result of the above three processes. Very high energy gamma radiation can also cause nuclear disintegration and can eject a nuclear particle such as a neutron or a proton. Various types of mesons can also be produced by gamma radiation of extremely high energy in its interaction with atomic nuclei. Gamma radiation is emitted as photons, or discrete quanta of energy (Solomon, 2005).

Rutherford's work in conjunction with numerous collaborators, including Frederick Soddy, led to the conclusion that one chemical element can transform into other element (Rutherford and Soddy, 1902). Atoms of a given element can have different numbers of neutrons, and thus different atomic mass (Rutherford 1913; Bohr 1913). Soddy named the forms of an element with different atomic masses, the "isotopes" of the element (Soddy, 1913a, b). He went further by alluding to the fact that not only can we consider the radioactive atoms of specific elements as isotopes, but that many, if not most of the stable elements may actually consist of a mixture of isotopes. Therefore, isotopes can simply be put as, nuclides that have the same atomic number

(Z), that is, the same number of protons but they differ in their number of neutrons (N). Thus, they differ in their mass number (A), which is the sum of the number of protons and neutrons in the nucleus. Because isotopes have the same atomic number, they are nuclides of the same chemical element (L'Annungiata, 2012).

Rutherford and Soddy also discovered that every radioactive isotope has a specific half-life (Rutherford and Soddy, 1902). Half the nuclei in a given quantity of a radioactive isotope will decay in a specific period of time. E.g., the half-life of uranium-238 is 4.5 billion years, which means that over that immense period of time, half the nuclei in a sample of uranium-238 will decay (in the next 4.5 billion years, half of what is left will decay, leaving one quarter of the original, and so forth). The isotope produced by the decay of uranium themselves promptly decay in a long chain of radiations. Radium and polonium are links in this chain (Fig.1).

Half-life of a given radioisotope is not affected by temperature, physical or chemical state, or any other influence of the environment outside the nucleus (except, from nuclear reactions), the radioactive samples continue to decay at a predictable rate. This makes several types of radioactive dating feasible (Pullman, 1998).

Radionuclides were first used for therapeutic purposes almost 100 years following the observation by Pierre Curie that radium sources brought in contact with the skin produce burns. Already by 1915, sealed sources of radium-226 and radon-222 were in use. By the 1950s radiotherapy had become much more widespread due to the development of remote source handling techniques and availability of reactor produced radionuclides such as cobalt-60 (Magill and Galy, 2004).

Ionizing radiations from radionuclides kill cells by damaging the DNA thereby inhibiting cellular reproduction. The energy of the radiation (in the form of photons, electrons, heavy particles, etc.)

required to damage DNA should be greater than a few electron volts (eV) corresponding to the binding energy of the outer electrons (Pullman, 1998).

Radioisotopes have been used as tracers. The first to use radioisotope as tracer was George de Hesevy (a colleague of Rutherford), who used radioisotopes to test his food when he suspected that the stew his landlady was serving him was made from the previous day leftovers (Pullman, 1998). The use of so-called "tracer" or "tap" techniques using radionuclides is based on the fact that radiation can be detected with very high sensitivity. A very small number of "tagged" or "labeled" molecules added to a material allow one to monitor chemical and physical behavior at both macro – and microscopic levels without disturbing the carrier material. A common problem in the oil industry is the detection of leaks. For this purpose, radionuclide tracers can be inserted into the pipe flow and will leak where the structure is damaged. If the pipe is not too deeply buried in the ground, the leak position can be identified from the gamma emission from the tracer radionuclide from the above soil (Magill and Galy, 2004).

1.5.1 Sources of Radiation

Radioactivity and exposure to ionizing radiation may occur naturally or produced artificially. While radiation may come from naturally occurring radionuclides, the usual method for artificially produced radioisotope is by the bombardment of stable nuclei with charged or uncharged particles. This can be achieved by the use of nuclear reactors (the primary source of radioisotopes for biological purposes), by particle accelerators, or by other neutron sources such as a neutron generator (Solomon, 2005).

1.5.1.1 Naturally Occurring Radionuclides

If we take into account the age of the earth, which is 4.5×10^9 years, and the characteristic property of the radionuclide half-life decay, one of the following conditions would have to be met for a natural radioactive nuclide to occur on earth: (i) the radionuclide would be produced

continuously on earth or its atmosphere by a natural phenomenon, (ii) the radionuclide would be very long-lived that is, it would have a half-life of the order of $\geq 10^9$ years, or (iii) a short-lived radionuclide would be in equilibrium with the naturally occurring long-lived parent radionuclide (L'Annungiata, 2012).

A number of radionuclides are produced on a continuous basis by the interaction of cosmic-ray particles with the nuclei in the earth's atmosphere. The cosmogenic isotopes are created by the interactions of high – energy primary and secondary particles of cosmic radiation with the nuclei of gaseous molecules of the atmosphere (e.g., N_2, O_2, Ar, etc.), resulting in the fragmentation of the target nuclei or by the capture of thermal neutrons of the cosmic radiation showers with target nuclei of the atmosphere (L'Annungiata, 2012). Lal (2009) reported that most of the cosmic-ray energy (>98%) is dissipated in the earth's atmosphere. Secondary particles of cosmic radiation produce nuclear reactions at a much reduced rate with the earth's superficial reservoirs, including the hydrosphere, cryosphere, and lithosphere (L'Annungiata, 2012). This means that, cosmogenic radionuclide are produced to a greater extent, in the earth's atmosphere. Examples of cosmogenic radionuclides are; ^{3}H, ^{7}Be, ^{10}Be, ^{26}Al, $^{14}CO_2$, ^{37}Ar, ^{39}Ar, etc.

Based on the age of the earth, we can expect that all non-cosmogenic radionuclides with a half-life $<10^8$ years, that were formed during the formation of the earth and are not in equilibrium with the parent nuclide in a naturally occurring decay chain, would have decayed to an undetectable level (L'Annungiata, 2012). Examples of naturally occurring radionuclide are; ^{238}U, ^{235}U, ^{232}Th, ^{40}K, (^{222}Rn, ^{220}Rn, ^{218}Po, ^{214}Bi), etc., where, the examples in parenthesis are daughter products of uranium and thorium decay series and have relatively very short half-lives.

The largest natural source of radiation exposure to humans is radon gas. While radon gas has always been in the environment, its contribution to human radiation exposure has increased in recent years. Radon's primary pathway is from the earth, through the basements of houses and

other buildings, and into inside air that people breathe. Radon exposures can vary depending on the soil and rock structure beneath buildings (Solomon, 2005).

1.5.1.2 Artificially Produced Sources

Man-made sources of radiation include medical exposures such as diagnostic x-rays, as well as from nuclear medicine involving diagnostic procedures such as the use of nuclear tracers. Very small amounts of radioactive materials, called tracers, are put into the blood stream, and their progress through the body is monitored with a radiation detector. With this, blocked or restricted blood vessels can be identified. Nuclear medicine also includes treatment of disease. Some examples are cobalt irradiation for the treatment of cancers, or the injection of radioactive iodine which concentrates in the thyroid for treatment of Graves' disease (Solomon, 2005).

Radiation is used in the manufacturing of many consumer products. It is used to sterilize products such as cosmetics and medical supplies. Radioactive materials are also used in other consumer products such as smoke detectors, while other consumer products that could expose people to radiation include smoking of cigarettes, burning gas lanterns, using natural gas for heating and cooking, using phosphate fertilizers, radiation from color television, as well as the use of cell phones. The dose rates from these sources are small and vary considerably (Solomon, 2005).

Other man made sources includes radiation exposures from fallout during international nuclear weapons testing programs and nuclear power plant accidents. For instance, high levels of radiation were created in the atmosphere after the Chernobyl accident in the then Soviet Union (April, 1986). Very recently radiation problems arising from the use of depleted uranium in war have been reported and investigations into the health and environmental consequences of this is continuing (United States Army Environmental Policy Institute, USAEPI 1994; United State Army Material Command- USAMC, 2000; United State Defense Department- USDD, 2000).

1.5.2 Radioactivity Pathways

Radionuclides travel through the environment along the same pathways as other materials. They travel through the air, in water (both groundwater and surface water), and through the food chain. Radionuclides may enter the human body by ingestion (eating or drinking), by inhalation, or through the skin. Radionuclides can also be released into the air by human activities or created in the atmosphere by natural processes such as the interaction of cosmic radiation with nitrogen to produce radioactive Carbon-14. Radionuclides in the air can settle out of the atmosphere if air currents cannot keep them suspended, and rain or snow can remove them. When these particles are removed from the atmosphere, they may land in water, on soil, or on the surfaces of living and non-living things (Solomon, 2005).

1.5.3 Radiation Surveys

Radiation survey involves the measurement of natural radiation levels, detection of radiation contamination, monitoring the effectiveness of shielding arrangements, as well as estimating radiation exposure to personnel. There are two main categories of radiation monitoring devices. They include gas filled detectors and scintillation detectors (Solomon, 2005).

Gas detection instruments are based on the principle that ions are produced when radiation passes through a gas-filled chamber. Electrons liberated in the chamber are attracted to the center electrode (anode) by a positive voltage potential, while positive ions are attracted towards the walls (cathode) of the chamber. This produces an electrical pulse or current which can then be detected and recorded by a scaler or rate-meter (Handloser, 1959; Price, 1964; Fenyves and Haiman, 1969; Ouseph, 1975). Gas filled detectors are of three types, namely ionization chambers, proportional counters, and Geiger – Müller detectors. The primary difference between these detectors is the voltage applied to the chamber, and the kind of detector to be used depends on the intensity and the type of radiation field encountered.

1.5.3.1 Ionization Chambers

Gas ionization detectors can be characterized by the effects created by different field strengths between the change – collecting electrodes (Steinhauser and Buchtela, 2012). At low field strength, many slowly migrating ion pairs still have the opportunity to recombine. This recombination region is not used for radioactivity detectors. As more voltage is applied, more ions and electrons produced by the ionizing radiation collected at the electrode. Finally, field strength is reached at which now rapidly migrating ions do not have a chance to recombine. Thus, a saturated region is reached where all the ions produced directly by the radiation event, the primary ions, are collected at the electrodes. A further increase of field strength cannot attract more ions because all of them have already been collected. Ion chambers operate in this region. The amount of charge collected at the electrodes directly shows the ionization effects of the incident radiation (Steinhauser and Buchtela, 2012).

1.5.3.2 Proportional Counters

If the field strength is increased further, additional ionization starts to occur because of the higher kinetic energy of the migrating primary ions. These primary ions now being accelerated to a higher energy than the ionization energy of the detector gas, produced secondary ions by impact. With increasing field strength, a great number of additionally produced ions are accelerated, the number still being proportional to the number of primary ions (Steinhauser and Buchtela, 2012). This gas ionization detector region is called proportional region. In that region, radiation with different abilities to produce primary ions (alpha, beta, or gamma radiation) can still be discriminated, or they are registered by "gross counting" without separation. Also, radiation of the same type but with different energies can be discriminated (Garcia-Leon, *et al*., 1984).

1.5.3.3 Geiger – Müller Counters

As the field strength is increased further, excitations of atoms and molecules are observed that, by the emission of ultraviolet light, can start additional ionization processes. In this region, referred to as the Geiger – Müller region, the total number of ions produced is independent of the number of primary ions and, therefore, also independent of the type and energy of radiation. A further increase of the field strength causes a continuous discharge (Steinhauser and Buchtela, 2012).

In the Geiger – Müller region, all primary ionization effects produce the same maximum response in the detector. Geiger – Müller counting tubes operate in this region and thus provide no direct information about the type and energy of radiation. Information related to the type and energy of radiation can be provided only by observing shielding effects related to this radiation. Alpha particles are stopped by a thin layer of matter, beta particles show a maximum range in penetrating a shielding material before they enter the detector, and photons show a somehow logarithmic decrease in intensity with increasing thickness of the material. In the earlier days of radiation measurements, such experimental setups were frequently used for rough determination of radiation type and energy (Chase and Rabinowitz, 1967).

1.5.3.4 Scintillation Detectors

Detection of ionizing radiation by scintillation detectors is based on the emission of light as a result of the interaction of the radiation with the detector material (called a scintillator) followed by collection of light and its conversion into electrical pulses using photomultiplier tubes or photodiodes. Scintillation detection is one of the oldest techniques in the measurement of radioactivity having had widespread application for the detection of alpha, beta and gamma radiation in the past (Vajda *et al*., 2012). At present, most of the applications are related to gross counting of alpha, beta, and gamma radiation due to the typically high counting efficiency and

the low cost of the instrumentation while radiation spectroscopy is limited by the insufficient energy resolution of the scintillators to allow the identification of the radionuclides in an isotope mixture. Scintillation gamma spectrometry was a basic tool until about the 1980s, but it was gradually replaced by semi-conductor spectrometry of much better energy resolution (Vajda, *et al*., 2012).

Scintillation detectors include solid and liquid scintillators as well as inorganic and organic scintillators. For all these different types, the basic process used for detection is fluorescence, which is the prompt emission of visible radiation (light). The main parts of the scintillation detector are the scintillator, which converts the radiation energy to visible light photons, and the photoelectron – multiplier (PM) tube containing the photocathode, the multi-stage electron – multiplying section made of a series of electron – multiplying dinodes and an anode for collection of the amplified charge situated in a glass vacuum envelope (Vajda, *et al*., 2012).

1.5.4 Radiation Dose

Radiation dose, also referred to as absorbed radiation dose, is the amount of energy deposited in a given mass of a medium by ionizing radiation (L'Annungiata, 2012). The basic units, used in the measurement of radiation dose are discussed as follows;

1.5.4.1 Count Rates

The standard unit of radioactivity is the Curie, which is defined as the number of disintegrations occurring in one gram of radium per second. Radium was chosen because it was available in pure form and has a long half-life, 1,600 years. The Curie is equivalent to 3.7 x 1010 disintegrations per second (dps). The Curie is a large unit, so several fractions of this unit are also used. These include the millicurie (mC), that is one-thousandth of a Curie, or 3.7 X 107 dps, and the microcurie, that is, one-millionth of a Curie, or 3.7 X 104 dps (Solomon, 2005).

The usual state of a radioisotope is as a mixture with a large amount of the stable isotopes of the same element. Specific activity therefore, is defined as the amount of radioactivity per given weight or weight equivalent of a sample. It expresses the relative abundance of a radioisotope in a sample. Specific activity is often expressed as dps or dpm, counting rates (counts per minute, cpm), or curies, mC, or micro C per unit weight (Solomon, 2005).

1.5.4.2 The Roentgen (R)

Radiation exposure was historically measured by roentgen (R), which is a measure of the quantity of radiation deposited in air from the amount of charge or ionization produced by the radiation in air (L'Annungiata, 2012). By definition;

$$1\ R = 2.58 \times 10^{-4}\ C/kg \text{ (of air at STP)}$$

(That is, one roentgen will produce 2.58×10^{-4} Coulombs of ion pairs in one kilogram of air)

The roentgen is a unit of exposure that is mostly historical and seldom used; it still occasionally appears on some dosimeter reading (L'Annungiata, 2012).

1.5.4.3 The Rad

Of more significance is the measure of absorbed dose, that is, the energy of radiation absorbed per unit mass of absorber. The original unit of absorbed doses is the "rad" which is derived from the term "Radiation Absorbed Dose" (L'Annungiata, 2007; 2012). The rad has been replaced with the gray (Gy), which is the SI unit of absorbed dose. The use of SI units is recommended by the International Commission on Radiation Units and measurements (ICRU) (L'Annungiata, 2012). The rad and gray have the following equivalents;

$$100\ rad = 10^4\ erg/g = 1\ Gy = 1J/kg$$

$$1\ rad = 10\ mGy = 100\ erg/g$$

$$1\ mrad = 10\ \mu Gy$$

As 1 eV = 1.602 x 10^{-19}J, gray can be converted to units of electron – volt energy deposited in a kg of absorber, (i.e.)

$$1 \text{ Gy} = 6.24 \times 10^{12} \text{ MeV/kg}$$

1.5.4.4 The Rem or Sievert

Another formerly common and historical unit of radiation dose is the "rem" (L'Annungiata, 2012). The rem is a measure of absorbed dose in biological tissue. This unit of measure is derived from the term "roentgen equivalent for man" or "roentgen equivalent mammal". The rem was created as a measure of dose of ionizing radiation to body tissue in terms of its estimated biological effects; its SI unit is the Sievert (Sv) and;

$$100 \text{ rem} = 1 \text{ Sv (i.e.) } 1 \text{ rem} = 10 \text{ mSv}$$

The rem or Sievert are referred to as units of equivalent dose, because the dose is measured on the basis of a weighting factor (W_R), which defines the relative hazards of radiation on the basis of the types and energies of the radiations by placing all radiation classes on the same dose level or equivalent (L'Annungiata, 1987). The dose in rem is the product of the dose in rad or gray (Gy) and a weighting factor (formerly known as quality factor, QF) (Solomon, 2005; L'Annungiata, 2012). According to International Commission on Radiation Protection and Measurement (1977), gamma rays, X-rays and beta radiation all have a quality factor of 1, neutrons (10), protons (10), alpha particle (20), and heavy ions (20). This quality factor depends on the relative biological effectiveness (RBE) of the type of radiation under consideration. The RBE is the ratio of the absorbed dose of photons of specific energy to the absorbed dose of any other ionizing radiation required to produce the same biologic effect (Noz and Maguire, 1979).

1.5.5 Maximum Permissible Dose

Over the years, research works in the field of radiation safety have shown that ionizing radiation is not only dangerous but could be lethal. For this reason, several international bodies have

worked on standards in relation to radiation hazards and this has led to the establishment of maximum permissible limit (MPL). Notably among these regulatory bodies are the National Academy of Science, National Research Council Advisory Committee on Biological Effect of Ionizing Radiation (BEIR), International Commission on Radiological Protection (ICRP), National Council on Radiation Protection and Measurement (NCRP), International Commission on Radiation Units and Measurements (ICRU), United Nations Scientific Committee on Effect of Atomic Radiation (UNSCEAR), International Atomic Energy Agency (IAEA) as well as World Health Organization (WHO) (IAEA, 1996).

In making the maximum permissible dose recommendations, both NCRP and ICRP divide the population into two groups namely members of the general public, and "radiation workers" who are exposed to radiation through their occupation. Government standards establish limits for occupational exposure that are greater than those established for the general public. The rationale is that "radiation workers" presumably accept the increased risk by informed consent as a trade-off in exchange for the benefits of employment. The maximum permissible dose for the general public is set at 1 mSv/yr by NCRP as well as ICRP and 0.1mSv/yr by WHO (ICRP, 1991; NCRP, 1993; WHO, 2009).

Chapter Two

LITERATURE REVIEW

2.1 REVIEW OF REGIONAL GEOLOGY AND HYDROGEOLOGY OF NIGERIA

2.1.1 Geology

Nigeria is situated within the Pan African mobile belt and sandwiched between the West African Craton to the west, the Tuareg Shield to the north and the Congo Craton to the south east (Fig. 5), which was affected by the Pan African orogeny about 600 MA. Opinions are divided concerning the evolution of the Nigerian Pan African terrain. The first and most popular opinion is that the Nigerian Pan African terrain is the result of tectonic processes involving continental collision between West African craton and the Pan African mobile belt (Burke and Dewey, 1972; Black, *et al*., 1979; Bertrand and Caby, 1978; Caby, *et al*., 1981; Trumpette, 1979). The resultant heat, deformation and partial melting of the upper mantle and lower crust led to the emplacement of the granites. This interpretation is based on the observation of a suture along the eastern margin of the West African Craton. The second opinion suggests that the Pan African Orogeny was more of aggregation of crustal blocks such as island arcs and older continental fragments than a simple collision between two entities (the West African Craton and the Pan African) (Wright and Ogezi, 1977; McCurry and Wright, 1977; Holt, *et al*., 1978). The interpretation is based on the close association of calc-alkaline volcanics, ultramafic and basic rocks with the two major NE – SW trending fracture systems established in the western part of Nigeria. Even though the former opinion has been widely accepted, some workers (Black, 1980 and Turner, 1983) have observed that the Pan African granites which extend to Nigeria and Cameroun, a distance of over 1500 km from the suture cannot be related to the same subduction zone. The Pan African event (600±150 Ma) was the latest reactivation that affect the whole region (Turner,

1983; Fitches, *et al*., 1985) and it caused regional metamorphism and deformation which imposed a generally N – S foliation trend and brought about the emplacement of granitoids.

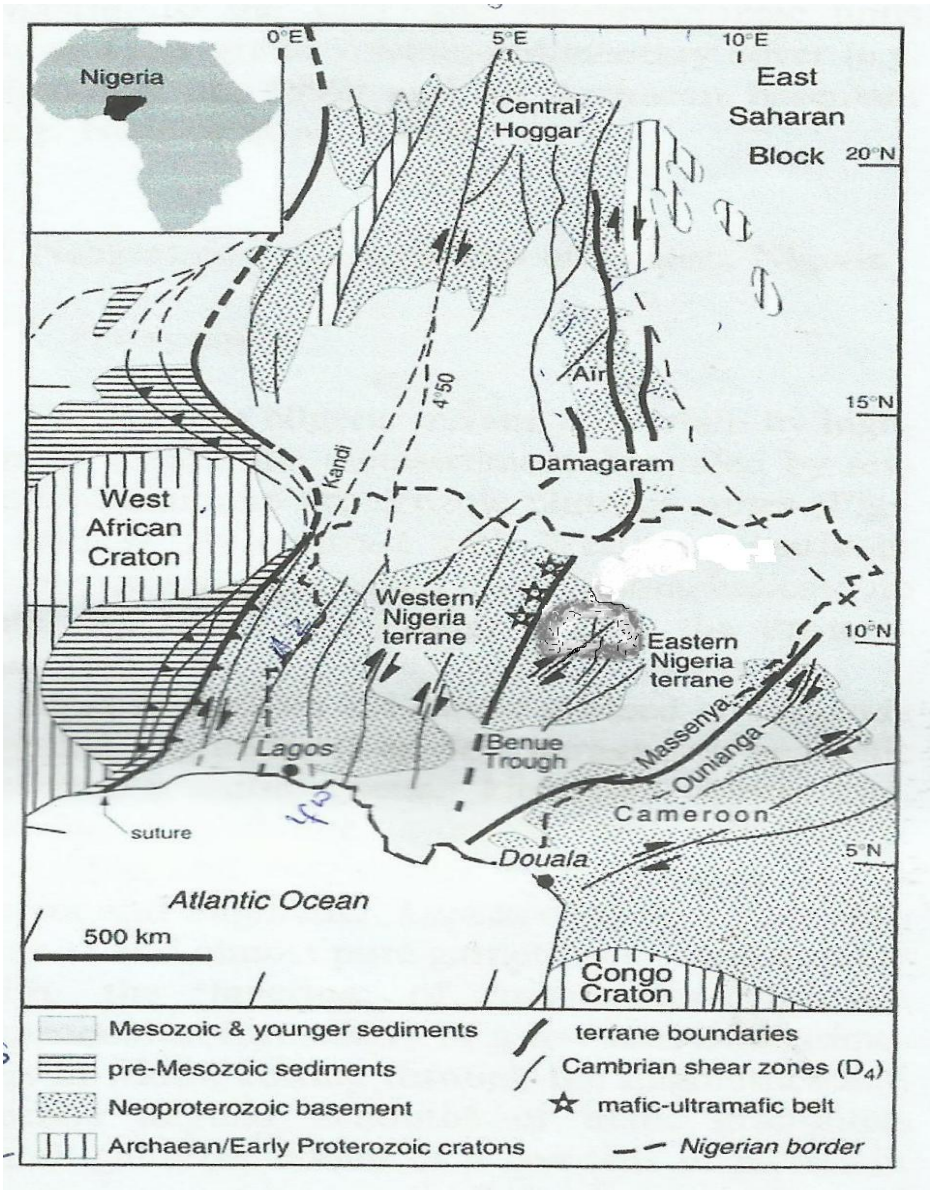


Fig 5: Geological setting of the Pan-African Belt of Nigeria in West Africa (modified after Caby 1989; Ajibade and Wright 1989; Affaton *et al*. 1991). Jurassic alkaline granites omitted. Inset:Southern Hoggar terranes (Liegeois *et al.* 1994).

The basement is usually sub-divided into three distinctive lithological units;

I. A migmatite – gneiss complex which constitute about 70% of the basement complex (Truswell and Cope, 1963; McCurry, 1976; Black, 1980) is a polymetamorphic complex

consisting of gneiss and migmatite with high grade supracrustal relics of basic and calcareous schists, marble and quartzites termed "Older metasediments" (McCurry, 1976). This unit is generally of lower amphibolites facie grade of metamorphism (Ogezi, 1977).

II. Schist belts consisting of low grade (supracrustal) metasediments and metavolcanics and are largely to the western half of the country although some relics of the schist bodies have been mapped around Jalingo to the northeast (Agunmanu, 1975) and on the Obudu plateau in the southeast (Okeke, 1979). These schist belts consist predominantly of pelites and semi-pelites with psammites, banded iron formation, metaconglomerate, metagreywackes and metavolcanics termed "Younger metasediments" and is generally of greenschist facie grade of metamorphism.

III. Older (Pan African) granites; this suite intrudes both gneiss and metasediments as swarms of plutons and batholiths covering a wide spectrum of rock types from tonalites through granite to diorite, syenite and charnockites. Age determinations indicate that they are Pan African bodies with ages ranging from 750 – 550Ma. The most predominant are the granodiorites. This rocks range in size from small subcircular crosscutting stocks to large elongated concordant batholiths bodies (Salau, 2000).

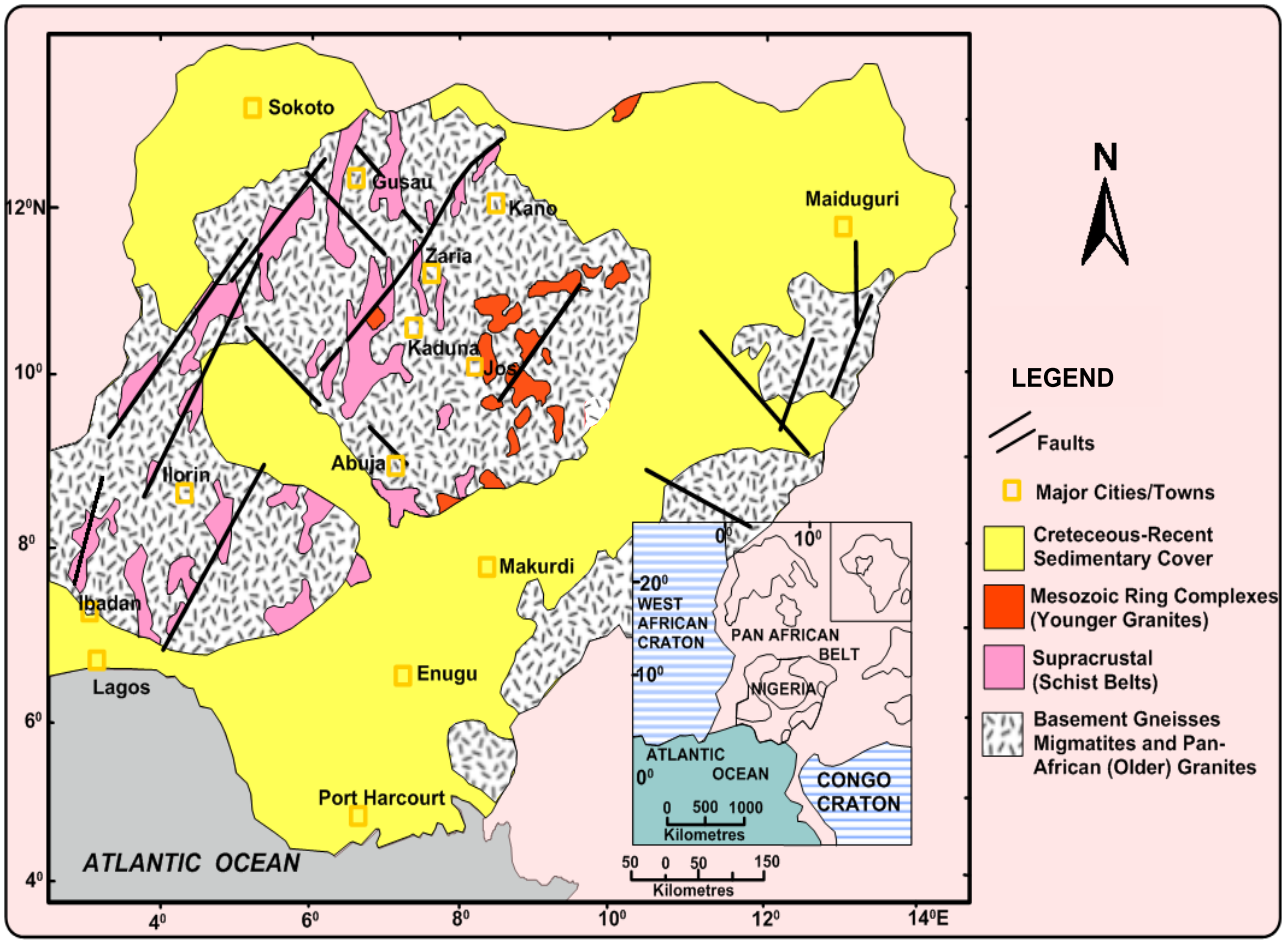


Fig 6: Geologic map of Nigeria showing basement and sedimentary terrains (Modified After Garba, 2003)

2.1.2 Hydrogeology

The water resources of Nigeria can be subdivided into surface sources (streams and rivers, lakes and ponds) and underground sources (groundwater). Groundwater exists in aquifers within the sedimentary terrain and also overburden and fractured aquifer within the basement terrain.

The Nigeria drainage system is dominated by the Rivers Niger and Benue which carry much of the run-off water from various catchments into the Atlantic Ocean in the south. Similarly, Lake Chad provides the emptying ground for a few rivers flowing northeastwards towards it, in the northern part of the country. The country is endowed by a closely knit networked river, and streams (Offodile, 2014). The system can therefore be divided into three groups, the bigger

group flowing into the Atlantic Ocean through the rivers Niger and Benue, the smaller and shorter rivers, nearer the coastline, flowing directly into the ocean, and the slightly longer ones emptying into Lake Chad, to the north. The drainage pattern is controlled by chains of mountains and hills marking the north central areas dominated by the Jos plateau, the south – western plateau, the Udi-Idah and the Cameroon ranges (including the Adamawa Massif) to the east (Offodile, 2014). The River Benue which reportedly contributes upto 50% of the water of River Niger, rises from the Cameroon mountains in the northeast, about 40 km north of Yola (Offodile, 2014).

2.2 REVIEW OF PREVIOUS WORK ON RADON

The increasing awareness on the negative effect of radon gas and its daughter progenies led to wide study of indoor radon as well as groundwater concentrations globally.

Alabdula'aly, (2014) studied the occurrence of radon in groundwater of Saudi Arabia where samples were collected from about 1025 wells supplying drinking water to the 13 regions of Saudi Arabia and analyzed for radon concentrations using the Liquid Scintillation counting method specified by USEPA, (1978). The report showed that the weighted radon median value for the entire country was 4.62 BqL^{-1} with a range of 0.01 to 67.4 BqL^{-1}. The percentage of samples with radon concentration equal to or greater than 11.1 BqL^{-1} (USEPA proposed MCL) was found to be 19.22%. It also reported that the range of radon in shallow wells varied between 0.06 and 67.4 BqL^{-1} with median value 5.1 BqL^{-1} and between 0.06 and 40.9 BqL^{-1} with median value 5.34 BqL^{-1} for deep wells. However, 50% of the samples analyzed had radon concentrations equal to or greater than 4.0 and 2.87 BqL^{-1} for the shallow and deep wells, respectively.

Jalili-Majareshin, *et al*., (2012), with the aid of RAD7 radon detector, studied the radon concentration in hot springs of the touristic city of Sarein in northwest Iran and methods to

reduce radon in water. The aim was to measure the efficiency of various simple methods to decrease the concentration of radon in the hot springs of the touristic city of Sarein. The concentration in water was observed to vary from 212 Bqm^{-3} to 3890 Bqm^{-3}. Using 250 mL vials half-filled with water samples, the report showed that when the temperature of the water increased from 17°C to 27°C, the radon concentration decreased from 3230 Bqm^{-3} to 745 Bq^{-3}. Also, the mixing of sample at a speed of 500 rpm for 12 mins led to a radon reduction of about 70%. Aeration of the water sample with 0.2 $Lmin^{-1}$ of ambient air resulted in a 90% decrease in radon concentration in 6 minutes. The report shows a strong exponential correlations (>95%), which verified the effectiveness of the methods employed in reducing dissolved radon gas in the waters.

Likewise, Kozlowska, *et al*., (2001) used a Wallac 1414 WinSpectral α/β Liquid Scintillation Counter method to determine ^{222}Rn in Radon-enriched spring water in the south of Poland. Samples were collected from springs in health resorts in the Sudety Mountains in Poland. The report showed that half of the studied water samples were radon enriched with an activity concentration higher than 74 BqL^{-1}. It concluded that the method introduced is very convenient and elegant for radon activity measurements.

Komal, *et al*., (2010) also used the electronic radon meter (RAD7) to measure radon concentration in groundwater and assessment of average annual dose in the environs of National Institute of Technology, Jalandhav (NITJ), Punjab, India. In the assessment of indoor radon, the LR–115 Type II plastic track detector was used. The report shows that the radon concentrations in drinking water vary from 2560 to 7750 Bqm^{-3} with an average value of 5143.33 Bqm^{-3} while pH value for the groundwater varies from 6.96 to 7.0 with an average value of 6.99. Their report showed that there is no correlation between the pH value and radon concentration values for the groundwater. The calculated indoor radon concentration values vary from 74 to 190 Bqm^{-3} with

an average value of 124.50 Bqm^{-3}. The report also shows that the calculated values for the absorbed dose ranged from 1.2 – 3.24 $mSv.y^{-1}$, which is well below the action level.

Ghokhale and Leung, (2010) studied the groundwater ^{222}Rn concentrations in Antelope creek, Idaho, USA. Groundwater samples were collected from eight wells in remote Antelope creek valley, Idaho. Seven out of eight locations showed that groundwater ^{222}Rn concentration were much greater than 11 BqL^{-1} (300 pCi/L), a maximum contaminant level (MCL) proposed by United States Environmental Protection Agency (USEPA). Rock and soil samples collected near the sampling wells revealed that ^{238}U contents were between 0.55 to 6.41 ppm. Minerals collected from different regions of the country with similar ^{238}U contents also showed high concentrations. Technique using Geographical Information System (GIS) software with available information also indicated a clear correlation between the rock types and ^{222}Rn concentrations in groundwater. Cancer rates near the study area were also reported to be higher than national average.

Greeman and Rose, (1995) measured emanation coefficients for ^{222}Rn and ^{220}Rn in 68 soil samples from 12 soil profiles from eastern U.S. These soils varied in soil type, parent material and location. Average emanation coefficients were 0.20 for ^{222}Rn and 0.16 for ^{220}Rn. Based on distribution of ^{226}Ra among the exchangeable, organic, Fe-oxide, sand, silt and clay fractions of the soils, a multiple regression indicated that the organic-exchangeable fraction, occurring mainly as coatings on grains, had an emanation coefficient for ^{222}Rn of 0.46, and the residual silt-clay fraction had 0.22. The organic fraction made the largest single contribution to Rn in soil gas. Mineral grains had twice the ^{222}Rn emanation as ^{220}Rn, implying that about half of the Rn atoms were emanated directly to the pore space, and the remainders were freed by track-etching and diffusion over a period of days.

LeDruillennec, *et al*., (2010) studied the hydrogeological and geochemical control of the variations of ^{222}Rn concentrations in a hard rock aquifer. This was aimed at showing an insight into the possible role of fracture – matrix exchange. To achieve this, a field study was carried out of a fractured aquifer in granite and the method was based on the insitu measurement of Rn in groundwater, aquifer tests for the determination of hydraulic characteristics of the aquifer and laboratory measurement of Rn exhalation rate from rocks. A simple crack model that simulates the Rn concentration in waters circulating in a fracture intersecting a borehole was also tested.

Similarly, Kumar, *et al*., (2003) studied the natural radioactivity and radon exhalation studies of rock samples from Surda Copper deposits in Singhbhum Shear zone. The report indicated that the wide spread uranium mineralization is associated with copper, nickel and other Sulphides in the Singhbhum Shear zone developed at the northern margin of the Singhbhum craton in the state of Jharkhand, India. CAN technique using LR–115 type II plastic track detector was used for the measurements. Uranium, thorium and potassium concentrations have been measured through low level gamma ray spectroscopy, which shows that uranium concentration (activity) was found to vary from 135.8 to 4607.8 Bq/kg whereas exhalation rate lies in the range 0.26 to 1.15 $Bqm^{-2}h^{-1}$. According to the report, a positive correlation has been found between uranium concentration and radon exhalation rates.

A couple of studies have also been carried-out by different scholars around Africa. Andam and Badoe, (2007) measured radon gas concentration in two deep gold mines in Ghana; Tarkwa Goldfields and Prestea Goldfields were reported. Radon concentrations measured underground at Tarkwa were in the range of 56 Bq/m^3 to 268 Bq/m^3. Corresponding values for Prestea were 43 Bq/m^3 to 878 Bq/m^3. These results represent the first published data on underground radon concentration in deep gold mines in Ghana. Measurement of the radon gas was done by means of

the solid state nuclear track technique, with CR – 39 plastic recording medium for the alpha particles from radon decay.

Garba, (2008) studied the natural radioactivity of groundwater of the Precambrian crystalline basement rocks around Zaria, north central, Nigeria and the results were correlated with the geology. About 180 groundwater samples were collected from different locations within the study area for gross alpha and gross beta ^{226}Ra and ^{228}Ra measurements as well as for ^{222}Rn using a gross alpha, gross beta and a liquid scintillation counter. 222Rn concentration in the groundwater ranges from 5.01 to 0.06 Bq/l. The values of 5.01, 4.28 and 2.77 Bq/l are from samples collected from boreholes. Open-well samples have values between 2.95 Bq/l to 0.06 Bq/l.

Arabi, *et al*., (2013) studied eighteen groundwater samples collected from wells in villages around Zona, an area reported to host uranium mineralization within Peta Gulf syncline, Northeast Nigeria. These were analyzed for mass/activity concentration of ^{226}Ra, ^{228}Ra and ^{232}Th. The results obtained were compared for compliance with international guidelines for radionuclides in drinking water. The results showed that activity concentration of ^{226}Ra, ^{228}Ra and mass concentration of ^{232}Th ranged from 0.05 to 6.7pCi/L, 0.2 to 4.8pCi/L and 0.02 to 1.10µg/L, respectively. In conclusion, the report indicated that all radionuclides analyzed fall within international guideline despite occurrence of uranium mineralization in the study area. The test method is based on the utilization of solid phase extraction of radium from water samples. The detection of the ^{226}Ra is by alpha spectrometry and ^{228}Ra via ^{228}Ac by gas flow proportional beta counter.

Garba, (2013) studied groundwater (well and borehole) samples from various locations of Zaria and environs including Sabongari, Tudunwada, Danmagaji, Samaru and Bomo for their ^{222}Rn concentrations using the liquid scintillation counter. The concentration of ^{222}Rn in open well

water was found to vary in the ranged from 0.77 to 28.37 Bq/l and 2.32 to 48.80 Bq/l for borehole, with a geometric mean of 12.43 and 11.16 Bq/l for borehole and well sources respectively. The results showed that ^{222}Rn concentration in borehole sources were both greater than the maximum concentration limit (MCL) of 11.1 Bq/l set by USEPA.

Nwankwo, (2013), in a report titled "Determination of Natural Radioactivity in Groundwater in Tanke-Ilorin, Nigeria", analyzed ten water samples by γ-ray spectroscopy to determine the ^{226}Ra and ^{228}Ra concentrations. The activity concentration values range from 0.81 ± 0.08 to 7.4 ± 2.2 Bq/l for ^{226}Ra and from 1.8 ± 0.3 to 5.6 ± 2.6 Bq/l for ^{228}Ra. The derived Annual Effective Dose received by the population as a result of the ingestion of ^{226}Ra was estimated to range from 0.08 ± 0.01 to 0.12 ± 0.07 mSv/yr, with an average of 0.39 ± 0.11 mSv/yr and ^{228}Ra range from 0.50 ± 0.32 to 1.42 ± 0.70 mSv/yr, with an average of 0.91 ± 0.31 mSv/yr. According to the report, the mean contribution of both ^{226}Ra and ^{228}Ra activities to the committed effective dose from a year of consumption of drinking water in the study area is higher than the tolerable level of 1 mSv/yr to the general public for prolonged exposure as recommended by ICPR, and much more than the new WHO recommended level of 0.1 mSv/yr for drinking water.

Arabi, *et al*., (2014) investigated the physico-chemical parameters of groundwater from areas of high radiometric anomalies in parts of northeastern Nigeria, together with radon and thoron gas to evaluate their implications on the worth of groundwater from the area for consumption. The study identified five water types (Mg-Ca-Na-HCO_3, Mg-Ca-Cl), with percentage distribution of 45.7%, 22.8%, 14.28%, 14.28% and 2.85% respectively. Radon concentration (Bq/m^3) ranges between 731 ± 4.9 to 84300 ± 530 with equivalent airborne radon contribution of 2.71 to 311.91 Bq/m^3, effective dose between 0.13 to 15.60 mSv/yr and a working level (WL) range of 0.09 to 4.39. Radon and thoron exhalation from aquifer materials in the area ranged between 62.5 ± 4 to 150 ± 10 Bq/m^3 and 12 ± 4 to 1250 ± 38 Bq/m^3, respectively. Based on the findings, it concluded

that water types and radon isotopes distribution were closely related to the groundwater flow pattern of the area and also, that most of the water samples (68.75%) will contribute to airborne radon that will translate to a dose >1 mSv/yr standard set for the public. The "HACH model" portable multi parameter (conductivity, pH, TDS) measurement device was used to determine the physico-chemical parameters, whereas, the RAD-H_2O method was to determine radon concentrations in groundwater.

Oni, *et al*., (2014), collected a total of 112 samples of groundwater in areas of elevated background radiation level in some cities and towns in southwestern Nigeria and was assayed for ^{222}Rn concentration. The measurement was carried-out using RAD7 (Durridge Company Inc., USA). The result revealed a steady trend of variation in the concentration of ^{222}Rn in water samples from different sources. Highest concentration was found in water from borehole sources. The concentration of radon in all the water samples were found to be above the maximum contaminant level (MCL) presented by the Standard Organization of Nigeria (SON). The ^{222}Rn concentrations from all the water from borehole sources were found to be higher than 11.1 Bq/l stated by USEPA. The report recommended consideration of possible remedial actions in the areas where 2.8% of the samples analysed had a concentration above 100 Bq/l, a MCL recommended by European Union for measurement that warrant possible remedial actions.

Chapter Three

MATERIALS AND METHODS;

3.1 INTRODUCTION

The study was carried-out in five stages, and these are:

I. Desk studies

II. Fieldwork

III. Laboratory analysis

IV. Analysis and presentation of results

V. Thesis write-up

3.1.1 Desk Studies

This involved collecting and reviewing available relevant literatures such as textbooks, research journals, equipment manuals, research bulletins, and unpublished research thesis/reports, geological and topographic maps.

3.1.2 Fieldwork

The fieldwork was carried-out in Mika and environs, part Monkin Sheet 216 and Dong Sheet 195 (Zing and Yorro local government areas), Taraba State. It was conducted between December, 2014 and February, 2015 (dry season period). The fieldwork involves field observations, water sampling, water level measurements, as well as rock sampling.

3.1.2.1 Field Observations

Variations in the rocks of the area with respect to texture and colour was taken note of, and also deformational structures observed were also captured on still photographs using a camera.

3.1.2.2 Water Sampling/ In-situ Measurements

Groundwater samples were collected from 15 boreholes equipped with hand pumps and 2 hand-dug wells. The sampling was carried-out based on sample availability and effort to ensure uniform spread, so that results may be a fair representation of the study area.

Boreholes were pumped continuously for at-least 5 minutes before sampling and the hand-dug wells chosen were in constant use. This is to ensure that "fresh" water samples were collected directly from the aquifer. Seventeen (17) groundwater samples were collected from 17 communities/settlements, in accordance with the standard procedure described in the RAD7 manual (for radon measurements) while, for physico-chemical measurements, a detailed procedure on water sampling as described in EPA, 2010 was adhered to. Sample containers (a 1 litre sampling container used) were washed with distilled water and rinsed with the sample before it was collected and sealed to ensure airtightness. Physicochemical parameters were measured in-situ using "HACH model" portable multi-parameter measurement device (Fig. 7), to measure pH, conductivity, TDS, and salinity.



Fig. 7: "HACH Model" Multi-parameter Conductivity/pH meter

3.1.2.3 Water Level measurement/Thickness of Dry Zone

Water level measurements were also carried-out in-situ to determine depth to water table and to be able to predict groundwater flow directions. These measurements were taken from a reference point above the ground. In cases where rims were used for hand-dug well completion (Plate 2), the entire height of the rim was used as a reference and later subtracted from the total well depth to get the depth of the well to ground surface which is the true depth of the well. A calibrated tape with a light metal weight attached to its end (to prevent the tape from sagging) was used to measure the rest water level. The rest water level measurements were taken from about 38 wells during the period of sampling (dry season).



Plate II: Measuring groundwater level at Madaki Open-Well

3.1.2.4 Rock Sampling

Rock samples were collected from locations in communities where there is an outcrop, to represent the aquifer material. The rock samples were collected using a geological hammer and the properly labeled sample containers were placed in a sampling bag for easy transportation to the laboratory. The rock samples were used as hand specimen for grain size description, gamma spectrometry analysis, exhalation rates measurement, emanation coefficient determination and γ-radiation dose estimations.

3.1.3 INSITU AND LABORATORY ANALYSIS

Radon in groundwater analysis was carried-out insitu (as provided by EPA, WHO and RAD7 manual) using RAD7 electronic radon detector (Fig. 9), because of the degassing tendency of radon gas, as considerable amount (if not all) will be lost if transporting the sample to the laboratory was considered. Meanwhile, radon analysis on rock samples, Radium (^{226}Ra), Thorium (^{232}Th) and Potassium (^{40}K) activity concentration in rocks, measured using gamma spectrometry technique as well as major cation and anioin analysis were all carried-out in the laboratory.

3.1.3.1 Radon in Water Analysis

The water samples were collected directly from the source into a clean 1 litre container previously rinsed with distilled water. During water sample collection, conscious effort was made to prevent bubbling of the water collected into a 250 ml vial having a septum cap (provided by Durridge Company as part of the RAD7 accessory) so as not to allow escape of dissolved radon in the water. A total of seventeen (17) groundwater samples (15 from hand-pump boreholes and 2 from hand-dug wells) were collected from the study area were assayed in-situ using RAD7, an electronic radon detector connected to a RAD-H_2O accessory. RAD7 is a well calibrated, fast and accurate radon detector. The RAD7 detector was used for measuring

radon in water by connecting it with a bubbling kit which enables it to degas radon from the water sample into the air in a closed loop. Within the closed loop is a desiccant to dry the air before entering the detector for radon concentration measurement. The detector uses alpha spectrometry technique. The RAD7 is capable of accurately measuring radon concentration in a water sample within 20 minutes. The time is very short compared with the 3.8 days half-life of radon, thereby making RAD7 superior to many other detectors for radon concentration in water measurement (Oni, *et al*., 2014). Each of the water samples was assayed for 15 minutes (making 3 runs each) and the machine was purged for 5 minutes between one and the next measurement. Purging of the machine is necessary in order to clear the system of previous radon concentration before the next sample is counted. The average concentration of ^{222}Rn was measured and recorded. The most widely supported sample sizes are 40 ml and 250 ml, as these correspond to the RAD7's built-in Wat-40 and Wat-250 protocols (Durridge RAD7 manual, 2014). Large water samples of up to 2.5L may be sampled using the big bottle RAD-H_2O kit. Radon concentration is being calculated using the provided CAPTURE software for Windows and OS X (Durridge RAD7 manual, 2014). Typical set-up of RAD7 electronic radon detector is presented in Fig. 9.



Fig 8: Alpha Spectrometer RAD7 Electronic Radon Detector



Fig 9: Typical set-up of RAD7 electronic radon detector

3.1.4 Radon Exhalation Rate measurement

Radon exhalation rate is defined as the radon activity released into the air per unit time from the mass of the matrix and is measured by enclosing the sample in a closed chamber and monitoring the buildup of radon concentration in the chamber at regular time intervals (Petropoulos, *et al*., 2001 and Chen, *et al*., 2010).

One kilogram (1kg) of each rock sample was used for this analysis. Each sample was placed in the sample chamber and radon emissions from the surface of the rock samples was counted for 24 hours, using the RAD7 electronic radon detector produced by Durridge Company. The analysis was carried-out according to the "Bulk Emissions" procedures described in the Durridge

RAD7 manual (2014). The Bulk Emission sample chamber is an airtight container with two well separated hose connectors. The two hose connectors has one as "inlet" where air from the RAD7 gets into the sample chamber, the other is the "outlet" where radon-filled air gets out of the sample chamber into the RAD7 radon detector through the radon inlet filter of the RAD7, for radon concentration counting. This measurement ensures a closed-loop operation. Fig. 10, demonstrates the processes leading to radon exhalation starting with emanation from either soil or rock materials to transportation and subsequent exhalation to the atmosphere.

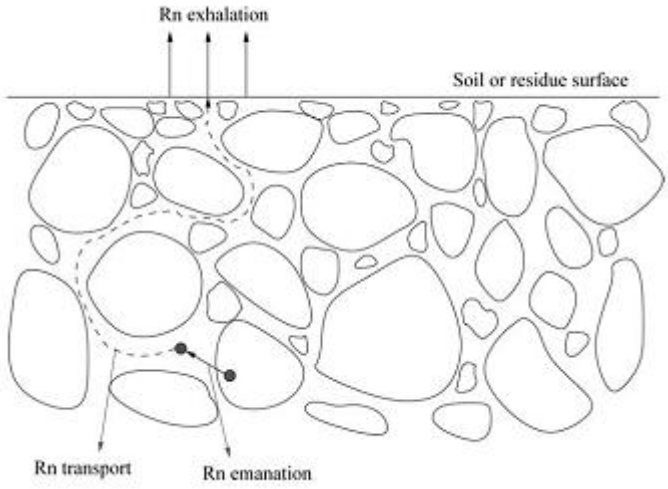


Fig 10: Schematic demonstration of Radon emanation, transport and subsequent exhalation from soil.

The exhalation rate was deduced from the formula of radon concentration C(t) at time t since the closing of the chamber builds up, as shown below;

$$E_m = \frac{CV\lambda}{M(T + \lambda^{-1}[e^{-\lambda T} - 1]}$$

Where;

E_m = is the mass exhalation rate ($Bq \cdot kg^{-1} \cdot h^{-1}$).

M = is the total dry mass of the sample (kg).

V = is the effective volume of chamber (m^3).

C = is the ^{222}Rn concentration present in the chamber volume (Bq/m^3).

λ = is the radioactive decay constant of ^{222}Rn (h^{-1}).

T = is the measurement time (h).

3.1.5 Radon Emanation Coefficient Measurement

The emanation coefficient is defined as the fraction of radon atoms generated that escape the solid phase in which they are formed and become free to migrate through the bulk medium. This term has also been referred to as the emanation fraction or the emanation power (Ishimori *et al*., 2013). The emanation coefficient can generally be evaluated by two methods; the combination of measurements of radium and radon, and gamma spectrometry under different conditions (Ishimori, *et al*., 2013). The total activity of radon released into the air from the sample material was evaluated using the RAD7 electronic radon detector, to measure radon concentration of each sample, whereas, the total activity of radium in a sample can be determined by various methods such as alpha spectrometry, gamma spectrometry, liquid scintillation spectrometry and mass spectrometry (IAEA, 2010). For the purpose of this work, the gamma spectrometry method was used.

The emanation coefficient was calculated using:

$$\mathbf{E = \frac{VC}{MR}}$$

Where;

E = the emanation coefficient

V = the effective volume of the sampling device (m^3)

C = the radon concentration (Bq/m^3)

M = the total mass of the sample (kg)

R = the radium activity concentration (Bq/kg)

3.1.6 Sample Preparation for NaI (TI) Gamma Spectrometry Measurement

Gamma spectrometry measurement was carried-out at the Centre for Energy Research and Training (CERT), Zaria – Kaduna State, Nigeria.

3.1.6.1 Rock Sample Collection

Method and instruments used in the rock sample collection was described earlier in section 3.1.

3.1.6.2 Rock Sample Preparation

Each of the rock samples collected was crushed to fine powder using a pulverizer. Packaging of the samples into radon-impermeable cylindrical plastic containers which were selected based on the space allocation of the detector vessel which measures 7.6 cm by 7.6 cm in dimension (geometry) was also carried-out. To prevent ^{222}Rn escaping, the packaging in each case was triple sealed. The sealing process included smearing of the inner rim of each container lid with Vaseline petroleum jelly, filling the lid assembly gap with candle wax to block the gaps between lid and container, and tight-sealing lid-container with masking adhesive tape. Radon and its short-lived progenies were allowed to reach secular radioactive equilibrium by storing the samples for 30 days prior to gamma spectrometry measurements.

3.1.6.3 Evaluation of Radioactivity of Samples

The analysis was carried-out using a 76x76 mm NaI (Tl) detector crystal optically coupled to a photomultiplier tube (PMT). The assembly has a preamplifier incorporated into it and a 1kilovolt external source. The detector is enclosed in a 6 cm lead shield with cadmium and copper sheets. This arrangement is aimed at minimizing the effects of background and scattered radiation.

The data acquisition software used is "Maestro" by Canberra Nuclear Products. The samples were analyzed for a period of 29000 seconds per sample. The peak area of each energy, in the spectrum was used to compute the activity concentration in each sample by the use of the following equation;

$$C\ (Bq.kg^{-1}) = \frac{Cn}{C_{fk}}$$

Where,

C = Activity concentration of the radionuclides in the sample given in $Bqkg^{-1}$

Cn = Count rate (counts per second)

C_{fk} = Calibration factor of the detecting system.

$$\text{Count per second (cps)} = \frac{\text{Net Count}}{\text{Live Time}}$$

3.1.6.4 Calibration and Efficiency Determinations

Calibration of the system for energy and efficiency were done with two calibration point sources, Cs-137 and Co-60. These were done with the amplifier gain that gives 72% energy resolution for the 66.16Kev of Cs-137 and counted for 30minutes.

3.1.6.5 Standards

The standards used to check for the calibration are the IAEA gamma spectrometric reference materials RGK-1 for K-40, RGU-1 for Ra-226 (Bi-214) and RTG-1 for Th-232 (Tl-208).

3.1.6.6 Background

The background count rate was done for 29000 seconds.

Table 1: Spectral Energy Windows used in the Analysis

Isotope	Gamma Energy (Kev)	Energy Window (Kev)
R-226	1764.0	1620 – 1820
Th-232	2614.5	2480 – 2820
K-40	1460.0	1380 – 1550

Table 2: Energy Calibration for Quantitative Spectral Analysis

Isotope	Calibration Factors		Conversion Factor($Bq.kg^{-1}$)	Detection Limit	
	10^{-3} (cps/ppm)	10^{-4} (cps/ppm)		ppm	Bq/kg
^{40}K	0.026	6.431	0.032	454.54	14.54
^{226}Ra	10.500	8.632	12.200	0.32	3.84
^{232}Th	3.612	8.768	4.120	2.27	9.08

3.1.7 Dose Rates Calculations

3.1.7.1 Radon Dose Calculation

Radon is soluble in water. Radon in water is due to the radium in the water, surrounding soil or bedrock. The concentration of radon in groundwater is usually much higher than it is in surface water (Clavensjo and Akerblom, 1994). Typical values of radon in surface water are around 40 Bqm^{-3}, while in groundwater it ranges from 4 to 1000kBqm^{-3} (UNSCEAR, 1982).

When water is used indoors, the radon in the water outgasses and become airborne (Makofske and Edelstein, 1988). Of the aggregate radiation dose received by human populations, the dominant portion is associated with inhalation of radon progeny. Table 3, shows the relative magnitude of the natural sources of radiation.

Table 3: Human Exposure to Radiation (UNSCEAR, 1988)

Component of Exposure	Annual Effective Dose (mSv)
Radon	**1.28**
Cosmic Rays	**0.38**
Cosmogenic Radionuclides	**0.01**
Terrestial Radiation: External Exposure	**0.46**
Terrestial Radiation: Internal Exposure	**0.23**
TOTAL	**2.40**

In order to estimate the annual effective dose rate received by the population, one has to take into account the conversion coefficient from the absorbed dose and the indoor occupancy factor. According to the UNSCEAR (2000) report, the committee proposed 9.0 x 10^{-6} mSv/h per Bq/m^3 to be used as a conversion factor, 0.4 for the equilibrium factor of ^{222}Rn indoors and 0.8 for the indoor occupancy factor. Occupancy factor of 0.5 was assumed and used as the time spent indoors by an average person in the study area (for the purpose of this present work). Calculating the annual effective dose to the population, the equation below was used (ICRP, 1993). At a certain radon concentration C_{Rn} in Bq/m^3, the annual absorbed dose, D_{Rn} is usually expressed in the unit of mSv from the following relation below:

$$\mathbf{D_{Rn}\ (mSv/yr) = C_{Rn}.D.H.F.T}$$

Where;

C_{Rn} = the measured Rn-222 concentration (Bq/m^3),

F = the Rn-222 equilibrium factor indoors (0.4),

T = the indoor occupancy time 24 h × 365 = 8760 h/yr

H = the indoor occupancy factor (0.5), and

D = the dose conversion factor (9×10^{-6} mSv/hr per Bq/m^3).

The annual effective doses due to the ingestion of radon (H_{ing}) in water were calculated from the mean activity concentration using the following equation;

$$\mathbf{H_{ing}\ (w) = DF_{Rn}\ x\ I_w\ x\ A_{222Rn}}$$

Where;

DF_{Rn} is the dose conversion factor by ingestion of ^{222}Rn in water by adult members of the public living in the study area, given as 10^{-8} $SvBq^{-1}$ (UNSCEAR, 1993), A_{222Rn} is the activity concentration of ^{222}Rn in water samples and I_w is the daily water consumption rate (L/a), considered to be 2 L/day (WHO, 2004).

To calculate the annual equivalent dose and effective dose, one has to apply a tissue and radiation weighting factors according to ICRP, 1991. The equivalent dose is the radiation-weighted absorbed dose. The radiation weighting (W_R) factor for alpha particles is 20 as recommended by ICRP (1991).With the effective dose, a tissue weighting (W_T) factor is applied. According to ICRP, the tissue weighting factor for lung is 0.12. The annual effective dose is then calculated according to the equation below:

$$\mathbf{H_E\ (mSv/yr) = D_{Rn}\ .W_R.W_T}$$

Where,

D_{Rn} = Annual Absorbed dose

W_R = Radiation Weighting Factor for Alpha Particles, 20

W_T = Tissue Weighting Factor for the Lung 0.12

3.1.7.2 Dose Rates due to γ Radiation

The absorbed dose rate (D) in $nGyhr^{-1}$ from ^{40}K isotope and the radionuclides from ^{226}Ra and ^{232}Th was calculated using the formula below;

$$\textbf{Dose Rate } (nGyhr^{-1}) = 0.460A_{Ra} + 0.614A_{Th} + 0.0418A_{K}$$

Where;

0.460, 0.614 and 0.0418 are the conversion factor ($nGyhr^{-1}/Bqkg^{-1}$) for ^{226}Ra, ^{232}Th and ^{40}K respectively, while A_{Ra}, A_{Th} and A_K are the radiological concentration ($Bqkg^{-1}$) for ^{226}Ra, ^{232}Th and ^{40}K respectively.

3.1.7.3 Annual Effective Dose Rate due to γ Radiation

The annual outdoor effective dose rate ($DE_{,out}$) to a member of the population within the study area was calculated from the absorbed dose rate (D), taking into account the conversion factor (CF) of the absorbed dose in air to the corresponding effective dose, and the occupancy factor (OF_{out}). This is equal to;

$$\textbf{DE}_{,out} = \textbf{D x CF x OF}_{out}$$

Where;

$DE_{,out}$ units are in $mSvyr^{-1}$, D units are in $nGyhr^{-1}$, CF = $0.7x10^{-6}$Sv/Gy (UNSCEAR, 2000), and OF = f_{out} x 24hrs x 365.25days. According to UNSCEAR (2000), humans are expected to spend 20% of their time outdoors and 80% indoors, this means that f_{out} = 0.2 and f_{in} = 0.8, for the annual outdoor and indoor effective dose rates respectively. The f_{out} and f_{in} proposed by UNSCEAR (2000) is not realistic for the settlers in the study area because they are mostly farmers, cattle/sheep rearers, hunters etc., so they spend much more time outdoors and less time indoors compared to the time proposed by UNSCEAR (2000), therefore, for this particular work, an average of 12 hours was taken (i.e. f_{out} = 0.5 which means f_{in} = 0.5) to estimate annual outdoor effective dose rates, assuming that 50% of their time is spent outdoors and 50% is spent indoors.

3.1.7.4 Radium equivalent (Ra_{eq}) Determination

Assessment of radiological hazards was made by calculating the radium equivalent activities index. The radium equivalent activity (Ra_{eq}) is a weighted sum of activities of the ^{226}Ra, ^{232}Th and ^{40}K based on the assumption that 370 Bq/kg of Ra, 259 Bq/kg of Th and 4810 Bq/kg of K produce the same gamma-ray dose rates (UNSCEAR, 2000) as given by the following equation;

$$\mathbf{Ra_{eq} = A_{Ra} + 1.43A_{Th} + 0.077A_K}$$

Where;

A_{Ra}, A_{Th}, and A_K are the activity concentration (in Bq/kg) of ^{226}Ra, ^{232}Th and ^{40}K, respectively.

3.1.7.5 External Hazard Index (H_{ex})

The model of the external hazard index (H_{ex}) places an upper limit to the external gamma radiation dose from materials to unity, which corresponds to a radium equivalent activity of 370 Bq/kg. It is defined;

$$\mathbf{H_{ex} = \frac{A_{Ra}}{370\ (Bqkg^{-1})} + \frac{A_{Th}}{259\ (Bqkg^{-1})} + \frac{A_K}{4810\ (Bqkg^{-1})} \leq 1}$$

Where;

A_{Ra}, A_{Th} and A_K are the mean activity concentrations of ^{226}Ra, ^{232}Th and ^{40}K in Bq/kg, respectively. The value of this index should be less than unity to keep the radiation hazard negligible (Berekta and Mathew, 1985).

3.1.8 Cations and Anions in Groundwater Analysis

Seventeen (17) groundwater samples were collected (15 borehole samples and 2 open-well samples) for major cations and anions analysis. pH, Total Dissolved Solid (TDS), Conductivity and Salinity values of the groundwater samples were all determined insitu using a pH and a

conductivity meter. Three methods of water analysis were used for major cations and anions determination. These methods include the use of Atomic Absorption Spectrometry (AAS), Flame Photometry and Titrimetric methods. The AAS was carried-out at the Multi-User Laboratory, Ahmadu Bello University, Zaria while, the Flame photometry and Titration was carried-out at the Department of Agriculture and Extension Laboratory, Ahmadu Bello University, Zaria.

3.1.8.1 Methodology And Procedures for Analysis

3.1.8.1.1 Atomic Absorption Spectrometry; Determination of Ca^{2+} and Mg^{2+}:

Quantitative estimation of Calcium (Ca) and Magnesium (Mg) were done by Atomic Absorption Spectrophotometer (Varian AA240FS fast Sequential AAS) (Fig.11) using different cathode lamps with air acetylene flame method. 100 ml of a well mixed acid preserved water sample was transferred into a beaker and 5 ml of concentrated nitric acid (HNO_3) was added to the mixture. The beaker was placed on a heater and allowed to evaporate to about 5 ml without boiling. This process took about 30 minutes, diluted to 100 ml in a volumetric flask and was ready for analysis. The two elements of interest (Ca and Mg) were assayed using the Varian AA240FS AAS method.

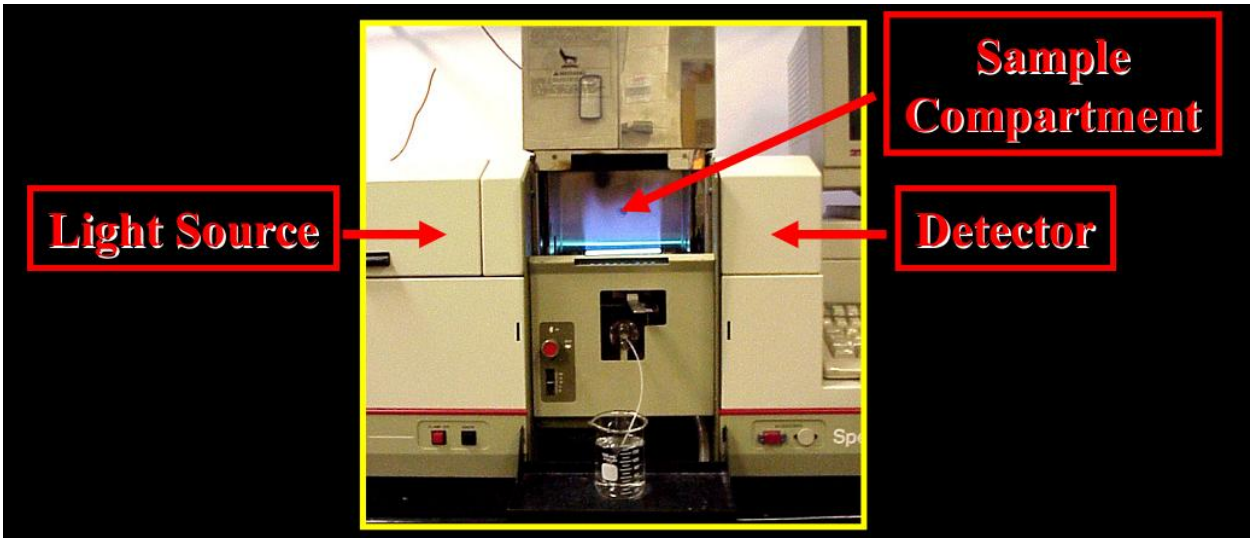


Fig 11 : A Varian AA240FS Atomic Absorbtion Spectrometer.

3.1.8.1.2 Flame photometry; Determination of Na^+ and K^+ Ions:

The concentrations of sodium and potassium ions in the water samples were determined using a flame photometric method (flame photometer model PFP 7, Jennywater product). Each of the water sample is passed into the flame photometer through the aspirator tube of the flame photometer and the concentration of the ions is then read when it has attain its highest peak and the peak is finally interpreted and recorded in milligram per litre (mg/l).

3.1.8.1.3 Titrimetric Method:

There are two (2) major phases involved in the analysis of the water samples;

PHASE I: Sedimented water samples (i.e. Water samples with sediment or water sample that is dirty or water sample that is muddy in nature). When analyzing such water sample, concentrated nitric acid (HNO_3) was added to the water sample in order to break up the bonds in the sediment. This is because some of the cations and anions to be determined are present in the particles of the sediments. The nitric acid would at the end make the sedimented water to become clearer water after dissolving the sedimented particles in the water samples.

PHASE II: Unsedimented water samples (i.e. clean water sample without sediment). In this case, the water does not require the procedure of adding nitric acid. Therefore, all the parameters to be determined were carried-out directly with the raw water sample, using the necessary assigned method and procedures.

Determination of Chloride (Cl^-) Ions

Methodology: Silver Nitrate Titrimetric Method.

Reagents: Silver Nitrate solution ($AgNO_3$) 0.01N and Potassium chromate indicator.

Procedure: 20mls of each water sample was measured into a 100 ml conical flask and immediately, 3 to 4 drops of potassium chromate indicator was then added, and swirled properly for a uniform mixture. It was then finally titrated with 0.01N $AgNO_3$ solution in order to obtain the titre value.

Calculations: The actual concentration of the ions in milligram per litre (mg/l) was then calculated using the formula below;

$$Cl^- \text{ (mg/l)} = \frac{10^3 \text{ x N x (ml of } AgNO_3 - B) \text{ x Df}}{A} = \frac{10^3 \text{ x N x (T} - B) \text{ x Df}}{A}$$

Where, N = Normality of $AgNO_3$ used (0.01N)

B = Blank or Control Reading

ml of $AgNO_3$ = Titre Value

Df = Dilution factor

A = Aliquote taken (Volume of water sample used)

Determination of Carbonate (CO_3^{2-}) and Bicarbonate (HCO_3^-):

Methodology: Sulphuric Acid (H_2SO_4) 0.02N method

Reagents: Concentrated Sulphuric Acid (H_2SO_4), Phenolphthalein indicator and Methyl-orange indicator.

Procedure: 20 ml to 30 ml of the water sample was measured into a 100 ml conical flask.

Test for Carbonate (CO_3^{2-}): Add few drops of the phenolphthalein indicator into the cornical flask containing each of the water samples and observe for the

presence of a pink colouration, which signifies that CO_3^- is present in the water sample. Finally, titrate to clear the pinkish colouration with 0.02N H_2SO_4, the solution turns colourless and the titre value, recorded. The actual concentration of the carbonate was determined by calculation using the formula below;

$$CO_3^{2-} \text{ (mg/l)} = \frac{10^3 \text{ x N x (ml of } H_2SO_4 - B) \text{ x Df}}{A} = \frac{10^3 \text{ x N x (T} - B) \text{ x Df}}{A}$$

Where; N = Normality of H_2SO_4 (0.02N)

B = Blank or Control Reading

Df = Dilution factor

A = Aliquote taken (Volume of water sample used)

ml of H_2SO_4 = Titre value

Test for Bicarbonate (HCO_3^-): Measure 20ml to 30ml of the water samples into a 100ml cornical flask and immediately add 3 to 4 drops of methyl orange indicator and swirl for uniform mixture. Finally, titrate with 0.02N H_2SO_4 and obtain the titre value. The actual concentration of HCO_3^- is calculated using the same formular used for carbonate determination.

Determination of Sulphate (SO_4^{2-}):

Methodology: Turbidimetric Method (Gelatine and $Bacl_2$ Extraction method)

Procedure: 10 ml of the water sample was pipetted into a 25 ml cornical flask and 1 ml of the gelatin/$Bacl_2$ solution was added to the water sample and diluted to 25 ml with distilled water and was allowed to stand for about 15 – 30 minutes. The concentration of sulphate (SO_4^{2-}) was determined calorimetrically, using a calorimeter at 430 nm.

Calculation: The concentration of SO_4^{2-} was calculated using the formula below;

$$SO_4^{2-} \text{ (ml/l)} = Df \times G \times Abs$$

Where; Df = Dilution factor = $\frac{\text{Volume of distilled water}}{\text{Aliquot}}$

G = Gradient = 66.67 (Constant factor from SO_4 standard)

Abs = Colorimeter Reading

Therefore;

$$SO_4^{2-} \text{ (mg/l)} = \frac{\text{Volume of Distilled water} \times Df \times G \times Abs}{\text{Aliquot (Volume of water sample)}}$$

3.2 Sodium Absorption Ratio (SAR) Determination

The concentrations of some constituents that contribute to the specific conductance of groundwater also determine the suitability of water for irrigation. In particular, large concentrations of sodium can have a negative effect on soils by causing dispersion and swelling. Soil dispersion can harden the soil and decrease infiltration rates at the surface and reduce the hydraulic conductivity of the soil (Hanson *et. al*., 1993). The ratio of sodium ions to calcium and magnesium ions can be used to predict the degree to which irrigation water tends to enter into the cation-exchange reactions in soil (U.S. Salinity Laboratory Staff, 1954). This ratio, called the sodium-adsorption ratio (SAR), is used to determine the sodium hazard for irrigation waters. As the SAR increases, the sodium hazard increases; therefore, the suitability of water for irrigation decreases. SAR can be determined by the following formula;

$$\mathbf{SAR} = \frac{\mathbf{Na}}{\sqrt{\frac{\mathbf{(Ca + Mg)}}{\mathbf{2}}}}$$

Richard (1954) classified SAR values as 0 to 10 (Excellent), 10 to 18 (Good), 18 to 26 (Fair) and > 26 (Poor). All the water samples collected from the study area can be said to be of excellent quality for irrigation, based on the calculated SAR values.

3.3 Percent Sodium (%Na) Determination

Irrigation water containing large amounts of sodium is of special concern due to sodium's effects on the soil and poses a sodium hazard. Excess sodium in waters produces the undesirable effects of changing soil properties and reducing soil permeability. Hence, the assessment of sodium concentration is necessary while considering the suitability for irrigation. Sodium content is generally expressed in terms of percent sodium or soluble sodium percentage and is given by the formula below;

$$\text{Na \%} = \frac{\text{Na}}{(\text{Ca} + \text{Mg} + \text{Na} + \text{K})} \times 100$$

Where; the quantities of all cations are expressed in milliequivalents per litre (Meq/l). The classification of groundwater was grouped based on percent Sodium as Excellent (<20 %), Good (20 to 40 %), Permissible (40 to 60%), Doubtful (60 to 80%) and Unsuitable (> 80%) (Wilcox, 1955).

3.4 Soil Permeability Index (PI) Determination

The soil permeability is affected by long term use of irrigation water. Sodium, calcium, magnesium and bicarbonate content of the soil influence it. Doneen (1964) evolved a criterion for assessing the suitability of water for irrigation based on the permeability index. Accordingly, waters can be classified under Class I, Class II and Class III orders. Class I and Class II waters are categorized as good for irrigation with 75% or more maximum permeability. Class III water are unsuitable with 25% of maximum permeability. The value of PI can be calculated as follows;

$$\text{PI} = \frac{\text{Na} + (\text{HCO}_3)^{½}}{\text{Ca} + \text{Mg} + \text{Na}} \times 100$$

3.5 Chloro Alkaline Index (CAI) Determination

Changes in chemical composition of groundwater along its flow path can be understood by studying the Chloro-Alkaline Indices (CAI). Schoeller (1967) has evolved a formula, Chloro

alkaline indices (CAI) to know the ion exchange between the ground water and its surroundings during residence or travelling in the aquifer. The CAI can be measured as;

$$\mathbf{CAI = \frac{[Cl^- - (Na^+ + K^+)]}{Cl^-}}$$

Where, all ionic concentrations are expressed in terms of meq/l. The negative value of CAI indicates that there is exchange between sodium and potassium ($Na^+ + K^+$) in water with calcium and magnesium ($Ca^{+2} + Mg^{+2}$) in the rocks by a type of base-exchange reactions. The positive value of CAI represents the absence of base-exchange reactions and existence of cation-anion exchange type of reactions (Raju, 2007).

Chapter Four

RESULTS

4.1 LITHOLOGICAL MAPPING

From the rock samples collected and field observations carried-out during fieldwork, a lithological map of the study area was produced (Fig 12). The medium-grained granite (Plate 4) dominated the study area. Pink coloured variety of medium-grained granite as described by Funtua, (1992) was noticed around the north-western part of the area while the greyish coloured medium-grained granite dominated the south and southwestern parts of the area. The Coarse-grained granites (Plate 3) represented by porphyritic granites dominated parts of the north and northeastern as well as the southeastern part of the study area. Extensively sheared zone was observed and the trending direction was noticed to be along the NE – SW.



Plate III: Part of the shear zone that cuts through the porphyritic granite, within the northeastern part of the study area.

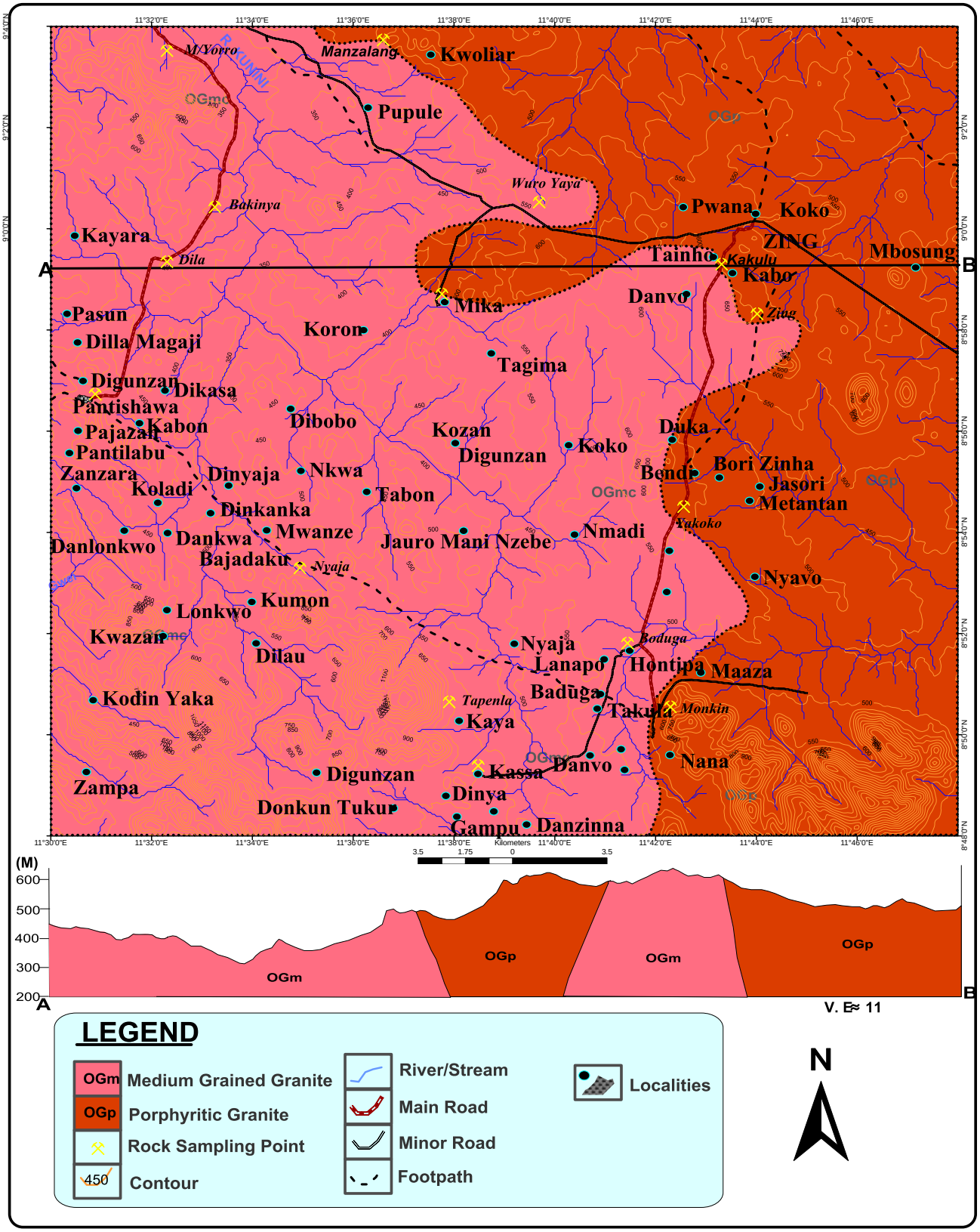


Fig 12: Lithological Map of the Study Area



Plate IV: Medium-Grained Granite section of the shear zone, within the southwestern part of the study area.

4.2 GROUNDWATER CONFIGURATION

Topographic map of the study area was used to produce the groundwater configuration map while the thickness of dry zone was measured in-situ. The groundwater flow direction map is presented in Fig. 13 and the thickness of the dry zones as measured with a calibrated tape is presented in Appendix 1.

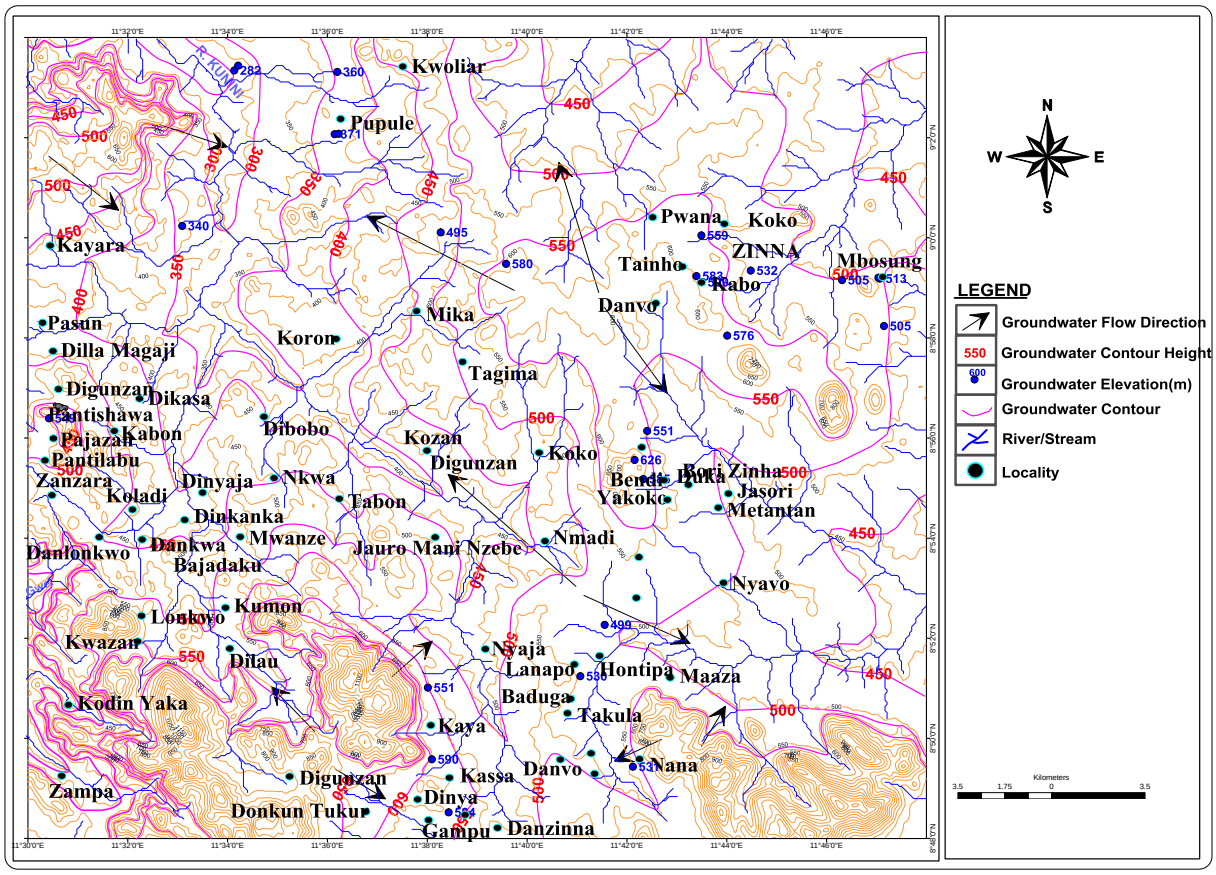


Fig 13: Groundwater flow direction map of the study area.

4.3 RADON IN GROUNDWATER

A total of seventeen (17) groundwater samples were analyzed for radon gas concentration, 15 of which were sampled from hand-pump boreholes while 2 of the samples were from hand-dug wells. Radon contour map of the area, radon contour map super-imposed on the texture-based Lithologic map of the area and radium distribution contour map super-imposed on the radon concentration contour map is presented as figures 14, 15 and 16, respectively. The results obtained from analysis using the RAD7 Electronic Radon detector is presented in Table 4 below;

Table 4: Measured Radon and Thoron Concentrations, Calculated Radon Annual Absorbed Dose, Annual Effective Dose and Annual effective dose due Ingestion by Drinking.

S/N	Sample ID	Coordinates	Location Name	^{222}Rn (Bq/m^3)	^{220}Rn (Bq/m^3)	Annual Absorbed Dose (DRn) ($mSvyr^{-1}$)	Annual Effective Dose (H_E) ($mSvyr^{-1}$)	$H_{ing}(w)$ ($mSvyr^{-1}$)	Well Type
1	GW01ZN	08º59.353'N 11º44.905'E	ZING	18,200 ± 900	142 ± 110	286.98	688.71	0.36	Borehole
2	GW02AB	08º55.947'N 11º42.596'E	ABUJA	30,100 ± 1100	201 ± 130	474.62	1139.09	0.60	Borehole
3	GW03MN	08º50.652'N 11º41.939'E	MONKIN	6,740 ± 520	114 ± 100	106.28	255.07	0.14	Borehole
4	GW04KK	08º59.028'N 11º43.165'E	KAKULU	3,540 ± 370	109 ± 90	55.82	133.97	0.07	Borehole
5	GW05KI	08º59.805'N 11º39.963'E	KAN-IYAKA	2,350 ± 300	65.3 ± 70	37.06	88.94	0.05	Open Well
6	GW06MK	08º58.718'N 11º37.653'E	MIKA	7,580 ± 550	66.9 ± 70	119.52	286.85	0.15	Borehole
7	GW07WY	09º00.511'N 11º39.588'E	WURO-YAYA	31,700 ± 1100	76.3 ± 80	499.85	1199.64	0.63	Borehole
8	GW08MZ	09º03.695'N 11º36.293'E	MANZALANG	39,900 ± 1200	109 ± 90	629.14	1509.94	0.80	Borehole
9	GW09KJ	09º03.558'N 11º34.238'E	KWOJI	44,300 ± 1300	193 ± 120	698.52	1676.45	0.89	Borehole
10	GW10MY	09º04.113'N 11º31.826'E	MARARABAN YORRO	42,600 ± 1300	450 ± 190	671.72	1612.13	0.85	Borehole
11	GW11BK	09º00.477'N 11º33.166'E	BAKINYA	34,100 ± 1200	382 ± 170	537.69	1290.46	0.68	Borehole
12	GW12DL	08º59.500'N 11º32.417'E	DILA	38,200 ± 1200	586 ± 210	602.34	1445.62	0.76	Borehole
13	GW13KPS	08º56.723'N 11º30.927'E	KPANTISAWA	46,200 ± 1300	322 ± 160	728.48	1748.35	0.92	Borehole
14	GW14NJ	08º53.458'N 11º34.694'E	NYAJA	45,900 ± 1300	510 ± 200	723.75	1737.00	0.92	Borehole
15	GW15TP	08º51.007'N 11º38.022'E	TAPENLA	41,300 ± 1300	348 ± 160	651.22	1562.93	0.83	Open Well
16	GW16KS	08º49.428'N 11º38.394'E	KASSA	37,100 ± 1200	203 ± 130	584.99	1403.98	0.74	Borehole
17	GW17BD	08º51.520'N 11º41.119'E	BODUGA	30,000 ± 1100	213 ± 130	473.04	1135.30	0.60	Borehole

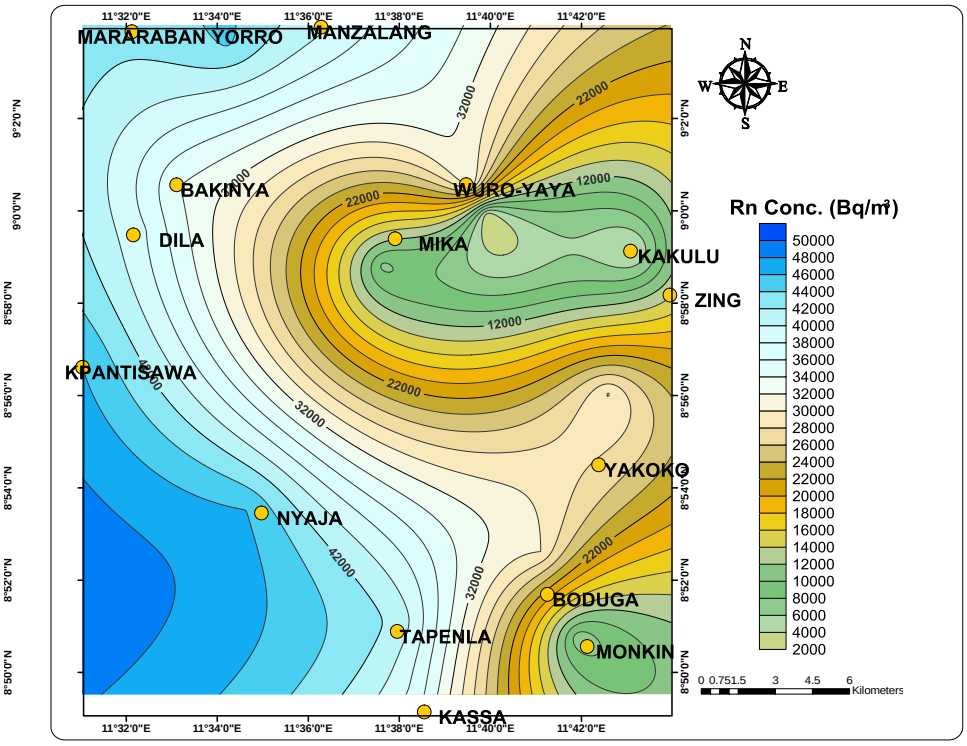


Fig. 14: Radon (in water) contour map of the study area

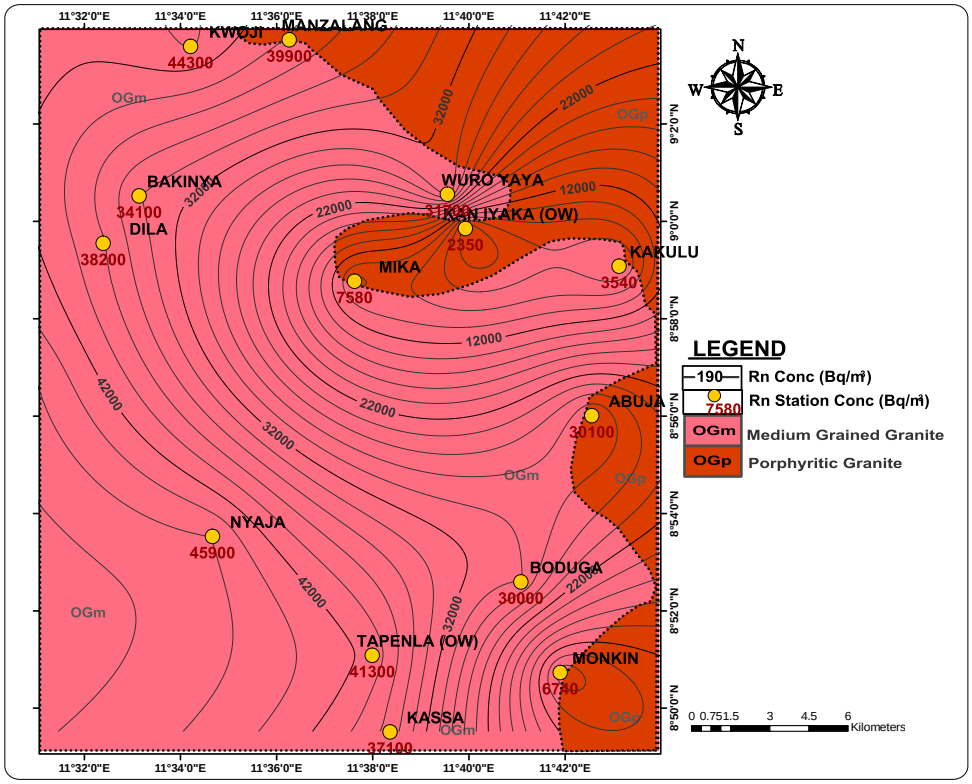


Fig. 15: Radon contour map super-imposed on the Lithologic map of the study area.

.

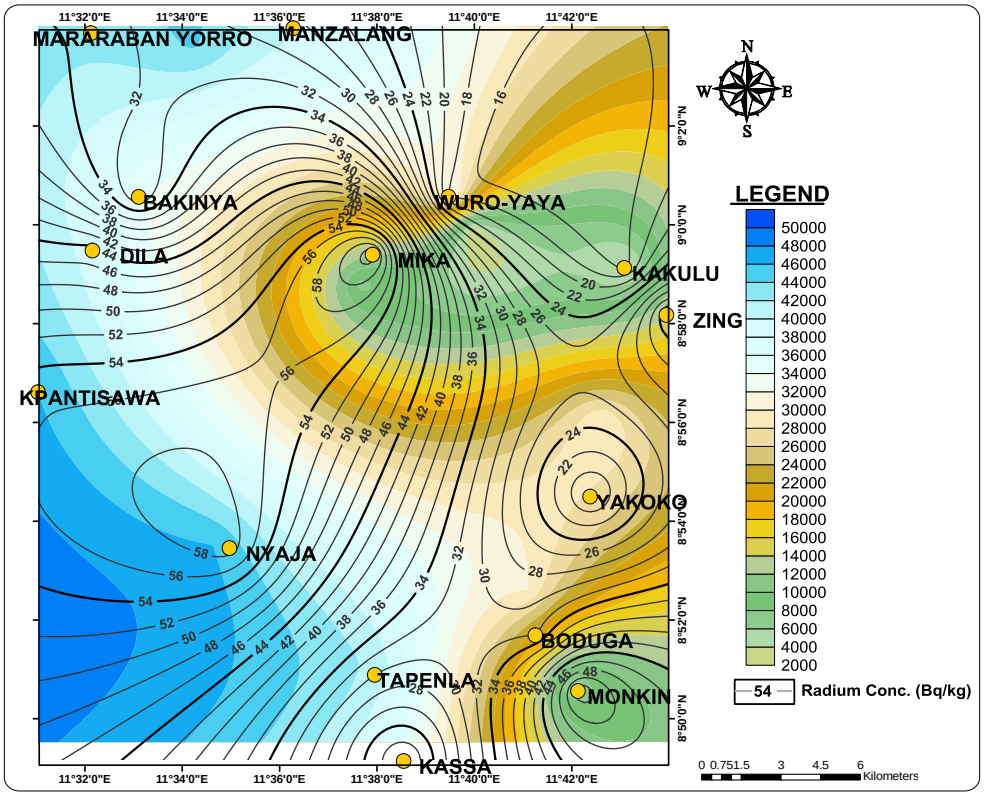


Fig. 16: ^{226}Ra concentration contour map superimposed on ^{222}Rn concentration in groundwater

4.4 RADON EMISSION FROM ROCK MATERIALS

Fifteen (15) rock samples were subjected to radon emission analysis in order to measure the radon exhalation rates from the rock material. This was done with the aim of estimating the amount of radon gas that is been emitted per unit mass (1kg) of a rock, into groundwater. RAD7 electronic radon detector was used for the analysis and counting took a period of 24 hours per sample. Radon concentrations were obtained in Bq/m^3, from the "CAPTURE" software computer interface after each rock sample analysis (radon concentration graph of each groundwater analysis is present in Appendix 3). The results of the measurements obtained were as follows;

Table 5: Radon Exhalation Results Measured on Rock Samples.

S/N	Sample ID	Coordinates	Sample Location	^{222}Rn (Bq/m^3)	^{222}Rn ($Bqm^{-3}h^{-1}$)
1	RK01ZN	08º58.121'N 11º43.988'E	ZING	211 ± 8	8.79
2	RKO2YK	08º54.431'N 11º42.419'E	YAKOKO	43.6 ± 4.5	1.82
3	RK03MN	08º50.481'N 11º42.168'E	MONKIN	138 ± 6	5.75
4	RK04KK	08º59.076'N 11º43.121'E	KAKULU	155 ± 33.2	6.46
5	RK05MK	08º59.354'N 11º37.941'E	MIKA	173 ± 11	7.21
6	RK06WY	09º00.520'N 11º39.505'E	WURO-YAYA	119 ± 6	4.96
7	RK07MZ	09º03.945'N 11º36.312'E	MANZALANG	39.7 ± 4	1.65
8	RK08MY	09º03.845'N 11º32.148'E	MARARABAN YORRO	114 ± 34.6	4.75
9	RK09BK	09º00.518'N 11º33.132'E	BAKINYA	262 ± 12	10.92
10	RK10DL	08º59.429'N 11º32.180'E	DILA	123 ± 6	5.13
11	RK11KPS	08º56.551'N 11º31.061'E	KPANTISAWA	216 ± 12	9.00
12	RK12NJ	08º53.384'N 11º34.999'E	NYAJA	123 ± 42.7	5.13
13	RK13TP	08º50.809'N 11º37.987'E	TAPENLA	134 ± 37	5.58
14	RK14KS	08º49.059'N 11º38.582'E	KASSA	76 ± 24.8	3.17
15	RK15BD	08º51.614'N 11º41.291'E	BODUGA	122 ± 6	5.08

Radon exhalation from rocks (Table 5) and radium concentrations (Table 6) obtained from gamma spectrometry analysis were used to calculate radon exhalation rates and radon emanation coefficients (Table 6) for each rock samples.

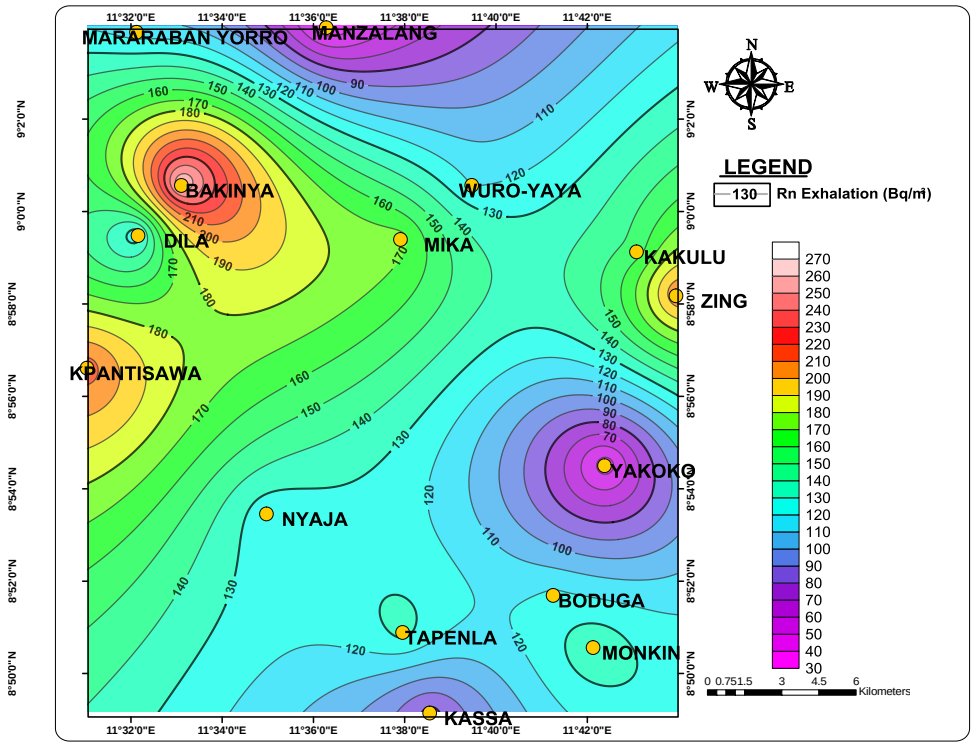


Fig.17: Contour Map of ^{222}Rn exhalation from rocks

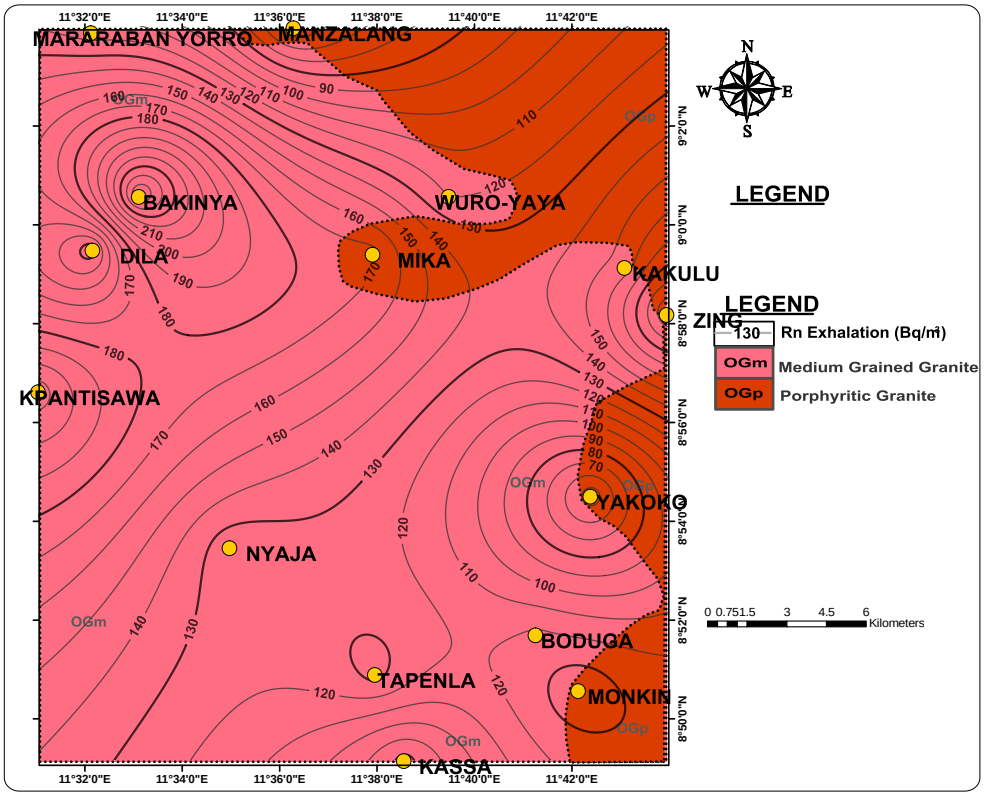


Fig. 18: ^{222}Rn exhalation map superimposed on Lithologic map of the study area

4.4.1 Radon Exhalation Rates and Emanation Coefficients

Radon emanation coefficients and its exhalation rates were calculated based on the measured values of radon exhalation. Radon exhalation, emanation coefficient and exhalation rate give good information about the radioactivity levels in the groundwater and naturally occurring radioactive materials (NORM). Therefore, measurement of these parameters is very important from point of view of radiation protection. The exhalation rates and the emanation coefficients of the rocks are presented in Table 6 and Fig. 19 shows the radon exhalation rate contours on the corresponding Lithology of the area.

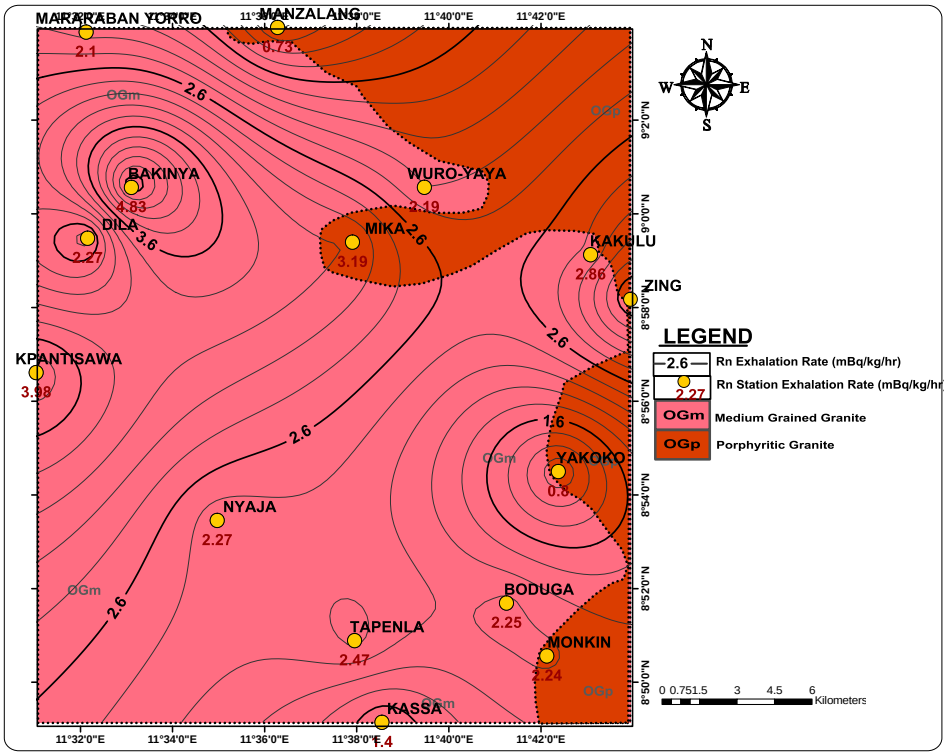


Fig 19: ^{222}Rn Exhalation Rate map superimposed on Lithologic map of the study area.

Table 6: Calculated Radon Emanation Coefficient and Exhalation Rate

	Sample ID	Coordinates	Sample Location	^{222}Rn (Bq/m^3)	Radium Activity (BqKg^{-1})	Exhalation Rate (mBqkg^{-1}hr^{-1})	Emanation Coefficient (%)
1	RK01ZN	08º58.121'N 11º43.988'E	ZING	211 ± 8	36.07 ± 1.97	3.89 ± 0.15	2.9 ± 0.11
2	RKO2YK	08º54.431'N 11º42.419'E	YAKOKO	43.6 ± 4.5	17.50 ± 1.28	0.80 ± 0.08	1.3 ± 0.13
3	RK03MN	08º50.481'N 11º42.168'E	MONKIN	138 ± 6	53.42 ± 2.69	2.24 ± 0.11	1.3 ± 0.06
4	RK04KK	08º59.076'N 11º43.121'E	KAKULU	155 ± 33.2	15.33 ± 3.82	2.86 ± 0.61	5.1 ± 1.08
5	RK05MK	08º59.354'N 11º37.941'E	MIKA	173 ± 11	63.38 ± 4.03	3.19 ± 0.20	1.4 ± 0.09
6	RK06WY	09º00.520'N 11º39.505'E	WURO-YAYA	119 ± 6	17.53 ± 2.49	2.19 ± 0.11	3.4 ± 0.17
7	RK07MZ	09º03.945'N 11º36.312'E	MANZALANG	39.7 ± 4	28.48 ± 1.02	0.73 ± 0.07	0.7 ± 0.07
8	RK08MY	09º03.845'N 11º32.148'E	MARARABAN YORRO	114 ± 34.6	33.49 ± 3.01	2.10 ± 0.64	1.7 ± 0.52
9	RK09BK	09º00.518'N 11º33.132'E	BAKINYA	262 ± 12	30.20 ± 2.16	4.83 ± 0.22	4.3 ± 0.20
10	RK10DL	08º59.429'N 11º32.180'E	DILA	123 ± 6	44.50 ± 1.99	2.27 ± 0.11	1.4 ± 0.07
11	RK11KPS	08º56.551'N 11º31.061'E	KPANTISAWA	216 ± 12	55.39 ± 3.59	3.98 ± 0.22	2.0 ± 0.11
12	RK12NJ	08º53.384'N 11º34.999'E	NYAJA	123 ± 42.7	59.10 ± 3.36	2.27 ± 0.79	1.0 ± 0.36
13	RK13TP	08º50.809'N 11º37.987'E	TAPENLA	134 ± 37	30.01 ± 2.83	2.47 ± 0.68	2.2 ± 0.62
14	RK14KS	08º49.059'N 11º38.582'E	KASSA	76 ± 24.8	19.58 ± 2.55	1.40 ± 0.46	1.9 ± 0.63
15	RK15BD	08º51.614'N 11º41.291'E	BODUGA	122 ± 6	31.87 ± 1.28	2.25 ± 0.11	1.9 ± 0.09

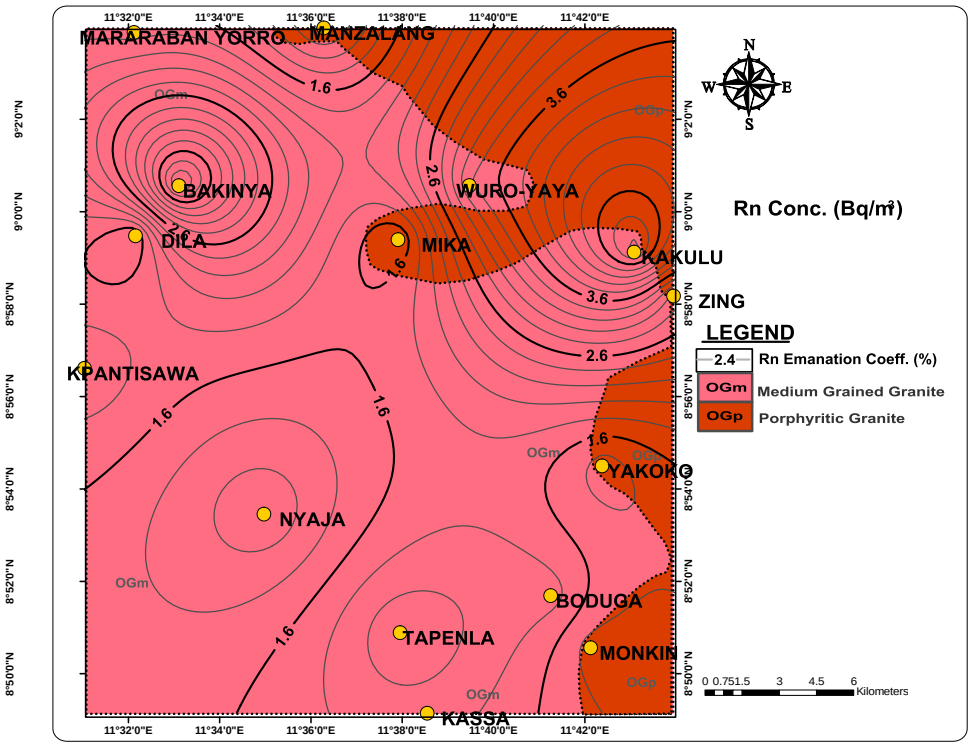


Fig 20: ^{222}Rn Emanation Coefficients map of the rocks within study area.

4.5 GAMMA RADIATION MEASUREMENTS AND DOSE RATES

The rock samples collected from the study area was subjected to gamma spectrometry analysis in order to determine concentrations of the most common naturally occurring radionuclides in the rocks and the gamma radiation doses they generate as a result of their combined effects. Thorium (^{232}Th), Radium (^{226}Ra) and Potassium (^{40}K) activity concentrations were measured.

The contour maps of ^{226}Ra, ^{232}Th and ^{40}K concentrations are presented as Figures 21, 22, and 23, respectively. Below is the detailed analysis result as obtained from gamma spectrometry analysis;

Table 7: Gamma Spectrometry Analysis Results

S/N	Sample ID	Location Name	K-40 (CPS)	Error± (CPS)	K-40 (Bq/kg)	Error± (Bq/kg)	Ra-226 (CPS)	Error± (CPS)	Ra-226 (Bq/kg)	Error± (Bq/kg)	Th-232 (CPS)	Error± (CPS)	Th-232 (Bq/kg)	Error± (Bq/kg)
1	RK01ZN	Zing	0.7539	0.0068	1172.457	10.5801	0.0311	0.0017	36.0718	1.9699	0.2926	0.0030	333.6374	3.4550
2	RK02YK	Yakoko	0.8637	0.0038	1343.235	5.9098	0.0151	0.0011	17.4971	1.2746	0.1782	0.0011	203.1813	1.2543
3	RK03MN	Monkin	0.1040	0.0036	161.726	5.5988	0.0461	0.0023	53.4183	2.6883	0.1508	0.0011	171.9498	1.2429
4	RK04KK	Kakulu	0.6090	0.0011	947.123	1.7107	0.0132	0.0033	15.3302	3.8239	0.0619	0.0015	70.5815	1.7104
5	RK05MK	Mika	0.9858	0.0026	1533.126	3.9814	0.0547	0.0035	63.3836	4.0325	0.2455	0.0012	279.9544	1.3113
6	RK06WY	Wuro-yaya	1.3931	0.0062	2166.563	9.5645	0.0151	0.0022	17.5330	2.4913	0.1205	0.0014	137.3888	1.6089
7	RK07MZ	Manzalang	0.6767	0.0027	1052.395	4.1991	0.0246	0.0009	28.4820	1.0197	0.1714	0.0012	195.4390	1.4139
8	RK08MY	Mararaban yorro	0.5939	0.0018	923.639	2.7994	0.0289	0.0026	33.4878	3.0128	0.0364	0.0024	41.5051	2.7366
9	RK09BK	Bakinya	0.9128	0.0059	1419.596	9.1291	0.0261	0.0019	30.1970	2.1553	0.1695	0.0020	193.2497	2.3162
10	RK10DL	Dila	0.5562	0.0070	864.992	10.8865	0.0384	0.0017	44.4959	1.9931	0.1541	0.0015	175.7126	1.6876
11	RK11KPS	Kpantisawa	0.7919	0.0065	1231.555	10.1089	0.0478	0.0031	55.3882	3.5921	0.2005	0.0016	228.6203	1.8130
12	RK12NJ	Nyaja	0.6594	0.0032	1025.505	4.9922	0.0510	0.0029	59.0962	3.3604	0.0409	0.0030	46.6363	3.4208
13	RK13TP	Tapenla	0.6743	0.0007	1048.678	1.0887	0.0259	0.0024	30.0116	2.8274	0.0739	0.0012	84.2645	1.3797
14	RK14KS	Kassa	0.8845	0.0039	1375.583	6.0653	0.0169	0.0022	19.5829	2.5493	0.0550	0.0010	62.7138	1.1403
15	RK15BD	Boduga	0.6639	0.00453	1032.504	7.0451	0.0275	0.0011	31.8656	1.2746	0.1781	0.00189	203.0787	2.1551

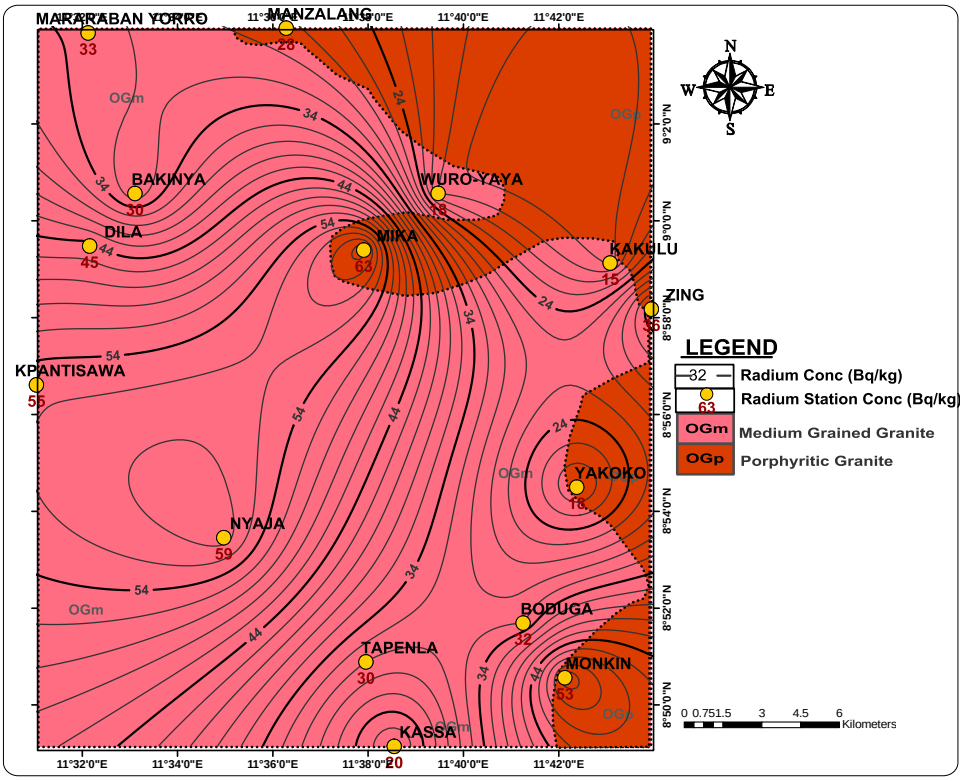


Fig. 21: ^{226}Ra Concentration Contour Map of the study area.

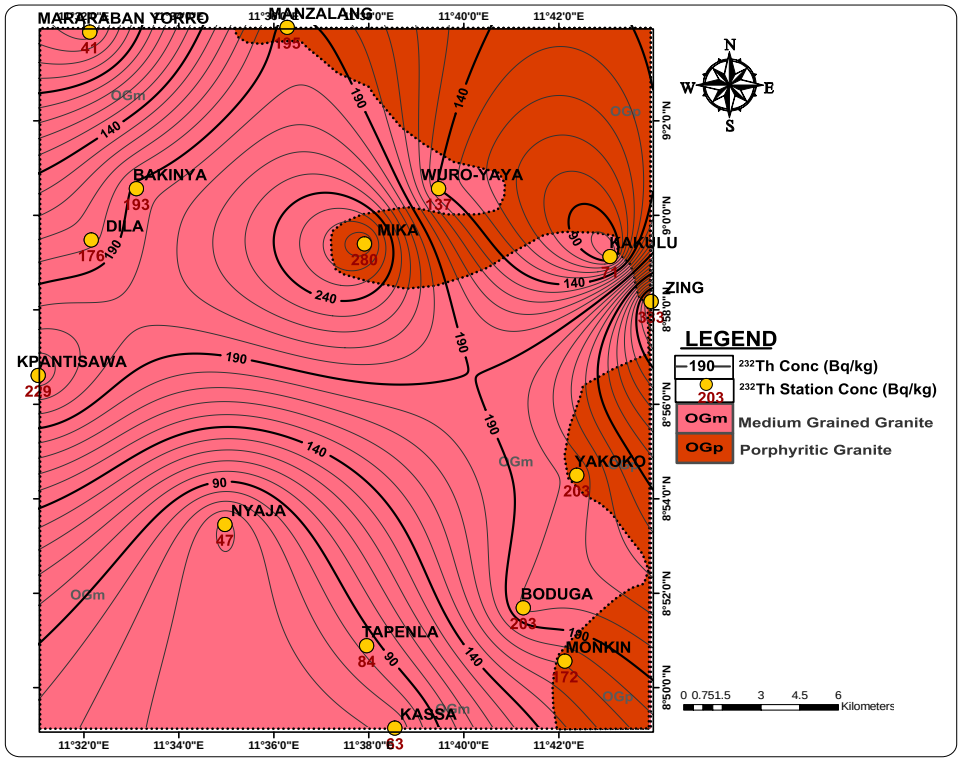


Fig. 22: ^{232}Th Concentration Contour Map of the study area.

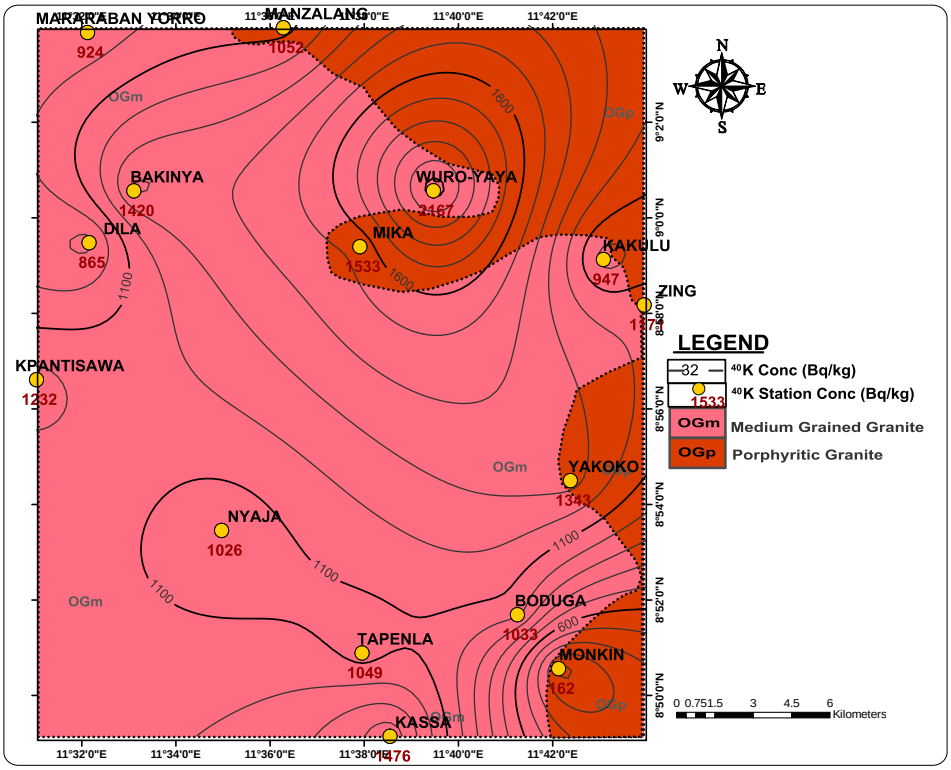


Fig. 23: ^{40}K Concentration Contour Map of the study area

The radioactivity of rocks contributes to the external gamma dose rate that human receive from the environment. The relationship between surrounding rocks and groundwater of a particular place cannot be over-emphasized therefore, it is important to measure the radioactivity of rocks and understand the dynamics of the radioisotopes in the natural environment.

4.5.1 Dose Rates due to Gamma Radiations

In order to evaluate radiation hazards, the radioactivity results were converted in three dose related quantities: the absorbed gamma radiation dose rate and the annual effective dose rate (IAEA, 2003), the radium equivalent (Ra_{eq}) and External hazard (H_{ex}) (Berekta and Mathew, 1985). Ra_{eq} and H_{ex} (Table 8) are parameters employed to check radioactivity hazards associated with naturally occurring radioactive rocks or any material used for construction purposes, e.g. granite chips used for borehole gravel packing, building constructions, etc.

Table 8: Calculated γ – Radiation Dose Rates, Annual Effective Dose Rate, Radium Equivalent and External Hazards.

S/N	Sample ID	Location Name	Rock Type	K-40 (Bq/kg)	Ra-226 (Bq/kg)	Th-232 (Bq/kg)	Dose Rate ($nGyhr^{-1}$)	Annual Effective Dose Rate ($mSvyr^{-1}$)	Radium Equivalent Activity (Ra_{eq}) (Bq/kg)	External Hazard (H_{ex})
1	RK01ZN	Zing	OG_P	1172.46 ± 10.58	36.07 ± 1.97	333.64 ± 3.46	270.46 ± 3.47	0.83 ± 0.011	603.46 ± 7.73	1.63 ± 0.02
2	RK02YK	Yakoko	OG_P	1343.24 ± 5.91	17.50 ± 1.28	203.18 ± 1.25	188.95 ± 1.60	0.58 ± 0.005	411.48 ± 3.52	1.11 ± 0.01
3	RK03MN	Monkin	OG_P	161.73 ± 5.60	53.42 ± 2.69	171.95 ± 1.24	136.91 ± 2.23	0.42 ± 0.007	311.76 ± 4.89	0.84 ± 0.01
4	RK04KK	Kakulu	OG_P	947.12 ± 1.71	15.33 ± 3.82	70.58 ± 1.71	89.98 ± 2.88	0.28 ± 0.009	189.19 ± 6.40	0.51 ± 0.02
5	RK05MK	Mika	OG_P	1533.13 ± 3.98	63.38 ± 4.03	279.95 ± 1.31	265.13 ± 2.83	0.81 ± 0.009	581.76 ± 6.21	1.57 ± 0.02
6	RK06WY	Wuro-yaya	OG_m	2166.56 ± 9.57	17.53 ± 2.49	137.39 ± 1.61	182.98 ± 2.53	0.56 ± 0.008	380.82 ± 5.53	1.03 ± 0.02
7	RK07MZ	Manzalang	OG_p	1052.40 ± 4.20	28.48 ± 1.02	195.44 ± 1.41	177.09 ± 1.51	0.54 ± 0.005	388.99 ± 3.36	1.05 ± 0.01
8	RK08MY	Mararaban yorro	OG_m	923.64 ± 2.80	33.49 ± 3.01	41.51 ± 2.74	79.50 ± 3.18	0.24 ± 0.010	163.97 ± 7.14	0.44 ± 0.02
9	RK09BK	Bakinya	OG_m	1419.60 ± 9.13	30.20 ± 2.16	193.25 ± 2.32	191.89 ± 2.80	0.59 ± 0.009	415.86 ± 6.18	1.12 ± 0.02
10	RK10DL	Dila	OG_m	864.99 ± 10.89	44.50 ± 1.99	175.71 ± 1.69	164.51 ± 2.41	0.51 ± 0.007	362.37 ± 5.25	0.98 ± 0.01
11	RK11KPS	Kpantisawa	OG_m	1231.56 ± 10.11	55.39 ± 3.59	228.62 ± 1.81	217.33 ± 3.19	0.67 ± 0.010	477.15 ± 6.96	1.29 ± 0.02
12	RK12NJ	Nyaja	OG_m	1025.51 ± 4.99	59.10 ± 3.36	46.64 ± 3.42	98.69 ± 3.85	0.30 ± 0.012	204.76 ± 8.64	0.55 ± 0.02
13	RK13TP	Tapenla	OG_m	1048.68 ± 1.09	30.01 ± 2.83	84.27 ± 1.38	109.38 ± 2.20	0.34 ± 0.007	231.27 ± 4.89	0.63 ± 0.01
14	RK14KS	Kassa	OG_m	1375.58 ± 6.07	19.58 ± 2.55	62.71 ± 1.14	105.01 ± 2.13	0.32 ± 0.007	215.18 ± 4.65	0.58 ± 0.01
15	RK15BD	Boduga	OG_m	1032.50 ± 4.99	31.87 ± 1.28	203.08 ± 2.16	182.51 ± 2.21	0.56 ± 0.007	401.78 ± 4.91	1.09 ± 0.01
	AM ± SD			1153.25 ± 6.11	35.72 ± 2.54	161.86 ± 1.91	164.02 ± 2.60	0.50 ± 0.008	355.99 ± 5.75	0.96 ± 0.02

Note: OG_P = Porphyritic Granite, OG_m = Medium-Grained Granite.

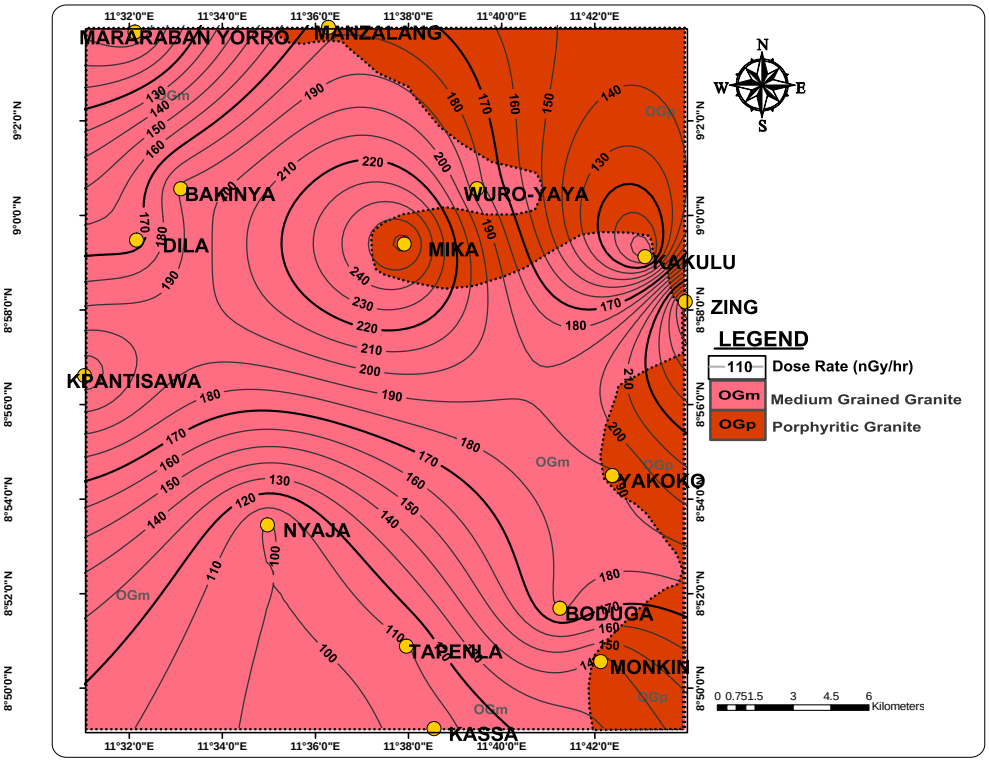


Fig. 24: Gamma Radiation Dose Rates of the rocks within the study area

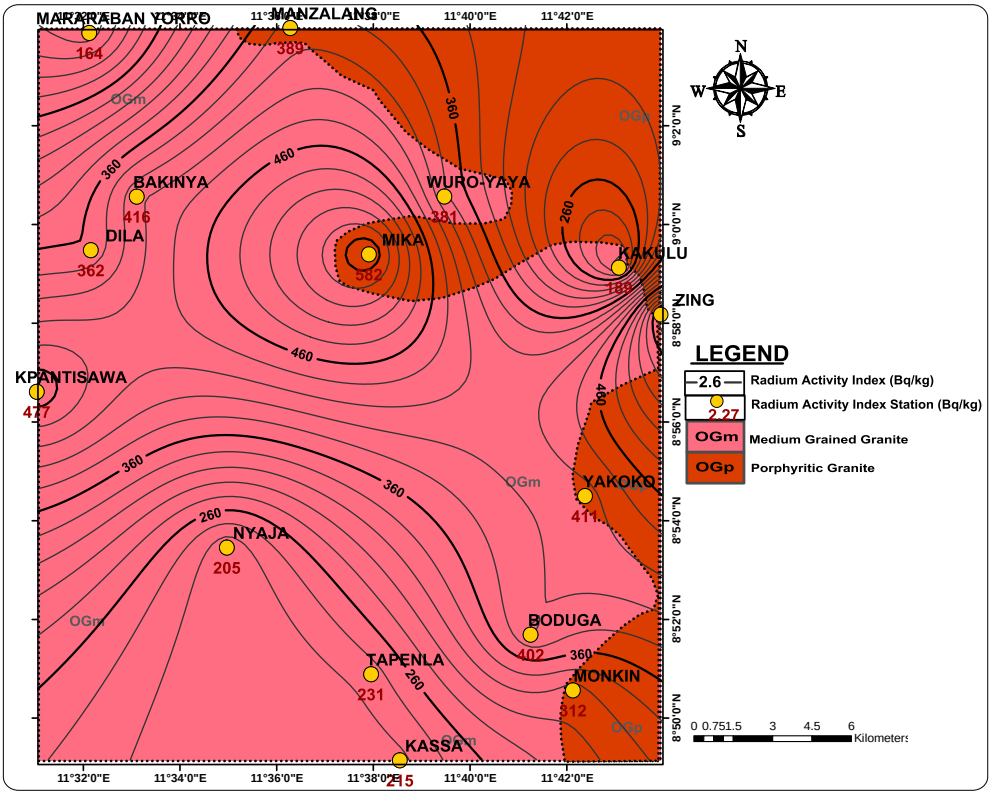


Fig. 25: Radium Equivalent Activity Index of the rocks of the study area

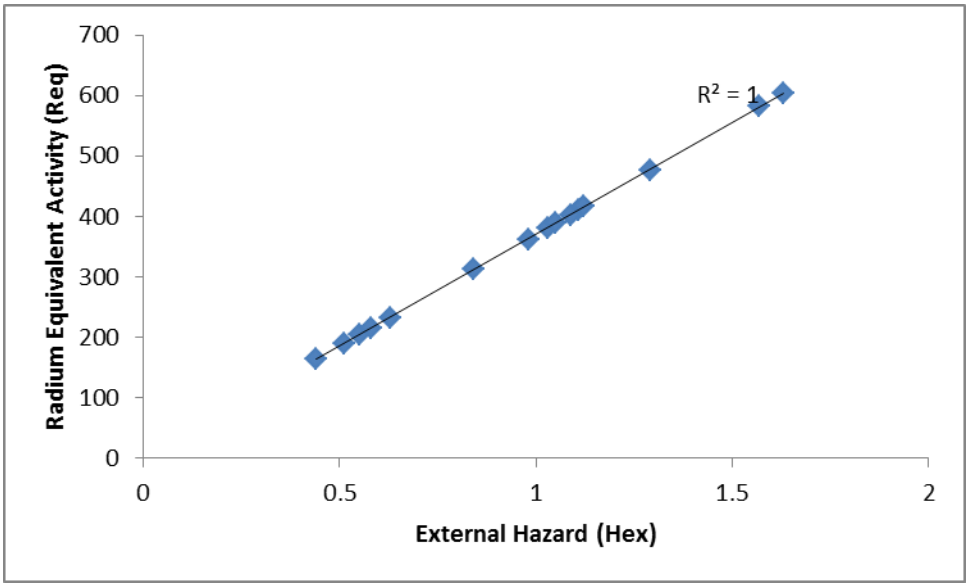


Fig. 26: A plot of Ra_{eq} vs. H_{ex}

4.6 HYDROCHEMISTRY OF THE STUDY AREA

The chemical characteristics of the groundwater in the study area is presented in this section based on the following physico-chemical parameters; Total Dissolved Solids (TDS), Hydrogen-Ion exponential (pH), conductivity, salinity, major cations and anions distribution, statistical and the graphical presentation of the hydrochemical data obtained. Table 9 below, shows a detailed physic-chemical analysis results and a statistical summary of the results compared with World Health Organization (WHO), United States Environmental Protection Agency (US. EPA) and the Nigerian Industrial Standard (NIS), recommended standards are presented in Table 10.

Table 9: Groundwater Physical and Chemical Analysis results

S/N	Sample ID	Ca^{2+} (mg/l)	Mg^{2+} (mg/l)	K^{+} (mg/l)	Na^{2+} (mg/l)	CO_3^{2-} (mg/l)	HCO_3^{-} (mg/l)	Cl^{-} (mg/l)	NO_3^{-} (mg/l)	SO_4^{2-} (mg/l)	TDS (mg/l)	pH	Conductivity (mS/cm)	Salinity
1	GW01ZN	107.38	5.66	2.3	52	0	2.4	3.10	0.02	2.83	4320	7.40	8.04	4.5
2	GW02AB	8.34	3.63	2.7	20	0	2.1	0.25	0.01	0.17	1176	7.00	2.32	1.2
3	GW03MN	7.47	8.90	1.4	42	0	3.3	0.75	0.03	0.17	2320	8.11	4.46	2.4
4	GW04KK	21.30	8.89	1.4	58	0	5.2	0.45	0.01	0.17	3040	7.45	5.77	3.1
5	GW05KI	2.69	10.20	0.6	40	0	2.7	0.45	0.01	0.33	1150	7.73	3.40	1.8
6	GW06MK	2.55	2.44	1.5	29	0	1.6	0.40	0.01	0.33	109.2	6.64	2.17	1.1
7	GW07WY	41.36	8.31	1.9	62	0	6.3	0.35	0.01	0.17	3470	7.59	6.57	3.6
8	GW08MZ	19.43	5.03	1.2	32	0	4.0	0.25	0.01	0.17	2200	7.87	4.24	2.2
9	GW09KJ	20.28	12.27	1.7	59	0	5.8	0.35	0.01	0.50	3280	7.73	6.20	3.4
10	GW10MY	7.15	3.01	4.0	44	0	1.7	0.90	0.01	0.83	1903	7.03	3.69	1.9
11	GW11BK	17.34	5.47	0.9	38	0	4.6	0.25	0.01	0.33	2420	7.55	4.64	2.5
12	GW12DL	20.12	10.01	2.2	42	0	4.8	0.65	0.01	0.17	2950	7.50	5.61	3.0
13	GW13KPS	37.17	11.89	1.8	41	0	3.4	1.65	0.01	1.83	3150	7.65	5.97	3.2
14	GW14NJ	24.70	9.70	2.1	36	0	3.1	1.40	0.01	0.17	2840	7.85	5.40	2.9
15	GW15TP	0	0	1.2	12	0	0.5	0.25	0.01	8.17	205	7.27	4.24	0.2
16	GW16KS	6.98	8.34	2.4	38	0	2.4	0.80	0.01	3.33	1992	7.51	3.84	2.0
17	GW17BD	8.57	6.96	1.2	51	0	3.5	0.55	0.01	0.67	2280	7.87	4.37	2.3
	Average	20.76	7.10	1.8	41	0	3.4	0.75	0.01	1.20	2282.66	7.52	4.76	2.4

Table 10: Statistical Summary of Physico-chemical Analysis Results.

Parameter	Unit	WHO (MCL)	NIS (MCL)	EPA, Sec (MCL)	Mean	Max	Min	Number of Samples
pH (Field)		6.5 – 8.5	6.5 – 8.5	6.5 – 8.5	7.52	8.11	6.64	17
Spec Cond	µS/cm	1400	1000		4.76	8040	2.19	17
TDS	mg/L	1000	500	500	2282.7	4320	109.2	17
Ca^{2+}	mg/L	75			20.75	107.4	0	17
K^{+}	mg/L	55			1.79	4.0	0.6	17
Mg^{2+}	mg/L	50	0.2		7.10	12.27	0	17
Na^{+}	mg/L	50	200		40.94	62	12	17
Cl^{-}	mg/L	250	250	250	0.75	3.1	0.25	17
HCO^{3-}	mg/L	1000			3.38	6.3	0.5	17
SO_4^{2-}	mg/L	250	100	250	1.2	8.17	0.17	17
CO_3^{2-}	mg/L			120	0	0	0	17
NO_3^{-}	mg/L	50	50	10	0.01	0.03	0.01	17

4.6.1 Correlation Matrix

Correlation Matrix is used to account for the degree of mutually shared variability between individual pairs of groundwater quality variables. The results of the correlation matrix for physico-chemical data obtained for the study area is presented in Table 11.

Table 11: Correlation Matrix

		pH	Cond.	TDS	Ca^{2+}	K^{+}	Mg^{2+}	Na^{+}	Cl^{-}	HCO_3^{-}	SO_4^{2-}
pH		1	-0.97	0.35	0.14	0.08	0.48	0.45	0.17	0.31	0.06
Cond	µS/cm		1	-0.25	-0.14	-0.03	-0.34	-0.40	-0.18	-0.20	-0.13
TDS	mg/L			1	0.76	0.14	0.49	0.77	0.56	0.67	-0.30
Ca^{2+}	mg/L				1	0.04	0.06	0.39	0.82	0.11	0.47
K^{+}	mg/L					1	0.16	-0.09	0.26	-0.07	-0.13
Mg^{2+}	mg/L						1	0.47	0.08	0.54	0.04
Na^{+}	mg/L							1	0.23	0.74	-0.46
Cl^{-}	mg/L								1	-0.19	0.15
HCO_3^{-}	mg/L									1	-0.56
SO_4^{2-}	mg/L										1

4.6.2 Water Types

The concentration of anions and cation arranged in order from the highest ion concentration to the lowest gives the water type of the samples collected as follows;

a) Bicarbonate – Sodium Water Type

$HCO_3^{2-} > Cl^- > SO_4^{2-} > NO_3^- / Na^+ > Ca^{2+} > Mg^{2+} > K^+$ (7 Samples)

$/ Na^+ > Mg^{2+} > Ca^{2+} > K^+$ (2 Samples)

$/ Na^+ > Ca^{2+} > K^+ > Mg^{2+}$ (1 Sample)

$HCO_3^{2-} > SO_4^{2-} > Cl^- > NO_3^- / Na^+ > Ca^{2+} > Mg^{2+} > K^+$ (4 Samples)

b) Sulphate – Sodium Water Type

$SO_4^{2-} > HCO_3^{2-} > Cl^- > NO_3^- / Na^+ > Mg^{2+} > Ca^{2+} > K^+$ (1 Sample)

$/ Na^+ > K^+ > Ca^{2+}$ & Mg^{2+} (1 Sample)

c) Chloride – Calcium Water Type

$Cl^- > SO_4^{2-} > HCO_3^{2-} > NO_3^- / Ca^{2+} > Na^+ > Mg^{2+} > K^+$ (1 Sample)

4.6.3 Graphical Presentation of Hydrochemical Data

Constituents in solution in water may be viewed as a chemical system with cations and anions in equilibrium with each other. There are several varieties of graphical techniques that have been developed for the presentation of chemical components of water. The major chemical constituents are usually used for the presentation. An important task of water investigation is the compilation and presentation of chemical data in a convenient manner for visual inspection. Graphs are used in comparing the similarities and differences in the concentration of the chemical constituents in each water sample analyzed. Graphs are also used in detecting mixing of water of different composition and identifying chemical processes occurring as water passed through the aquifer system. For this work, Piper, Durov and Schoeller diagrams were used to show the different hydrochemical species within the study area.

4.6.3.1 Piper Diagram

This method was developed by Piper, (1944). Diagram reveals similarities and differences among large number of groundwater samples because those with similar qualities will tend to plot together as groups. By the use of Piper diagram chemical relationship among waters may be brought out in more definite terms than is possible with any other plotting graphical procedure. It is most useful for representing and comparing water quality because it reveals the similarities and difference among water samples, it directly gives you the various water types and it can handle results of many samples of water within the same graph although conversely, it is not good for a few data sets that make it hard to be compared. The Piper diagram of the study area is shown below (Fig. 27);

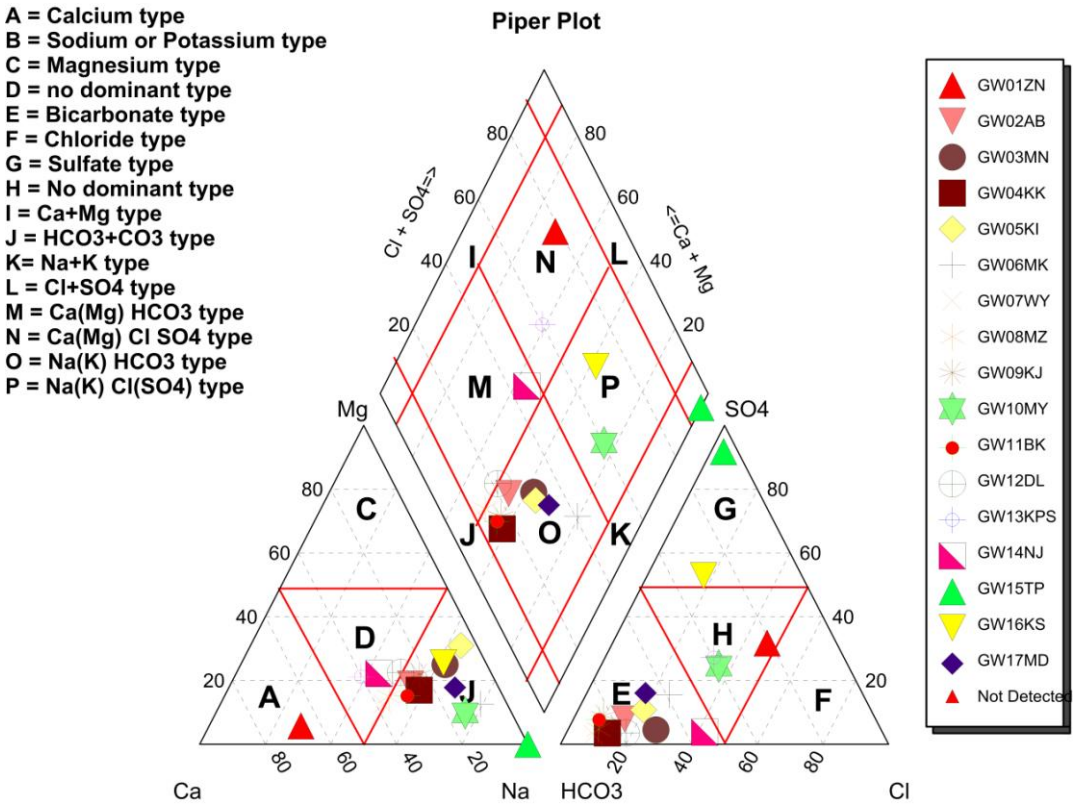


Fig 27: Piper Diagram of groundwater of Mika Area and Environs.

4.6.3.2 **Durov Plot**

Durov plot is a composite plot consisting of 2 ternary diagrams where cations of interest are plotted against the anions of interest; sides form a binary plot of total cations versus total anions concentration and the expanded version may include TDS (mg/l) and pH data added to the sides of the binary plot to allow for further comparison. This plot is used to graphically illustrate cation/anion concentrations, relative to TDS and pH. Durov plot for the study area (Fig. 28) is presented below;

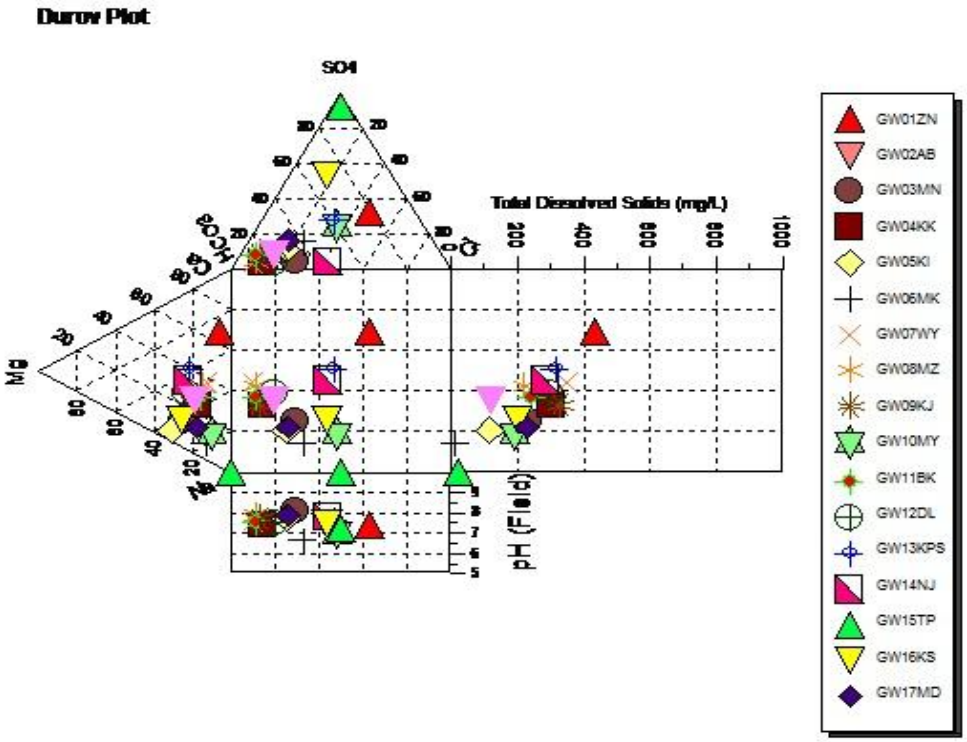


Fig 28: Durov plot of groundwater of Mika area and environs.

4.6.3.3 Shoeller Diagram

Schoeller (1977) diagram (Fig. 29) was also used to present average chemical composition of the groundwater at Mika and Environs. From the plots, the relative tendency of ions in mg/l showed that Na > Ca > Mg and HCO_3 > Cl > SO_4.

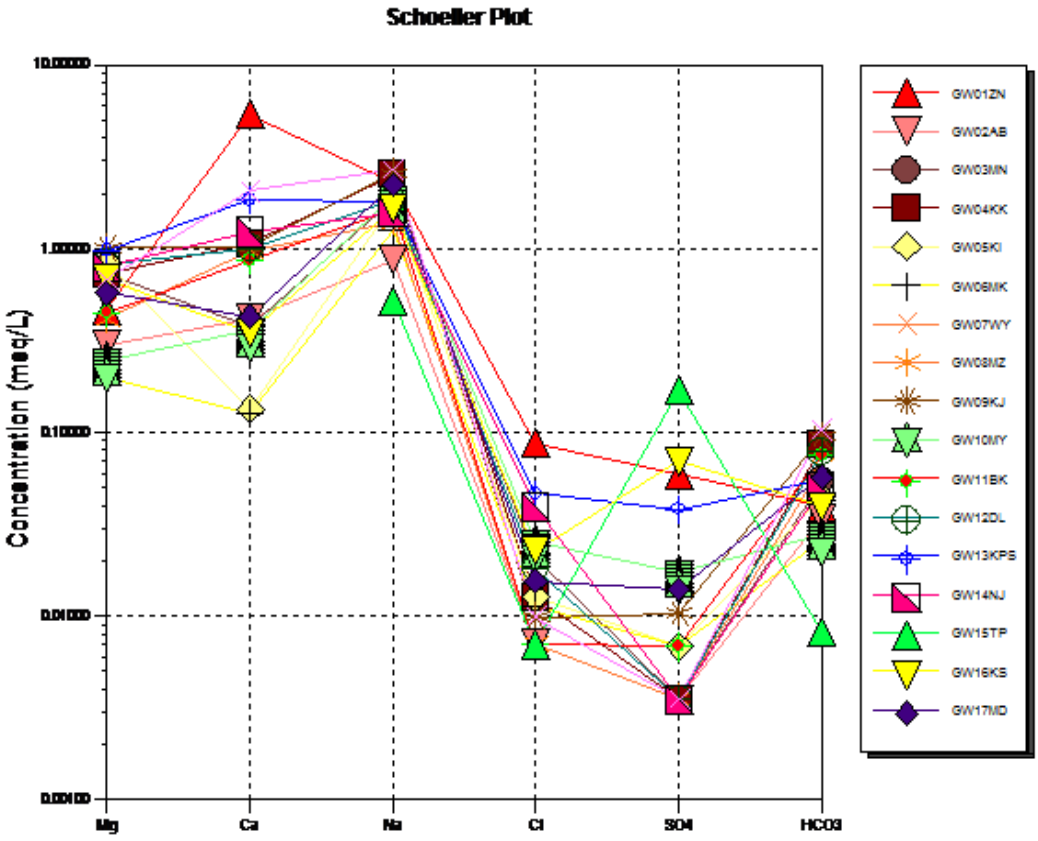


Fig 29: Schoeller Plot of the Study Area.

4.6.4 Assessment of Groundwater Quality for Irrigation Purposes

Assessment of the groundwater quality for irrigation in the study area was done based on calculated Sodium Adsorption Ratio, Percent sodium, Soil permeability Index, Chloro-Alkaline Indices as well as measured Electrical Conductivity and Chloride content of the groundwater.

Table 12: Calculated values of Sodium Adsorption Ratio (SAR), Percent sodium (%Na), Permeability Index (PI) and Chloro-Alkaline Indices (CAI).

Sample ID	Sample Location	SAR	%Na	PI	CAI
GW01ZN	**Zing**	**1.32**	**28.43**	**30.37**	**- 24.8**
GW02AB	**Abuja**	**1.45**	**56.63**	**65.61**	**- 93.0**
GW03MN	**Monkin**	**2.46**	**62.75**	**69.85**	**- 92.5**
GW04KK	**Kakulu**	**2.65**	**58.58**	**65.13**	**- 225**
GW05KI	**Kan-Iyaka**	**2.47**	**64.00**	**71.06**	**- 175**
GW06MK	**Mika**	**3.10**	**79.76**	**90.14**	**- 129**
GW07WY	**Wuro-Yaya**	**2.30**	**49.91**	**55.24**	**- 274**
GW08MZ	**Manzalang**	**1.56**	**50.53**	**58.16**	**- 141**
GW09KJ	**Kwoji**	**2.56**	**56.25**	**62.74**	**- 260**
GW10MY	**Mararaban Yorro**	**3.46**	**76.72**	**82.67**	**- 66**
GW11BK	**Bakinya**	**2.02**	**55.67**	**64.86**	**- 166**
GW12DL	**Dila**	**1.91**	**50.67**	**57.57**	**- 93.5**
GW13KPS	**Kpantisawa**	**1.49**	**39.10**	**43.74**	**- 35.6**
GW14NJ	**Nyaja**	**1.55**	**44.14**	**49.55**	**- 39.5**
GW15TP	**Tapenla**	**0**	**100**	**119.23**	**- 54**
GW16KS	**Kassa**	**2.28**	**61.96**	**68.52**	**- 84.5**
GW17MD	**Madaki**	**3.12**	**60.02**	**76.31**	**- 111.5**

Note: All calculations are based on converted milli-equivalent per litre (Meq/l) value of mg/l

Table 13: Summarized classification of groundwater for irrigation in the study area.

Classification Basis	Categories	Ranges	Percentage of Samples	No. of Samples
Sodium Absoption Ratio (SAR)	**Excellent**	**0 – 10**	**100**	**17**
	Good	**10 – 18**	**-----**	**-----**
	Fair	**18 – 26**	**-----**	**-----**
	Poor	**> 26**	**-----**	**-----**
Richard (1954)				
Percent Sodium % Na	**Excellent**	**0 – 20**	**-----**	**-----**
	Good	**20 – 40**	**11.8**	**2**
	Permissible	**40 – 60**	**52.9**	**9**
	Doubtful	**60 – 80**	**29.4**	**5**
Wilcox (1955)	**Unsuitable**	**> 80**	**5.9**	**1**
Soil Permeability Index (PI)	**Class I**	**> 75**	**23.5**	**4**
	Class II	**25 – 75**	**76.5**	**13**
	Class III	**< 25**	**-----**	**-----**
Doneen (1964)				
Electrical Conductivity (EC)	**Excellent**	**< 250**	**-----**	**-----**
	Good	**250 – 750**	**-----**	**-----**
	Permissible	**750 – 2250**	**5.9**	**1**
	Doubtful	**2250 – 5000**	**52.9**	**9**
Wilcox (1955)	**Unsuitable**	**> 5000**	**41.2**	**7**
Chloride (Cl^-)	**Extremely Fresh**	**< 0.14**	**-----**	**-----**
	Very Fresh	**0.14 – 0.85**	**76.5**	**13**
	Fresh	**0.85 – 4.23**	**23.5**	**4**
	Fresh-Brackish	**4.23 – 8.46**	**-----**	**-----**
	Brackish	**8.46 – 28.21**	**-----**	**-----**
	Brackish Salt	**28.21 – 282.06**	**-----**	**-----**
	Salt	**282.06 – 564.13**	**-----**	**-----**
Stuyfzand (1989)	**Hyper Saline**	**> 564.13**	**-----**	**-----**
Chloro-Alkaline Indices (CAI)	**Base – Exchange Reaction**	**-ve Value**	**100**	**17**
Schoeller (1967)	**Cation – Anion Exchange Reaction**	**+ve Value**	**-----**	**-----**

Note: -ve (negative), +ve (positive)

Chapter 5

DISCUSSION

5.1 GEOLOGY OF THE STUDY AREA

The Study area is located within the basement (granitoids) of the area in northern part of Adamawa Massif which is dominated by porphyritic granites and medium-grained granite. Other rock units include fine-grained granites, Olivine basalt, brecciated rhyolite and siliceous veins, with pegmatites as the only minor rock unit (Funtua, 1992). Textural varieties exist within the medium-grained granite but are difficult to demarcate. It is greyish to pinkish in colour with some orientation of feldspar crystals (Funtua, 1992). These rocks form prominent rocky hills in the study area and exhibit considerable textural variation and contact relationships. The area is characterized by extensive fractures and shear zones. The mineralogy of the granites of the study area are generally characterized by three major minerals; plagioclase, biotite, and microcline, even though hornblende was also reported around the south-eastern part of the area (Funtua, 1992; Haruna, *et al*., 2013). The high relief in the area as shown on the topographic and digital elevation maps (Figures 3 and 4) with a maximum elevation of about 2400m asl, run-off is relatively high and infiltration rate is low. Groundwater storage has also been limited due to climate conditions. Soil erosion has become prominent phenomenon and is ravaging the landscape of the study area.

Fine-grained granite was sampled, sandwiched in-between medium-grained granite along Yakoko – Monkin road, southeastern part of the study area (N08°52’25.4; E11°42’11.0) and also bounding coarse-grained granite at Manzalang (Northern part of the study area). The fine-grained granite outcrops could not be mapped as a separate unit, in this work and by previous workers, due to their small size. The area to the north, northeast and southeast are underlain by the porphyritic granite while, the areas to the south, southwest and northwest are dominated by

medium-grained granite (Fig. 12). Sheared granite occurs mostly as long ridges enclosing siliceous veins and rhyolites at the centre of the shear zone. The siliceous veins occur as the north – west trending ridges in the central parts and the almost north – south ridge at the lower part of the area, all measuring over 120 m in width. Rhyolite veins occur in similar fashion to the sheared granite, but occur only in the northern half of the area with predominantly north – south alignment (Funtua, 1992).

From the emplacement of the granitic bodies, the geological events that can be inferred in the area are the formation of shear zones with quartz veins, mostly in the NE – SW direction; dilation of some of the shear zones and emplacement of rhyolite bodies and further shearing that affected parts of the rhyolites and granites (Funtua, 1992).

Funtua (1992) produced a Rose diagram for Joint trends of Mika area with the majority of the joints and fractures falling in the range $0 – 20^0$, $60 – 80^0$, $80 – 100^0$ and $140 – 180^0$ which correspond with the major lineaments of the area. These major lineaments are the N – S subvertical foliation trend found in the porphyritic granite, which along with the conjugate E – W, are the common features of the Pan-African basement, the NE – SW lineaments that are prominently observed in the Upper Benue are the N140E and N170E trend of some sheared granite and rhyolite bodies. These groups of fractures are also believed to conjugate to the NE – SW sinistral faults contemporaneous with the genesis of the Benue trough (Benkhelil and Robineau, 1983).

5.2 GROUNDWATER CONFIGURATION WITHIN THE STUDY AREA

The groundwater configuration map (Fig. 13) shows that streams and groundwater flow of the area is controlled by the high relief. Water flow is in the direction of the steepest slope. The flow system exists on a local scale, characterize by the topography of each catchment area. There is no clear evidence that the flow systems are responsible for the chemical difference between the

sampled groundwater, most especially radon concentration in the groundwater. The depth to groundwater or thickness of the dry zone ranges from 0.95 to 21.22 m (Appendix 1). This measurement was carried-out during the dry season; therefore, it is expected to be lower during the wet season.

5.3 RADON CONCENTRATION IN GROUNDWATER

The result of radon concentration in groundwater (Table 4) showed that radon (^{222}Rn) concentration measured in Becquerel per cubic metres (Bq/m^3) range from 2340 ± 300 to 46,200 ± 1300 with an average of about 29,400 ± 1000. The mean value is far above the upper value of the ICRP reference level of 1500 Bqm^{-3}, while thoron (^{220}Rn) concentration also measured in Bq/m^3 range from 65.3 ± 70 to 586 ± 210, with an average value of about 240 ± 130. The calculated potential dose rate due to the degassing of radon from the groundwater shows an average annual absorbed dose of 463.59 mSv and average annual effective dose (for the human lungs) value of 1112.62 mSv, respectively. The 4th schedule in the Nigeria Basic Ionization Radiation Regulations of 2003, under the heading "Dose limits" specified classes of persons to who dose limits apply, to include persons of 18 years or above and 18 years or below (FGN, 2003). 76.5% of the calculated doses are above the highest regulatory limit of 500 $mSvyr^{-1}$ which represents limit on equivalent dose for the skin, hands, forearms, feet and ankle while about 23.5% are below. The annual effective dose due to ingestion (H_{ing}) of ^{222}Rn in groundwater varied from 0.05 to 0.92 $mSvyr^{-1}$, with an average value of 0.59 $mSvyr^{-1}$. These are within the ICRP recommended reference level of 1 $mSvyr^{-1}$ for the intake of radionuclide in water by the general public for a prolonged exposure. 11.77% representing two (2) groundwater samples are within WHO recommended reference level of 0.1 $mSvyr^{-1}$ while 88.23% of the sampled groundwater showed an annual effective dose higher than the recommended level. The open-well

at Kan-Iyaka and the borehole at Kakulu recorded the lowest H_{ing} while boreholes at Kpantisawa and Nyaja recorded the highest.

In the environment, the concentration of ^{222}Rn in waters is highly variable because of the variations in the rock characteristics and flow distribution. It is noteworthy that groundwater from fractured igneous and high-grade metamorphic rocks frequently exhibit high activity of dissolved ^{222}Rn (Wood, *et al*., 2004), this is evident from the result of radon concentrations presented in Table 4, which shows high radon concentration values in the groundwater, as samples were collected from wells drilled within the uranium mineralized granitic rocks. 76.5% of the samples in the area under study have ^{222}Rn concentrations far above the United States Environmental Protection Agency (USEPA) maximum contaminant level (MCL) of 11.1 Bq/l (for States without radon monitoring policy and enhanced indoor air programs) (NAS, 1999) while 23.5% have values lower. All radon values are below the MCL recommended by European Union (EU), 100.0 Bq/l (measurement that warrants consideration of possible remedial actions) and 1000.0 Bq/l (upper bound above which remedial action is definitely required) (EU, 2001). But on the other hand, all the samples have radon values far above the Standards Organization of Nigeria (SON) recommended an MCL of 0.1 Bq/l (for radionuclide concentration in drinking water in Nigeria) (SON, 2007). The highest ^{222}Rn concentration of 46,200 ± 1300 Bq/m^3 was measured from a borehole at Kpantisawa town while the lowest concentration 2350 ± 300 $Bq/m^3$was recorded from an open-well at Kan-Iyaka community. It is worthy to note here that, higher radon concentrations were recorded in borehole waters. Low radon value recorded at Kan-Iyaka may be due to degassing of ^{222}Rn from the open-well before sampling/measurement because of direct contact with the atmosphere (Sampling and measurements from open-well was deliberately carried-out for comparison purpose) but ^{222}Rn concentration from Tapenla (open-well) show a high value of about 41,300 ± 1300 Bq/m^3, this might be because as at the time of

sampling/measurement of water from Tapenla, the open-well was in continual use, which means that "fresh" water sample (from the aquifer) was collected and immediately analyzed, therefore, did not allow time for much radon to degas. Kakulu recorded the lowest ^{222}Rn concentration obtained from borehole samples; boreholes showing very high radon concentration relative to others may have numerous fractures intersecting the borehole, with each fracture contributing to the total radon concentration in the borehole. This is because radon content of fluids is expected to respond to variations in ^{222}Rn flux as well as the extent and length of water/rock contact, which in-turn depends on the fracture surface (Le Druillennec *et al.*, 2010). The radon concentration results presented in the Table 4, is similar with radon concentration ranges in Swedish groundwater from Uranium-rich granites, reported by Akerblom, *et al*., (2005). It is generally accepted that high radon levels will be found in terrain of high grade metamorphic rock or granites (Brutsaert, *et al*., 1981), most especially Uranium-rich ones.

A superimposed map of radon concentration (Fig. 14) on the lithologic map of the study area (Fig. 12), shows that radon concentrations are higher in groundwaters within the medium-grained granites than in groundwaters within the coarse-grained granite (Fig. 15). A map of radium (^{226}Ra) distribution (Fig. 19) in rocks of the study area super-imposed on radon concentration in groundwater (Fig. 14), showed that relatively higher radium distribution within the medium-grained granite is responsible for the higher radon concentrations in groundwaters within the medium-grained granite (Fig. 16). Although, the grain sizes of a rock has been reported to play an important role in increasing exhalation of radon from the rock into the groundwater, thereby increasing radon concentrations in groundwater, the higher concentrations of radon in groundwater within the medium-grained granite can be clearly attributed to radium distribution.

5.4 RADON EMMISSION FROM ROCK MATERIALS

Table 5 shows the results of radon exhalation or emmission from the rock samples collected within the study area. The radon emmissions from the rocks ranged from 39.7 ± 4 to 262 ± 12 Bq/m^3 with an average of 137 ± 17 Bq/m^3 which translate approximately into a range of 1.65 $Bq/m^3/hr$ to 10.92 $Bq/m^3/hr$. The medium-grained granite at Bakinya recorded the highest radon exahalation while the porphyritic granite at Manzalang recorded the lowest exhalation.

The ^{222}Rn exhalation contour map (Fig. 17) super-imposed on the lithologic map of the study area (Fig. 12) showed that exhalation of ^{222}Rn is more towards the western part of the area, within the medium-grained granite rocks and also the eastern part within the porphyritic granite (Fig. 18). This might be due to the relatively smaller grain sizes of the medium-grained granite compared to the porphyritic granite and/or may be due to the effect of shearing that affected areas around the mid-part of the area (Fig. 12) which is evident by the presence of boulders scattered on outcrops (Plate 4). This may affect the grain structures of the rocks thereby influences increased ^{222}Rn exhalation.

5.4.1 Radon Exhalation Rates and Emanation Coefficients of the Rocks

The radon emanation coefficient also known as radon emanation power of the sampled rocks in the study area, calculated in percentage (%), ranges between 0.7 ± 0.07 to 5.1 ± 1.08 with a mean value of 2.17 ± 0.29 across the study area. The highest calculated value of 5.1% was recorded from Kakulu while Manzalang rocks have the lowest radon emanation power of 0.7%. One of the most important factors affecting the radon emanation coefficient is distribution of radium activity within the grains. Particularly if it is concentrated within the thin surface layers of the grains, the radon generated will increase and the number of radon atoms escaping into pore spaces could also increase, thereby increasing the radon emanation coefficient. On the other hand, the internal structure of the materials (e.g., macroscopic properties, crystallization of the grains' surfaces,

and the texture and size of grains) also affect the emanation coefficient. For example, the radon emanation coefficient could be higher if the particles are crumbly (grain) rather than solid, even if both particles have the same radium concentration (Nazaroff, 1992). The shear zone in the area cuts through the coarse-grained granite of Kakulu (where the highest value was recorded), the deformational effect of shearing that have affected crystal structures of the rocks within that locality might be the influence on the emanation coefficient of radon within the lattice structure. The calculated radon exhalation rates ranges between 0.73 ± 007 to 4.83 ± 0.22 $mBqkg^{-1}h^{-1}$ with a mean value of 2.52 ± 0.30 $mBqkg^{-1}h^{-1}$. The medium-grained granites of Bakinya exhibits the highest radon exhalation rate while the coarse-grained granite of Manzalang producing the least radon exhalation rate. This variation may be attributed to differences in radium concentration in the rock, porosity (micro-fractures) and surface crystallography (Sato and Nakamura, 1993, Sahu *et al*., 2014). Table 6 show the details of the results obtained from the calculation of emanation coefficients, exhalation rates and radium concentration from gamma spectrometry analysis while Fig. 19 and Fig. 20 shows radon exhalation rates and radon emanation coefficient distributions within the rocks of the area, respectively.

5.5 GAMMA RADIATIONS WITHIN THE STUDY AREA

Activity concentration of ^{232}Th ranged from 41.51 ± 2.74 to 333.64 ± 3.46 Bq/kg, of ^{226}Ra from 15.33 ± 3.82 to 63.38 ± 4.03 Bq/kg and of ^{40}K from 161.73 ± 5.60 to 2166.56 ± 9.57 Bq/kg. Wuroyaya recorded the highest ^{40}K value of 2166.56 Bq/kg while the lowest value (161.73 Bq/kg) was recorded at Monkin (Table 7 and Fig. 23), Mika town recorded the highest ^{226}Ra activity concentration of 63.38 Bq/kg while Kakulu recorded the lowest value of 15.33 Bq/kg. For ^{232}Th, the highest activity concentration of 333.64 Bq/kg was recorded at Zing town while the lowest concentration of 41.51 Bq/kg was recorded at Mararaban Yorro community. The reported world mean radioactivity levels for ^{226}Ra, ^{232}Th, ^{40}K are 35, 30, and 400 Bq kg^{-1},

respectively (UNSCEAR, 2000). The wide variation between the concentrations of the radionuclides within the study area compared with the world mean values means that the study area is contributing high amount of gamma radiation to the environment. The results obtained shows that 40% of the samples have values greater than the world mean radioactivity level for ^{226}Ra while 60% have values lower than the world mean level. For ^{232}Th, all the samples have values higher than the world mean radioactivity value meanwhile, 93% of the samples have values higher than the world mean radioactivity value for ^{40}K and only 7% have values lower.

The distribution of the radionuclides within the study area is shown on the contour maps of ^{226}Ra, ^{232}Th and ^{40}K presented in Figures 21, 22 and 23, respectively.

5.5.1 Dose Rates due to Gamma Radiations within the Study Area

Calculated dose rates from the study area ranged from 79.50 ± 3.18 $nGyhr^{-1}$ (at Mararaban Yorro community) to 270.46 ± 3.47 $nGyhr^{-1}$ (at Zing town). Mika town recorded the second highest dose rate with 265.13 ± 2.83 $nGyhr^{-1}$ and the second lowest was recorded at Kakulu with dose rate of 89.98 ± 2.88 $nGyhr^{-1}$. The mean dose rate across the study area is 164.02 ± 2.60 $nGyhr^{-1}$. All the dose rates calculated from the study area (Fig. 26) are higher than the world mean value of 60 $nGyhr^{-1}$ (UNSCEAR, 2000).

5.5.2 Annual Effective Dose Rates

The calculated annual effective dose in the study area ranged from 0.24 ± 0.01 to 0.83 ± 0.011 $mSvyr^{-1}$, with an average value of 0.50 ± 0.008 $mSvyr^{-1}$. The rocks within Zing and Mika towns recorded the highest and the second highest annual effective dose rates, respectively, while the rocks within Mararaban Yorro and Kakulu recorded the lowest and the second lowest annual effective dose rates, respectively. WHO recommended a level of 0.1 $mSvyr^{-1}$ (WHO, 2000) for annual effective dose while according to ICRP recommendations, the public should not be exposed to more than an average of 1 $mSvyr^{-1}$ (ICRP, 1991). Based on the parameters used to

calculate the annual effective dose rates, all the samples have values higher than WHO recommended limit but lower than ICRP recommended tolerable limit.

5.5.3 Radium Equivalent Activity Index (Ra_{eq}) of the rocks

The calculated Radium Equivalent of the granite rock samples collected from the study area varied from 163.97 ± 7.14 to 603.46 ± 7.73 Bq/kg with an arithmetic mean value of 355.99 ± 5.75 Bk/kg. A comparison of the calculated radium equivalent index from the measured samples with the corresponding world accepted upper limit (Ra_{eq} = 370 Bq/kg, UNSCEAR, (1982)), reveals that 53% of the rock samples (these includes rocks from Zing, Yakoko, Mika, Wuro-yaya, Manzalang, Bakinya, Kpantisawa and Boduga) have Ra_{eq} values higher than the world accepted limit with the highest Ra_{eq} value recorded on the very coarse-grained granite of Zing town while 47% of the rock samples have Ra_{eq} values within the world accepted value, the least value was recorded on the rock sample collected at Mararaban Yorro. The derived average value of 355.99 Bq/kg within the study area is much higher than the average global value of 35 Bq/kg (UNSCEAR, 1982).

5.5.4 External Hazard Index (H_{ex}) of the rocks

The calculated external hazard index (H_{ex}) ranged from 0.44 ± 0.02 to 1.63 ± 0.02 with an average value of 0.96 ± 0.02. The values of the external hazard index (H_{ex}) of the rocks of the study area is directly proportional to the values of the radium activity index (Ra_{eq}) as shown on a statistical plot of Ra_{eq} values against H_{ex} values (Fig. 26). The plot showed a perfect linear correlation between the two parameter with $R^2 = 1$, which means that an increase/decrease in one of the parameter will also mean an increase/decrease in the other. The world accepted upper limit for the external hazard index is unity (i.e.) H_{ex} = 1. This value corresponds with the world accepted upper limit of 370 Bq/kg for radium equivalent index (Ra_{eq}), which means that all rocks with H_{ex} less than 1 will also have Ra_{eq} less than 370 Bq/kg and all rocks with H_{ex} more than 1

will have Ra_{eq} also more than 370 Bq/kg. Therefore, the rocks at Zing, Yakoko, Mika, Wuro-yaya, Manzalang, Bakinya, Kpantisawa and Boduga also have H_{ex} values above the world accepted limit.

5.6 PHYSICAL AND CHEMICAL CHARACTERISTICS

The physical and chemical properties of the groundwater within study area was analyzed based on Total Dissolved Solids (TDS), Hydrogen-Ion exponential (pH), conductivity, salinity, major cations and anions distribution, statistical and graphical presentations to establish its suitability consumption and for irrigational purposes.

5.6.1 Total Dissolved Solids (TDS)

Total Dissolved Solids (TDS) content of water is related to the concentration of major ions and other minor constituents. The study area is entirely covered by granitic rocks, and mafic minerals, when weathered release significant amount of associated ions into the groundwater. The TDS values obtained in-situ within the study area ranged from 109.2 to 4320 mg/l with an average value of 2282.66 mg/l. The values are similar to the TDS values obtained from an Iron Ore mining site within a basement complex, at Itakpe, Kogi State (Akpah, 2008). These values are commonly associated with brackish water having high concentration of calcium ions, magnesium ions, sodium ions, sulphate ions and bicarbonate ions as the dominant ions (Freeze and Cherry, 1979). The highest TDS value was observed at Zing borehole while the least TDS was observed at a borehole in Mika town and an open-well at Tapenla community. Only the groundwater at Tapenla and Mika have TDS values falling within the “Fresh water” category according to Davis and Dewiest, (1966) classification while the remaining samples fall within the brackish water category. This can also explain the reason for the salty taste of the groundwater. High TDS values in the groundwater of the study area could also be the result of

high evaporation intensity, considering the period at which the samples were collected (peak of dry season).

Table 14: Groundwater Classification based on TDS Values; (Davis and Dewiest, 1966)

Fresh Water	**TDS up to 1000 mg/l**
Brackish Water	**TDS (1000 – 10,000) mg/l**
Salty Water	**TDS (10,000 – 100,000) mg/l**
Brine	**TDS > 100,000 mg/l**

Fifteen (15) of the groundwater samples (88.2%) have TDS value higher than NIS, EPA and WHO recommended limits of 500, 500 and 1000 (NIS, 2007; EPA, 2004 and WHO, 2011) respectively, for TDS in water used for drinking purposes, only two (2) groundwater samples (11.8%), (i.e.) from Mika and Tapenla communities have values within the recommended limits.

Table 15: Classification of irrigation water based on TDS as follows; (Wilcox, 1955)

Best Quality Water	**TDS (200 – 1000) mg/l**
Water Involving Hazard	**TDS (1000 – 3000) mg/l**
Used for Irrigation only with Leaching and Perfect Drainage	**TDS (3000 – 7000) mg/l**

Based on this classification by Wilcox (1955), only the groundwater from an open-well at Tapenla is of best quality for irrigation, 58.8% of the samples are waters involving hazard and 29.4% of the groundwater samples require leaching and perfect drainage for it to be used for irrigational purposes. The groundwater sample at Mika with TDS of 109.2 mg/l is out of the ranges based on Wilcox's classification, therefore it is assumed "not good" to be used for irrigation.

5.6.2 Hydrogen-Exponential (pH)

The Hydrogen-ion exponential (pH) values measured insitu from the study area ranged from 6.64 to 8.11 with an average of 7.52. Based WHO, EPA and NIS guidelines which all limits pH values within the range of 6.5 to 8.5 (WHO, 2011; EPA, 2004 and NIS, 2007), it is safe to

conclude that all the sampled groundwater from the study area are within permissible limit but the groundwater sample at Mika borehole is slightly acidic with a pH value of 6.64.

5.6.3 Conductivity and Salinity

The conductivity values measured in-situ, of the sampled groundwater within the study area ranged from 2.17 to 8.04 mS/cm with a mean value of 4.76 mS/cm. All the groundwater samples have values higher than the guideline of 1400 µS/cm recommended by the World Health Organization (WHO, 2011) and 1000 µS/cm recommended by the Nigerian Industrial Standards (NIS, 2007). The highest conductivity value of 8.04 mS/cm (equal to 8,040 µS/cm) was observed at Zing borehole. This, and with the large variation in the groundwater salinity also observed at Zing borehole, groundwater sample could be influenced by different processes such as evaporation, anthropogenic activity and the interaction water – rock mixing processes.

Salinity values ranged from 0.2 to 4.5 with an average value of 2.4. The borehole at Zing show the highest salinity as expected considering the corresponding electrical conductivity (EC) value and the open-well at Tapenla show the least value of 0.2. However, it is note-worthy that sampling was carried-out during the dry season; therefore reduced salinity is expected during wet season due to groundwater recharge from meteoric source and subsequent mixing.

5.6.4 Major Cations and Anions Distribution

The chemical composition of groundwater reflects the chemical composition of the geologic units found within the drainage basin and provides valuable information on the presence of contaminants from anthropogenic sources and/or contributions from external sources (e.g., inflows from the rivers, canals, and the sea) (Güler, *et al*., 2002).

5.6.4.1 Cations

Calcium (Ca^{2+}): Calcium concentrations in the study area, ranges from 0 to 107.38 mg/l with an average of 20.76 mg/l. From the results, Zing town has a relatively

higher concentration with 107.38 mg/l which is more than twice the concentration at Wuro-yaya with 41.36 mg/l, which is the second highest calcium concentration from the study area and Tapenla has no (0 mg/l) calcium concentration. Such wide ranges of Calcium concentrations suggest that multiple sources and/or complex hydrochemical processes affected the distribution of this particular element in groundwater. Calcium (Ca) is one of the elements considered essential to human and animal health. Lack of it can result to poor development of bones and dentition (WHO, 1997). WHO (1997), recommended an upper limit of 200 mg/l and a lower limit of 75 mg/l. 1000 mg/l daily dietary intake is recommended by the US Committee on Dietary Reference Intake (1997). Only the water sample at Zing borehole met the minimum calcium requirement as recommended by the WHO, all others are below the minimum requirement and all the sample are below the required daily dietary intake recommended by US Committee on Dietary Reference Intake. This low concentration in calcium concentration could give rise to serious deficiencies in both humans and animals unless a supplementary source is provided.

***Magnesium (Mg^{2+})*:** Magnesium (Mg^{2+}) concentrations in the study area ranged from 0 to 12.27 mg/l with an average of 7.10 mg/l. The groundwater at Kwoji recorded the highest magnesium concentration while the open-well at Tapenla showed no magnesium concentration in it at all, it may be that it occurs below the detection limit of the instrument used. This result showing a wide range could also imply multiple sources and/or complex hydrochemical processes. All the samples analyzed are below WHO recommended limit of 50 mg/l (WHO, 2011) but only the open-well at Tapenla met the NIS recommended limit of 0.2 mg/l (NIS, 2007), as all the other samples are above the limit recommended by Nigerian Industrial Standards (NIS). Magnesium is

common in natural waters as (Mg^{2+}), and along with calcium, is a main contributor of water hardness.

The source of magnesium (Mg^{2+}) in the groundwater from the study area is most-likely to be contribution from the leaching of biotite, visibly present in most of the rock of the study area. Natural concentrations of magnesium in fresh waters may range from 1 to > 100 mg/l, depending on the rock types within the catchments (Chapman, 1996).

Sodium (Na^+): Sodium (Na^+) concentrations in the groundwater of the study area ranged from 12 to 62 mg/l, having an average of 40.94 mg/l. Wuro-yaya has the highest while Tapenla has the lowest sodium concentrations. The World health Organization (WHO) proposed a guideline limit of 50 mg/l while NIS proposed 200 mg/l as its guideline limit for sodium concentration in water for consumption (WHO, 2011; NIS, 2007). All the samples analyzed are within NIS recommended limit while 70.58% of the samples are below the WHO recommended limit and 29.41% of the samples are above the WHO proposed limit. The likely source of sodium in the groundwater of the study area is the leaching of sodium from plagioclase feldspars common in all the granite rocks sampled.

Potassium (K^+): Potassium and sodium are common constituents of natural waters, even though sodium is being more prevalent than potassium; it also plays an important role in the classification of the chemistry of natural waters. Potassium (K^+) concentrations from the study area, varies from 0.6 to 4.0 mg/l with a mean value of 1.79 mg/l. WHO proposed a guideline of 55 mg/l for potassium, (WHO, 2011). As of the time of this report, no guideline is reported for either NIS or EPA. All the samples analyzed are well below the recommended limit proposed by the World Health

Organization. Potassium (K^+) in the groundwater of the study area may have been from either the microcline or the biotite (or both) components of the granites of the study area.

5.6.4.2 Anions

***Bicarbonate (HCO_3^-)*:** Bicarbonate is an ion that is common to all natural waters and it is the predominant anion. Apart from the simple HCO_3^- ions occur in ionic associates with calcium and magnesium, $[CaHCO_3]^+$ and $[MgHCO_3]^+$.

Bicarbonate concentrations in the groundwater of the study area ranged from 0.5 to 6.3 mg/l, with an average of 3.38 mg/l. WHO proposed a guideline of 1000 mg/l for bicarbonate concentration in water used for consumption purposes. All the samples are below this limit proposed by the World Health Organization. Bicarbonate concentration in groundwater of the study area is most-likely to be of meteoric source.

***Sulphate (SO_4^{2-})*:** Sulphate in the study area has concentrations ranging from 0.17 to 8.17 mg/l, with an average value of 1.20 mg/l. The open-well at Tapenla has the highest sulphate concentration while boreholes at Abuja, Monkin, Kakulu, Wuro-yaya, Manzalang, Dila and Nyaja have the lowest sulphate concentrations. The WHO, EPA and NIS recommended a maximum limit of 250, 250 and 100 mg/l respectively, for sulphate in drinking water. All the samples analyzed have concentration lower than the maximum recommended limits with the highest concentration of just 8.17 mg/l at Tapenla. High sulphate concentrations can influence the taste of water and can also have laxative effects. It occurs in water predominantly in the form of simple SO_4^{2-}. Schoeneich and Garba (2010) actually reported that sulphate concentrations

above 250 mg/l in non-polluted water on the Crystalline Hydrogeological province of Nigeria have not yet been reported.

Chloride (Cl$^-$): According to Schoeneich and Garba (2010), chloride (Cl^-) concentration in water, in the crystalline aquifers, is entirely of atmospheric origin, as no chloride is released in the process of weathering. Chloride in the groundwater of the study area ranged from 0.25 to 3.10 mg/l, with an average value of 0.75 mg/l. The highest concentration was observed at Zing borehole water sample. The relatively high chloride concentration at Zing could be due to effluent contributions from sewage drains as a result of growing urbanization due to the recently transferred State College of Education to the area. A proposed guideline of 250 mg/l was recommended by WHO, EPA and NIS. All the samples analyzed are within the proposed limits.

***Nitrate (NO_3^-)*:** Nitrate (NO_3^-) in groundwater of the study area ranged between 0.01 to 0.03 mg/l, having an average of approximately, 0.01 mg/l. Nitrate is the stable oxidation state of nitrogen. It is formed by oxidation of nitrite, NO_2. Organic substance in soil is decomposed to ammonia, it is oxidized by nitrosifying bacteria to nitrite (NO_2), and at the end oxidized by nitrifying bacteria to nitrate (NO_3). It can also be of meteoric origin. Nitrate is an important indicator of faecal pollution and other organic pollution. WHO and NIS set a Maximum Contaminant Levels (MCL) of 50 mg/l while EPA gave an MCL of 10 mg/l. All the samples analyzed are within the limits recommended, therefore, the waters in the study area can be said to be safe for consumption, based on its nitrate content.

5.6.4.3 Correlation Matrix

Variables having coefficient (r) values ranging from 0.99 to 1.00 are considered "Perfect correlation coefficient". "Strong" correlation coefficient ranged from 0.80 to 0.98. Parameters showing correlation coefficients, r > 0.5 to 0.80 are considered to be "moderate" correlation while, "weak" correlation coefficient is considered when r < 0.5. The negative values show inverse relationships between chemical parameters. The strong to perfect correlation between the chemical parameters, is an indication of a common source (El Arabi, *et al*., 2013).

The correlation matrix obtained (Table 13) showed a strong correlation coefficient between Ca^{2+} and Cl^{-} (0.82) which indicates that they are of common source. A moderate correlation exists between Mg^{2+} and HCO_3^{-} (0.54), Na^{+} and HCO_3^{-} (0.74), while a weak correlation is shown between Ca^{2+} and SO_4^{2-}, Ca^{2+} and Mg^{2+}, etc.

5.6.5 Water Type/Specie

Based on reported concentrations (Table 11) of the major cations and anions, three water types were identified as Chloride – Calcium water type, Bicarbonate – Sodium water type and Sulphate – Sodium water type. The concentration of anions and cations when arranged in order from highest concentration to the lowest showed that fourteen (14) of the groundwater water samples have HCO_3^{2-} as the dominant anion and Na^{+} as the dominant cation, two (2) groundwater samples have SO_4^{2-} as the dominant anion while Na^{+} is the dominant cation and one (1) groundwater sample has Cl^{-} as the dominant anion while Ca^{2+} is the dominant cation. Therefore, Bicarbonate – Sodium water type is the most dominant water type within the study area. This is also confirmed by the graphical presentations using Piper, Durov and Schoeller diagrams of the cation and anion values for the study (Figures, 27, 28 and 29).

5.6.6 Assessment of Groundwater Quality for Irrigation Purposes

The inhabitants of the communities under study are mostly farmers and the groundwater can play an important role in aiding irrigation practices. Therefore, the suitability of the groundwater was assessed using Sodium Absorption Ratio (SAR), Percent Sodium (%Na), Soil Permeability Index (PI) and Chloro-Alkaline Index (CAI).

5.6.6.1 Sodium Absorption Ratio (SAR)

According to Richard (1954) classification with respect to SAR, all the calculated SAR values for the groundwater samples collected within the study area and analyzed have values within the range of SAR values which indicates that there is no sodium hazard and can be considered of "excellent" quality for irrigational use.

5.6.6.2 Percent Sodium (%Na)

The suitability of the groundwater for irrigation using Percent Sodium (Wilcox, 1955), showed that 11.8% of the samples collected can be considered "Good" for irrigation purposes (these includes groundwater samples from Zing, and Kpantisawa boreholes), 52.9% are "Permissible" (includes groundwater samples from Abuja, Kakulu, Wuro-Yaya, Manzalang, Kwoji, Bakinya, Dila, Nyaja and Madaki), 29.4% are considered "Doubtful" (includes groundwater samples from Monkin, Kan-Iyaka, Mika, Mararaban Yorro and Kassa), while, the groundwater at Tapenla is of "Poor" quality, therefore, should not be used for irrigation.

5.6.6.3 Soil Permeability Index (PI)

According to Doneen (1964) classification using Soil Permeability Index (PI), the groundwater samples collected within the study area have thirteen (13) of the samples fall under Class I order (groundwater from Zing, Abuja, Monkin, Kakulu, Kan-Iyaka, Wuro-Yaya, Manzalang, Kwoji, Bakinya, Dila, Kpantisawa, Nyaja, and Kassa), while, four (4) of the groundwater samples are of

Class II order (groundwater from Mika, Mararaban Yorro, Tapenla and Madaki), therefore, they are all good to be used for irrigation.

5.6.6.4 Chloro-Alkaline Index (CAI)

The Chloro-Alkaline Index (CAI) of the groundwater samples collected from the study area (Table 14) showed that all the samples analyzed have negative CAI values, indicating a base – exchange reaction between Na^+ and K^+ in the groundwater with Ca^{2+} and Mg^{2+} in the rocks.

Chapter Six

SUMMARY, CONCLUSION AND RECOMMENDATIONS

6.1 Summary and Conclusion

This study was set-out to evaluate; radon concentration in groundwater and exhalation from rocks, associated radiological hazards as well as hydrochemistry of the groundwater with respect to major cations and anions, around Mika uranium mineralization. To achieve this, a texture-based (grain sizes) lithological map of the study area was produced. The map revealed the dominance of medium-grained granites within the study area. A shear zone was delineated on the produced lithological map.

A clear influence of groundwater flow direction on the radon concentrations within the study area could not be established. The groundwater flows away from areas that recorded higher radon concentrations. This could be attributed to these reasons; radon is a gas, and it has a short half-life (3.82 days), therefore cannot travel long distance in groundwater before they decay. Radon is mostly found not far from where it is produced.

Radon concentrations tend to increase towards the southern and western parts of the study area mostly dominated by the medium-grained granites which also corresponds to radium distribution within the study area. Therefore, radon concentrations in the groundwater of the study area are to a large extent controlled by radium distribution within the rocks.

Potential dose rates from the degassing of radon in groundwater was calculated and the result obtained show an average annual absorbtion dose of 463.59 mSv/yr, average annual effective dose of 1112.62 mSv/yr and an average annual effective dose due to ingestion of groundwater was calculated to be 0.59 mSv/yr. These values are above the regulatory limits specified in the Nigeria Basic Ionization Radiation Regulation (FGN, 2003). The doses due to ingestion were within ICRP recommended limit of 1 mSv/yr for radionuclides ingestion through water. But only

11.77% were found to be within WHO recommended reference level of 0.1 mSv/yr, the remaining 88.23% are above this limit.

Radon concentrations measured on rock samples show an exhalation ranges of between 39.7 to 262 Bq/m^3 and an average value of 137 Bq/m^3. The calculated emanation coefficient and exhalation rates ranges from 0.7 to 5.1 (average; 2.17) and 0.73 to 4.83 $mBqkg^{-1}h^{-1}$, respectively. The exhalation rates and emanation coefficients of the rocks are mainly influenced by radium distribution within the rocks and also by extensive rock deformations that characterize the study area.

Gamma spectrometry, revealed the background radioactivity of the rocks with respect to ^{226}Ra, ^{232}Th and ^{40}K within the study area. These results showed average activity concentrations of 35.72, 161.86 and 1153.25 Bq/kg as against the world median radioactivity levels of 35, 30 and 400 Bq/kg for ^{226}Ra, ^{232}Th and ^{40}K, respectively. Comparatively, only ^{226}Ra is very close to the world median value. Thus, ^{232}Th and ^{40}K are contributing the most, to the background radioactivity within the study area. Dose rates as a result of the background activity of these radionuclides ranges from 79.50 to 270.46 nGy/hr. This dose rates were found to be higher than the world median value of 60 nGy/hr. The average annual effective dose due to gamma radiations from the radionuclides within the study area is 0.59 mSv/yr, this value is above the WHO recommended level of 0.1 mSv/yr but lower than ICRP recommended limit of 1 mSv/yr.

Hydrochemical studies of the area including graphical presentations using Piper, Durov and Schoeller plots revealed the dominance of HCO_3 – Na water type/specie. This indicates recharge of the aquifer to be mainly from meteoric source. The groundwater was also evaluated to determine its suitability for use in irrigation.

On a general note, the groundwater quality with regards to chemical elements can be said to be safe for drinking and other domestic uses and can also be considered good for irrigational

purposes, but with regards to radon content, groundwater pose a health risk to the inhabitants within the study area, as prolonged exposure will result in lung cancer.

6.2 Recommendations

Epidemiological evidence indicates that indoor radon is responsible for a substantial number of lung cancers in the general public. It is a unique environmental threat, in that it cannot be perceived, sensed or experienced. Accepting the saliency of the threat requires the need for appropriate actions. Therefore the following are recommended;

i. Greater public education about radon as a health threat and the accomplishment of radon mitigation is recommended. The public need to understand radon is a health threat, especially in high risk prone areas.

ii. Conscious efforts should be made by relevant authorities to develop a framework for the selection of radon and other radionuclide measuring devices and procedures for a continuous and reliable measurement of NORM's both in water, air and materials used for construction purposes.

iii. Measures should be put in place by relevant authorities to control or restrict the use of the rocks and other naturally occurring radioactive materials (NORM) within the study area for construction of both human and animal dwellings.

iv. Mitigation or remediation programmes should be properly planned and initiated by government authorities, in areas considered to be of high risk.

v. A National/State programmes and frameworks should be initiated under a new or existing platforms, in accordance with global practices so that national radionuclides reference limits could be set, ensure radon risk reduction and create national policy options for prevention and mitigation.

vi. Taraba State government should also embark on serious and continual monitoring of groundwater quality to ensure safe use, as increased farming activities within the study area may affect the quality of the groundwater in future.

vii. This work was carried-out during the dry season only, therefore, similar work is recommended to be carried-out during the wet season in-order to ascertain if some environmental factors associated with wet season, influences radon concentration in groundwater, its emanation coefficient and exhalation, and also hydrochemistry of the groundwater.

viii. Exhalation studies was carried-out on outcrops only, to represent rocks in contact with groundwater, therefore it is recommended that further exhalation studies should be done on rock chips collected during borehole drilling so that rock in direct contact with groundwater may be truly represented.

REFERENCES

Adebo, B.A. and Adetoyinbo, A. A. (2009). Assessment of groundwater quality in unconsolidated sedimentary coastal aquifer in Lagos State, Nigeria. *Scientific Research and Essay,* 4 (4), pp. 314 – 319.

Affaton, P., Rahaman, M.A., Trompetre, R. and Sougy, J. (1991). The Dahomeyide orogen: tectonothermal evolution and relationships with the Volta Basin. In: Dallmeyer, R.D and Lec'orc'he, J.P. (eds) The West African Orogens and Circum-Atlantic Correlatives. IGCP, Special Publications. *Springer* Verlag, Berlin, pp. 107 – 122.

Agunmanu, A.E. (1975): Geological Survey of Nigeria, Unpublished Report of Geology of sheet 215.

Ajibade, A.C and Wright, J.B. (1989). The Togo-Benin-Nigeria Shield: evidence of crustal aggregation in the Pan-African Belt. *Tectonophysics,* 165, pp. 125 – 129.

Akerblom, G., Falk, R., Lindgren, J., Mjones, L., Ostergren, I., Soderman, A.L., Nyblom, L., More, H., Hagberg, N., Andersson, P. and Ek, B.M. (2005). Natural radioactivity in Sweden, exposure to internal radiation. Radiological Protection in Transition. Proceeding of the XIV Regular Meeting of the Nordic Society for Radiation Protection, NSFS, Rattvik, Sweden. pp. 211 – 214.

Akpah, F.A. (2008). Hydrochemistry and Impact of Iron Ore Mining on Groundwater Quality in Itakpe and its Environs. Kogi State, Central Nigeria. An Unpublished Msc. Thesis, University of Nigeria, Nsukka.

Alabdula'aly A. I. (2014). Occurrence of Radon in Groundwater of Saudi Arabia. *Journal of Environmental Radioactivity*, 138, pp. 186 – 191.

Ames, L. L., McGarrah, J. E., and Walker, B. A. (1983). Sorption of trace constituents from aqueous solutions onto secondary minerals. I. Uranium. *Clays and Clay Minerals*, 31, pp. 321 – 334.

Arabi, A. S. (2012). Radioactivity and Chemistry of Groundwater from Uranium Mineralized Areas around Gubrunde, North Eastern Nigeria. Unpublished PhD Thesis, A.B.U. Zaria Nigeria.

Arabi, A.S., Funtua, I.I., Dewu, B.B.M., Adeyemo, D.J., Abafoni, J.D., Garba, M.L. and Garba, I. (2013). Activity and Mass Concentration of ^{226}Ra, ^{228}Ra and ^{232}Th in Groundwater around the Zona Uranium Occurrence, Peta Gulf Syncline, Northeast Nigeria. *International Journal of Advanced Earth Science and Engineering*, 2, Issue 1, pp. 57 – 68.

Arabi, A.S., Funtua, I.I., Dewu, B.B.M., Muhammad, A.M. and Mahed, G. (2014). Radon in Groundwater and Exhalation from Aquifer Materials Around Areas of High Radiometric Anomalies in Parts of Northeastern Nigeria.

Asonye, C.C., Okolie, N.P., Okenwa, E.E. and Iwuanyanwu, U.G. (2007). Some Physico-chemical characteristics and heavy metal profile of Nigerian rivers, streams and waterways. *African Journal of Biotechnology,* 6(5), pp. 617 – 624.

Badoe, L. G., (2007). Measurement of Radon gas level in Ashanti Region and design of a radon vulnerability map for Ghana. *Nuclear Tracks and Radiation Measurements,* 20, pp. 276 – 281.

Becquerel, A.H., (1896a). On the rays emitted by phosphorescence. *Comptes Rendus de l'Académie des Sciences Paris,* 122, pp. 420.

Becquerel, A.H., (1896b). On the invisible rays emitted by phosphorescent bodies. *Comptes Rendus de l'Académie des Sciences Paris,* 122, pp. 501.

Becquerel, A.H., (1903). On radioactivity, a new property of matter. Nobel lecture, december 11, 1903. "Nobel Lectures, Physics, 1901 – 1921." (1967). In: Science Incorporated Elsevier (Ed.), Nobel Lectures in Physics, 1901 – 1970, vol. 1. *Elsevier* Publishing, Amsterdam.

Benkhelil, J. and Robineau, B. (1983). Le fosse de la Benoue est-il un rift? Bulletin Des *Centres Recherches Exploration Production Elf Aquitaine*, 12, pp. 29 – 128.

Beretka, J. and Mathew, P.J. (1985). "Natural Radioactivity of Australian building materials, industrial wastes and by -products," *Health Physics,* 48, pp. 87 – 95.

Bertrand I.M.L. and Caby Y.R. (1978). Geodynamic evolution of the Pan-African orogenic belt, A new interpretation of the Hoggar Shield (Algerian Sahara), *Geology Rundsch,* 67, pp. 357 – 388.

Black R. (1980). Granite: From Segregation of Melt to Emplacement, *Episodes,* 4, pp. 3 – 8.

Black R., Caby R., Pouchkine A., Bayer B., Bertrand J.M., Boullier A.M., Fabre J. and Lesquer A. (1979) Evidence for Late Precambrian plate tectonics in West Africa, *Nature*, 278, pp. 223 – 227.

Bohr, N., (1913). On the constitution of atoms and molecules. *Philosophical Magazine,* 26 (6), pp. 1 – 25.

Boswinkel J. A. (2000) Information Note, International Groundwater Resources Assessment Centre (IGRAC), Netherlands Institute of Applied Geoscience, Netherlands.

Brutsaert, W.F., Norton, S.A., Hess, C.T., and Williams, J.S. (1981). Geologic and hydrologic factors controlling radon-222 in ground water in Maine. *Ground Water,* 19, pp. 407–417.

Burke K.C. and Dewey F.J., (1972). Orogeny in Africa, In: T.F.J. Dessauvagie and A.J. Whiteman (Editors) African Geology, Geology Department, University of Ibadan, Nigeria, pp. 583 – 608.

Caby Y.R., Bertrand J.M. and Black R. (1981). Pan African ocean closure and continental collision in the Hoggar-Iforas segment, Central Sahara, In: A Kroner (Editor) Precambrian plate Tectonics. *Elsevier*, Amsterdam, pp. 407 – 434.

Caby, R (1989). Precambrian terranes of Benin-Nigeria and Northeast Brazil and the Late Proterozoic South Atlantic fit. In: Dallmeyer, R.D. (ed.) Terranes in the Circum-Atlantic Palaeozoic Orogens. Geological Society of America Special Papers, 230, pp. 145 – 158.

Chase, G.D. and Rabinowitz, J.L., (1967). Principles of Radioisotope Methodology, third ed. Burgess Publishing Company, Minneapolis, pp. 140 – 143.

Chen, J., Rahman, N.M., Abuatiya, I.A (2010). Radon Exhalation from Building Materials for Decorative Use, *Journal of environmental radioactivity*, 1014, pp. 317 – 322.

Clavensjö B, Åkerblom G. (1994). The radon book. Measures against radon. - Stockholm, Ljunglöfs Offset AB, 1994.

Committee on Dietary Reference Intake (1997). Dietary Reference Intakes for Calcium, Phosphorus, Magnesium, Vitamin D, and Fluoride, National Academy Press, Washington D.C.

Curie, P., (1905). Radioactive substances, especially radium. Nobel lecture on June 6, 1905. In: Science Incorporated Elsevier (Ed.), Nobel Lectures in Physics, 1901 – 1970, 1. *Elsevier* Publishing, Amsterdam.

Darby, S., Hill, D., Auvinen, A., Barros-Dios, J.M., Baysson, H., Bochicchio, F., et. al., (2005). Radon in homes and risk of lung cancer: collaborative analysis of individual data from 13 European case-control studies. *British Medical Journal*, 330, pp. 223 – 227.

Davis, S. N. and Dewiest, J. M. (1966). Hydrogeology, John Wiley and Sons, Inc. New York, London, Sydney.

Doneen L. D. (1964). Notes on water quality in agriculture. Published as a Water Science and Engineering Paper 4001, Department of Water Science and Engineering, University of California.

Durridge RAD7 manual (2014). Durridge Radon Instrumentation: RAD7 Radon Detector Manual.

Edsfeldt, C. (2001). The Radium Distribution in Some Swedish Soils and its Effect on Radon Emanation. Division of Engineering Geology, Department of Civil and Environmental Engineering; Royal Institute of Technolgy Stckholm, Sweden. Unpublished PhD Thesis.

El Arabi, N., Idris, Y. and Fekry, A. (2013). Temporal and Spatial Change Detection of Variations in the Groundwater Composition by Multivariate Statistical Techniques. *New York Science Journal,* 6(11), pp. 38 – 48.

Environmental Protection Agency (EPA), (2004). Assessment of Risks from Radon in homes Office of Radiation and Indoor Air. US Environmental Protection Agency.

Environmental Protection Agency (EPA), (2010). The Analysis of regulated contaminant occurrence data from public Water systems in support of the second six-year review of National Primary Drinking Water Regulations. Office of Water (4607M) EPA-815-B-09-006 Revised September 2010.

European Union (EU), (2001). European Union Commission Recommendation on the protection of the public against exposure to radon in drinking water supplies. Office Journal of the *European Community*, L 344, 28 December, pp. 85 – 88.

Federal Government of Nigeria (FGN), (2003). Nigeria Basic Ionization Radiation Regulations. Federal Republic of Nigeria; Official Gazette. Government notice No. 218. Published by Federal Government of Nigeria Press: FG097/22004/650(OL163). pp. 42.

Fenyves, E. and Haiman, O. (1969). The physical principle of nuclear radiation measurements. Academic, New York. pp. 256.

Fitches, W.R., Ajibade, A.C., Egbuniwe, I.G., Holt, R.W., and Wright, J.B. (1985): Late proterozoic schist belts and plutonism in NW Nigeria. *Journal of the Geological Society London*, 142, pp. 319 – 337.

Freeze, R.A. and Cherry, J.A., (1979). Groundwater; Prentice Hall. Inc, Eaglewood Cliffs, N.J. pp. 249 – 250.

Funtua, I. I. (1992). Geology and Geochemistry of Uranium Mineralization in Mika North Eastern Nigeria. Unpublished Ph.D Thesis, A.B.U. Zaria Nigeria.

Gabelman, J. W. (1977). Migration of uranium and thorium - exploration significance. AAPG Studies in Geology no 3. American Association of Petroleum Geologists. Tulsa, Oklahoma. pp. 168.

Garba, I. (2003). Geochemical Discrimination of Newly Discovered Rare-Metal Bearing and Barren Pegmatites in the Pan-African (600 ± 500 Ma) Basement of Northern Nigeria. *Journal of Applied Earth Science, 112,* pp. 287 – 292.

Garba, M.L. (2008). Natural Radioactivity of Groundwater in the Precambrian Crystalline Rocks Around Zaria, North Central Nigeria. Unpublished Ph.D Thesis. pp. 48 – 77.

Garba, N.N., Rabi'u, N., Dewu, B.B.M., Sadiq, U. and Yamusa, Y.A. (2013). Radon Assessment in Around Water Sources from Zaria and Environs, Nigeria. *International Journal of Physical Sciences,* 8(42), pp. 1983 – 1987.

Garcia-Leon, M., Garcia-Montano, E., and Madurga, G., (1984). Characterization of ^{99}Tc by Shape of its Plateau with a Gas-Flow Proportional Counter. *The International Journal of Applied Radiation and Isotopes,* 35, pp. 195 – 200.

Geological Survey of Nigeria (GSN), (1975). Airborne Spectrometric Survey Map of Contours of Total Count, Selected Anomalies and Anomalous Zones. Airborne Geophysical Series (Monkin, Sheet 216).

Gokhale, B. and Leung, S. (2010). Groundwater Radon-222 Concentrations in Antelope Creek, Idaho: Measurement and Interpolation. *The Open Environmental & Biological Monitoring Journal*, 3, pp. 12 – 20.

Greeman, D. and Rose, A. (1995). Factors Controlling the Emanation of Radon and Thoron in Soils of the Eastern U.S.A. *Chemical Geology*, 129, pp. 1 – 14.

Güler, C., Thyne, G.D., McCray, J.E., Turner, A.K., (2002). Evaluation of graphical andmultivariate statistical methods for classification of water chemistry data. *Hydrogeology Journal*, 10, pp. 455–474.

Handloser, J. S. (1959). Health physics instrumentation. *Pergamon*, New York. pp. 338.

Haruna I.V., Orazulike D.M. and Samaila N.K. (2013). Trace and Rare Earth Elements Petrochemical Constraint on Tectonogenetic Evolution of the Granitoids of Zing-Monkin area, Adamawa Massif, N.E. Nigeria. *Research Journal of Chemical Sciences*, 3(1), pp. 32 – 42.

Herschy R. W. (1999). Hydrometry Principles and Practices (2nd Edition) John Wiley & Sons, Chicchester.

Holt R.W., Egbuniwe I.G., Fitches W.R. and Wright J.B. (1978). The relationships between low grade metasedimentary belts, calc-alkaline volcanism and the Pan-African orogeny in NW Nigeria, *Geology Rundsch*, 67, pp. 631 – 646.

International Atomic Energy Agency (IAEA), (2003). Extent of Environmental Contamination by Naturally Occurring Radioactive Material (NORM) and Technological Options for Mitigation, Technical Reports Series no. 419, IAEA, Vienna.

International Atomic Energy Agency (IAEA), (1996). International Basic Safety Standards for Protection against Ionization Radiation and for the Safety of Radiation Sources. (Safety Series. ISSN 0074 – 1892; 115. Safety Standards).

International Atomic Energy Agency (IAEA), (2010). Guidelines for radioelement mapping using gamma ray spectrometry data.

International Commission on Radiation Protection (ICRP), (1991). 1990 Recommendations of the International Commission on Radiological Protection – User's Edition. ICRP Publication 60.

International Commission on Radiation Protection (ICRP), (1993). Publication 65, Protection against Radon-222 at home and at work, Annals of the ICRP, Oxford, U.K., *Pergamon*, l23(2).

International Commission on Radiological Protection and Measurement (ICRP), (1977). Recommendations of the International Commission on Radiological Protection. ICRP Publication, 1(3), pp. 26.

Ishimori, Y., Lange, K., Martin, P., Mayya, Y. S. and Phaneuf, M. (2013). Measurement and Calculation of Radon Releases from NORM Residues. Technical Report Series No. 474. International Atomic Energy Agency, Vienna.

Jalili-Majareshin, A., Behtash, A. and Rezaei-Ochbalagh, D. (2012). Radon Concentration in Hot Springs of the Touristic City of Sarein and Methods to Reduce Radon in Water. *Radiation Physics and Chemistry*, 81, pp. 749–757.

Kendall G. M. and Smith T. J. (2002). Doses to organs and tissues from radon and its decay products. *Journal of Radiological Protection*, 22(4), pp. 389 – 406.

Komal B., Mehraa, R. and Sonkawade, R. G. (2010). Measurement of radon concentration in ground water using RAD7 and assessment of average annual dose in the environs of NITJ, Punjab, India. *Indian Journal of Pure and Applied Physics*, 48, pp. 508 – 511.

Kozlowska, B., Hetman, A., Dorda, J. and Zipper, W. (2001). Radon-enriched Spring Waters in the South of Poland. *Radiation Physics and Chemistry*, 61, pp. 677 – 678.

Kumar, R., Sengupta, D. and Prasad, R. (2003). Natural radioactivity and radon exhalation studies of rock samples from Surda Copper deposits in Singhbhum shear zone. *Radiation Measurements*, 36, pp. 551 – 553.

L'Annungiata, M.F., (1987). Radionuclide Tracers, Their Detection and Measurement. Academic Press, London, pp. 505.

L'Annungiata, M.F., (2007). Radioactivity: Introduction and History. *Elsevier Science*, Amsterdam, pp. 609.

L'Annungiata, M.F., (2012). Radiation Physics and Radionuclide Decay. Handbook of Radioactivity Analysis. *Elsevier Science*, pp. 2 – 148.

Lal, D., (2009). Cosmogenic isotopes. In: Steele, J., Thorpe, S., Turekian, K. (Eds.), Encyclopedia of Ocean Sciences. Academic Press/*Elsevier Science* Publishers, Amsterdam, pp. 678 – 687.

Langmuir, D. (1978). Uranium solution-mineral equilibria at low temperatures with applications to sedimentary ore deposits. *Geochimica et Cosmoschimica Acta*, 42, pp. 547 – 569.

Le Druillennec, T., Ielsch, G., Bour, O., Tarits, C., Tymen, G., Alcalde, G. and Aquilina, L. (2010). Hydrogeological and Geochemical Control of the Variations of ^{222}Rn Concentrations in a Hard Rock Aquifer: Insights into the possible role of fracture-matrix exchanges. *Applied Geochemistry*, 25, pp. 345 – 356.

Liegeois, J.P., Black, R., Navez, J. and Latouche, L. (1994). Early and late Pan-African orogenies in the Air assembly of terranes (Tuareg shield, Niger). *Precambrian Research*, 67, pp. 59 – 88.

Magill, J., Galy, J., (2005). Radioactivity, Radionuclides, Radiation. Springer-Verlag Berlin Heidelberg and European Communities, Karlsruhe. pp. 116.

Makofske, W.J. and Edelstein, M.R. (1988). Radon and the Environment. Park Ridge, NJ (USA): Noyes. ISBN 0-8155-1161-2.

Mason, B., and Moore, C. B. (1984). Principles of Geochemistry. 4th edition. John Wiley & Sons, Inc., New York. pp. 344.

McCurry P. and Wright J.B. (1977). Geochemistry of calc-alkaline volcanics in northwestern Nigeria, and a possible Pan-African suture zone, *Earth Planet Science Letters,* 37, pp. 90 – 96.

McCurry, P. (1976): The Geology of the Precambrian to Lower Paleozoic Rocks of Nigeria – A Review in Geology of Nigeria (Kogbe, C.A. ed). Elizabethan Publishers Co. Lagos. pp. 18 – 39.

Molinari, J., and Snodgrass, W. J. (1990). The chemistry and radiochemistry of radium and the other elements of the uranium and thorium natural decay series. In: The Environmental Behavior of Radium; Volume 1. IAEA Technical Reports Series No 310. International Atomic Energy Agency, Vienna. pp. 11 – 56.

National Academy of Science (NAS), (1999). Report of the Committee on Risk Assessment of Exposure to Radon in Drinking Water, Board on Radiation Effects Research, Commission on Life Sciences, National Research Council, National Academy Press, Washington, DC.

National Council on Radiation Protection, (1993). Limitation of Exposure to Ionizing Radiation. National Council on Radiation Protection and Measurements. Bathesda, MD: NCRP; NCRP Report No. 116.

Nazaroff, W.W. (1992). Radon transport from soil to air. *Reviews of Geophysics,* 30, pp. 137–160.

Nigerian Industrial Standards (NIS), (2007). Nigerian Standard for Drinking Water Quality, NIS 554: 2007. Approved by Standard Organization of Nigeria, ICS 13.060.20

Noz, M. E. and Maguire, G. Q. (1979). Radiation Protetion in the Radiologic and Health Sciences. Henry Kimpton Publishers. London. pp. 211.

Nwankwo, L.I. (2013). Determination of Natural Radioactivity in Groundwater in Tanke-Ilorin, Nigeria. *West African Journal of Applied Ecology*, 21(1), pp. 111 – 119.

Offodile, M. E. (2014). Hydrogeology: Groundwater Study and Development in Nigeria; 3rd edition. pp. 19 – 51.

Ogezi, A.E.O. (1977): Geochemistry and Geochronology of the basement rocks from NW Nigeria. Unpublished Ph.D. thesis, University of Leeds. pp. 295.

Okeke, P.I. (1979): Report on the geology of Gaiza, sheet 114. Geological Survey of Nigeria.

Oni, O.M., Oladapo, O.O., Amuda, D.B., Oni, E.A., Olive-Adelodun, A.O., Adewale, K.Y. and Fasina, M.O. (2014). Radon Concentration in Groundwater of areas of High Background Radiation Level in Southwestern Nigeria. *Nigerian Journal of Physics* Vol. 25(1) June 2014. pp. 64 – 67.

Oruonye, E.D. (2014). An assessment of the Trend of Climate Variables in Taraba State, Nigeria. *Global Journal of Science Frontier Research: H Environmental and earth Science*, (14).

Ouseph, P. J. (1975). Introduction to nuclear radiation detectors.Vol. 2. Plenum Press. New York.

Petropoulos, N.P., Anagnostakis, M.J., Simopoulos, S.E. (2001). Building Materials Radon Exhalation Rate: ERRICCA intercomparison exercise results, *science of the total environment*, 272. pp. 1–3; pp. 109–118.

Price, W. J. (1964). Nuclear Reaction Detection. 2nd ed. McGraw-Hill, San Francisco.

Pullman, B. (1998): The Atom in the History of Human Thought. Oxford University Press, 1998.

Raju N. J. (2007). Hydrogeochemical parameters for assessment of ground water quality in the upper Gunjanaeru River basin, Cuddapah District, Andhra Predesh, South India, *Environmental Geology*, 52, pp. 1067-1074.

Ray, H.H. and Yusuf, M.B. (2011). The Incidence of Soil Erosion in Zing Local Government Area of Taraba State, Nigeria. *Ethiopian Journal of Environmental Studies and management*. (4) No. 2.

Richard L. A. (1954). Diagnosis and improvement of saline and alkali soils, Agric Handbook 60, USDA, Washington D.C., pp. 160.

Rogers, J. J. W, and Adams, J. A. S. (1969). Uranium. In: Handbook of Geochemistry. Edited by Wedepohl, K. H. *Springer*-Verlag Heidelberg. pp. 92.

Rutherford, E. and Soddy, F., (1902). The cause and nature of radioactivity. *Philosophical Magazine,* 4, pp. 370 – 396.

Rutherford, E., (1903). The magnetic and electric deviation of the easily absorbed rays from radium. *Philosophical Magazine,* 6, pp. 177 – 187.

Rutherford, E., (1913). The structure of the atom. *Nature* 92 (No. 2302), pp. 423.

Sahu, P., Panigrahi, D.C. and Mishra, D.P. (2014). Sources of Radon and its Measurement Techniques in Underground Uranium Mines – An Overview. *Journal of Sustainable Mining*, 13(3), pp. 11 – 18.

Salau, S.L. (2000): The Geology, Geochemistry and Possible Origin of Gold Mineralization at Dukki Old Mine, Maru – Zamfara State, Nigeria.Unpublished Msc. Thesis, Ahmadu Bello University, Zaria.

Sato, J. and Nakamura, T. (1993) Leaching of radon from weathered granite into water. *Radioisotopes,* 42, pp. 667 – 675.

Schoeller H. (1967). Geochemistry of ground water. An international guide for research and practice, UNESCO, 15, pp. 1 – 18.

Schoeneich, K. and Garba, M. L. (2010). Hydrogeology note (Geol. 405), an Unpublished Material on Hydrogeology, Ahmadu Bello University Zaria.

Skeppstrom, K. and Olofsson, B. (2007). Uranium and Radon in Groundwater: An overview of the problem. E. W. Publication. *European Water*, 17/18, pp. 51 – 62.

Soddy, F., (1913a). Inter-atomic charge. *Nature,* 92, pp. 399 – 400.

Soddy, F., (1913b). Radioactivity. *Chemical Society*. Annual Reports, 10, pp. 262 – 288.

Solomon, A.O., (2005). A study of Natural Radiation Levels and Distribution of Dose Rates within the Younger Granite Province of Nigeria. An Unpublished Ph.D. Thesis, University of Jos, Nigeria. pp. 31 – 33.

Standards Organization of Nigeria (SON), (2007). Nigeria standard for drinking water. NIS554:2007.

Steinhauser, G. and Buchtela, K., (2012). Gas Ionization Detectors. Handbook of Radioactivity Analysis. *Elsevier Science*. pp. 191 – 195.

Stuyfzand P. J. (1989). Nonpoint source of trace element in potable ground water in Netherland. In: Proceeding of the 18th TWSA Water Working, Testing and Research Institute, KIWA, Nieuwegein, The Netherlands.

Thomson, J.J., (1897). Cathode Rays. *Philosophical Magazine,* 44, pp. 293 – 316.

Trumpette R. (1979). The Pan-African Dahomeyide fold belt: a collision orogeny? (Abstract), 10th *Colloque de Geologic Africaine, Montepellier*, pp. 72 – 73.

Truswell, J.F., and Cope, R.N. (1963): The geology of parts of Niger and Zaria provinces Northern Nigeria. *Geological Survey of Nigeria Bulletin,* 29, pp. 53.

Turner D.C., (1983). Upper Proterozoic schist belts in the Nigerian sector of the Pan African province of West Africa, *Precambrian Research*, 21, pp. 55 – 79.

United Nation Environmental Protection (UNEP), (2002). Vital Water Graphics – An Overview of the State of the World's Fresh and Marine Waters, UNEP, Nairobi, Kenya; 2002.

United Nations Scientific Committee on the Effects of Atomic Radiation (UNSCEAR), (2000). Sources and Effects of Ionizing Radiation. Report to General Assembly, Vol. 1, Annex B, United Nations, New York.

United Nations Scientific Committee on the Effects of Atomic Radiation (UNSCEAR), (1982). Ionising Radiation Sources and Biological Effects; 1982 Report to the General Assembly.

United Nations Scientific Committee on the Effects of Atomic Radiation (UNSCEAR), (1988). Ionising Radiation Sources and Biological Effects; UNSCEAR 1988 Report to the General Assembly.

United Nations Scientific Committee on the Effects of Atomic Radiation (UNSCEAR), (1993). Sources and effects of ionizing radiation. UNSCEAR report to the general assembly with scientific annexes, United Nations, New York.

United State Army Material Command, (2000). Tank-Automotive and Armaments Command (TACOM) and army Material command (AMC). Review of transuranics (TRU) in depleted uranium armor. 19 January, 2000. Memorandum. 5001 Eisenhower Avenue, Alexandria, VA 22333-001.

United State Department of Defense, (2000). Environmental exposure report. Depleted uranium in the Gulf (II).

United States Army Environmental Policy Institute, (1994). Health and environmental consequences of depleted uranium use by the U.S. Army. Technical report, June 1995. Army Environmental Policy Institute.Champaign, Illinois, 1994.

United States Environmental Protection Agency/EERF Manual 78 – 1, (1978). The Determination of Radon in Drinking Water.

United States Salinity Laboratory (1954): Diagnosis and Improvement of Saline and Alkali Soils. U.S. Departmen of Agric. Handbook 60.

Vajda, N., Martin, P., and Kim, C. (2012). Alpha Spectrometry. Handbook of Radioactivity Analysis. *Elsevier Science*. pp. 375 – 379.

Villard, P., (1900a). Sur la re´flexion et la refraction des rayons cathodiques et des rayons de ´viables du radium. *Comptes Rendus de l'Académie des Sciences, Paris*, 130, pp. 1010 – 1012.

Villard, P., (1900b). Sur le rayonnement du radium. *Comptes Rendus de l'Académie des Sciences, Paris,* 130, pp. 1178 – 1179.

Wanty, R. B., Johnson, S. L., Briggs, P. H. (1991). Radon-222 and its parent nuclides in groundwater from two study areas in New Jersey and Maryland, U.S.A. *Applied Geochemistry*, 6, pp. 305 – 318.

Wilcox L. V. (1955). Classification and use of irrigation water, *Agric circular* 969, USDA, Washington D.C., pp. 19.

Wood, W.W., Kraemer, T.F., Shapiro, A., (2004). Radon (^{222}Rn) in ground water of fractured rocks: a diffusion/ion exchange model. *Ground Water,* 42, pp. 552–567.

World Health Organization (WHO), (1997). Guidelines for drinking-water quality, 2nd ed. Vol. 3. Surveillance and control of community supplies. Geneva.

World Health Organization (WHO), (2000). Guidelines for drinking-water quality.

World Health Organization (WHO), (2003). Report of the WHO workshop: Nutrient minerals in drinking water and the potential health consequences of long-term consumption of demineralized and remineralized and altered mineral content drinking waters. Rome, 11–13 November 2003 (SDE/WSH/04.01).

World Health Organization (WHO), (2004). Guidelines for Drinking Water Quality. 3rd Edn., World Health Organisation Recommendations, Geneva, ISBN: 92-45-154638 7.

World Health Organization (WHO), (2009). WHO Handbook on Indoor Radon: a public health perspective edited by Hajo Zeeb and Ferid Shannoun. pp. 3 – 14.

World Health Organization (WHO), (2011). Guidelines for Drinking Water Quality, 4th Edition.

Wright J.B. and Ogezi A.E.O., (1977). Serpentinite in the Basement of Northwestern Nigeria, *Journal of Mining and Geology*, 14, pp. 34 – 37.

Appendix 1:

Table 16: Groundwater Elevation and Thickness of Dry Zone (Depth to WT)

Well Location	Coordinates	Elevation (m)	Depth to Water Table (m)	Groundwater Elevation (m)
ZING	08º59.154'N 11º46.307'E	509.85	5.10	504.75
LAMMA	08º58.044'N 11º44.005'E	582.21	6.40	575.81
KODUGA	08º56.137'N 11º42.402'E	553.00	1.58	551.42
ABUJA	08º55.556'N 11º42.150'E	631.54	5.40	626.14
YAKOKO	08º55.248'N 11º42.372'E	596.16	10.97	585.19
YAKOKO(BENDI)	08º55.174'N 11º42.325'E	596.56	11.37	585.19
MADAKI	08º52.257'N 11º41.550'E	514.35	15.15	499.20
MONKIN(DOSHETI)	08º49.419'N 11º42.115'E	552.28	21.22	531.06
ZING AREA	08º59.113'N 11º43.497'E	590.51	0.95	589.56
KAKULU	08º59.235'N 11º43.389'E	593.58	10.50	583.08
BODUGA	08º51.230'N 11º41.063'E	534.95	4.91	530.04
KASSA	08º48.506'N 11º38.424'E	588.65	4.79	583.86
TAPENLA	08º51.001'N 11º38.008'E	596.91	4.27	592.64
KPANTISAWA	08º56.389'N 11º30.416'E	561.72	12.22	549.50

Appendix 2a.

Table 17: Specific Activity Concentration (Bq/kg)

Country	N	^{226}Ra	^{232}Th	^{40}K	Ra_{eq}	Reference
Australia	7	51.5	48.1	114.7	129.4	Berekta and Mathew (1985)
Austria	18	26.7	14.2	210	63.1	Sorantin and Steger (1984)
Algeria	12	41	27	422	112	Amrani and Tahtat (2001)
Brazil	1	61.7	58.5	564	188.8	Malanca, *et. al.* (1993)
China	46	56.5	36.5	173.2	122	Zinwei (2005)
Egypt	85	78	33	337	151	El-Afifi *et al.* (2006)
Ghana	38	12.5	23.9	206.2	62.5	Faani, *et al.* (2011)
India	1	37	24.1	432.2	104.7	Kumar, *et al.* (1999)
Japan	16	35.8	20.7	139.4	-----	Suzuki, *et al.* (2000)
Netherland	6	27	19	230	71.9	Ackers, *et al.* (1985)
Tunisia	2	21.5	10.10	175.5	49.7	Hizem, *et al.* (2005)
Turkey	145	40	28	248.3	99.1	Turham and Gurbuz (2008)
Nigeria	15	35.7	161.9	1153.3	356	This Work

N= Number of samples; Ra_{eq}= Average Radium Equivalent concentration

Appendix 2b.

Table 18: Radon Concentration in Water across the Globe (UNSCEAR, 1982)

Location	Average concentration ($kBqm^{-3}$)
Austria	
Salzburg	1.5
Finland	
Helsinki and Vantaa	1200
Other areas	280
Italy	80
Sweden	19
United States	
Aroostock, Maine	48
Cumberland, Maine	1000
Hancock, Maine	1400
Lincoln, Maine	560
Perrobscut, Maine	540
Waldo, Maine	1100
Yolk, Maine	670
Nigeria	
Southwest:	
Agbeloba Quarry (Abeokuta)	1.59 (Oni, *et al.*, 2013)
Idofin (Imesi-Ile)	49.00 ,,
Northwest:	
Zaria	12.43 (Garba, *et al.*, 2013)
Northeast:	
Mika Uranium Mineralization	29.4 (Present Work)

Appendix 2c.

Table 19: Radon Concentration in Outdoor Air (UNSCEAR, 1982)

Location	Mean Value (Bqm^{-3})
Austria	7.0
Bolivia	1.5
Finland	2.3
France	9.3
Germany	2.6
India	3.7
Japan	2.1
Peru	1.5
Philippines	0.3
Poland	3.3
United States (Cincinnati)	9.6
Norwegian Sea	0.2

Table 20: Radionuclides (World Average vs. Present Work)

Radionuclide	World Average (UNSCEAR, 2000)	This Work
^{226}Ra	35 Bq/kg	35.72 Bq/kg
^{232}Th	30 Bq/kg	161.36 Bq/kg
^{40}K	400 Bq/kg	1153.25 Bq/kg
^{222}Rn	40 Bq/m^3	136.62 Bq/m^3

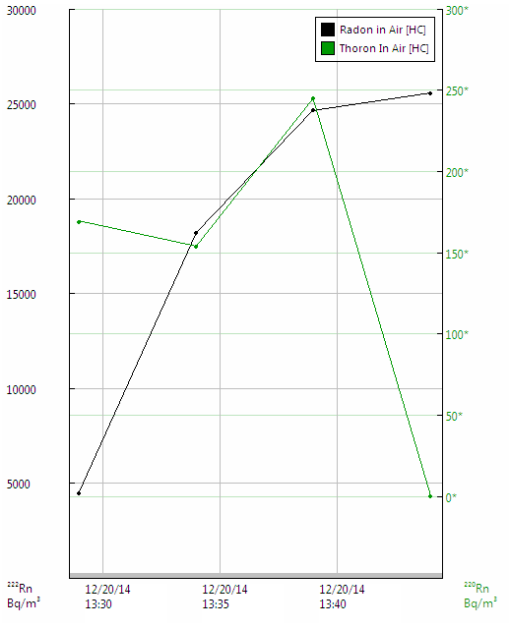


Fig 30: ^{222}**Rn** and ^{220}**Rn** concentration graph of Zing town (borehole).

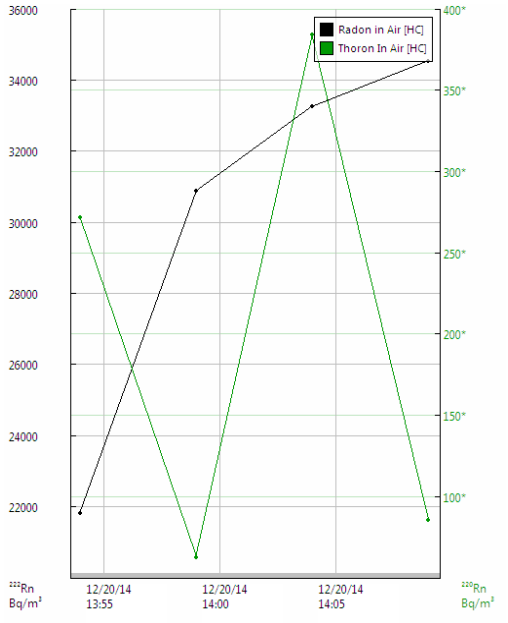


Fig 31: ^{222}**Rn** and ^{220}**Rn** concentration graph in of Abuja Village (borehole).

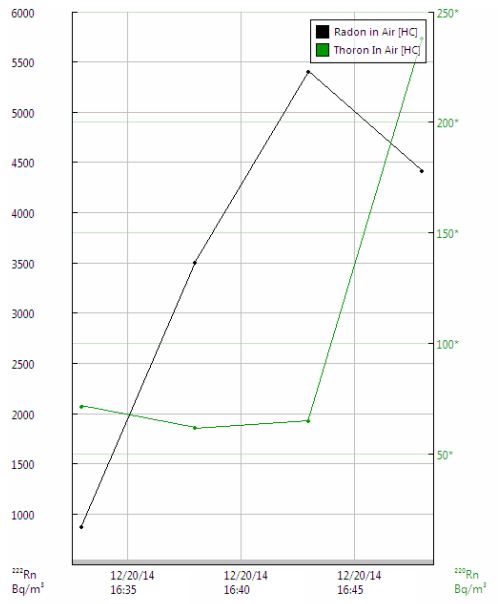


Fig 32: ^{222}**Rn** and ^{220}**Rn** concentration graph of Monkin town (borehole).

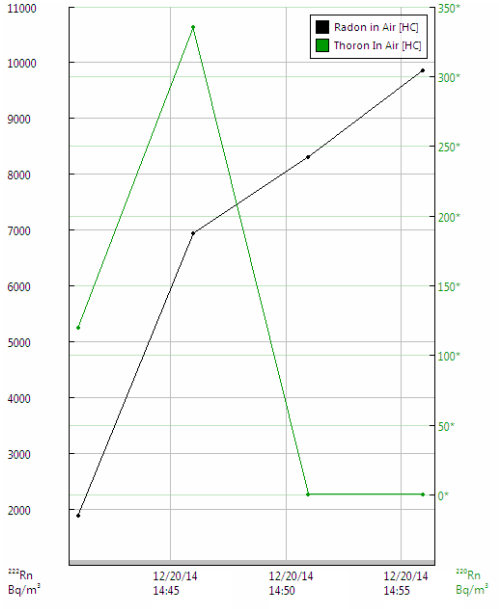


Fig 33: ^{222}**Rn** and ^{220}**Rn** concentration graph of Kakulu town (borehole).

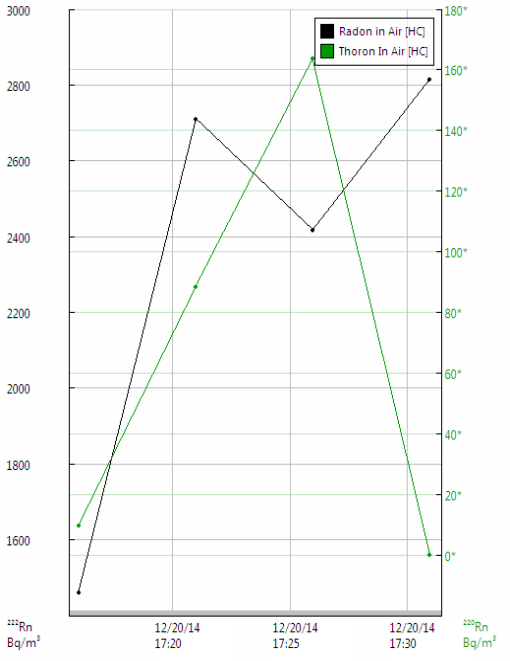


Fig 34: ^{222}**Rn** and ^{220}**Rn** concentration graph of Kan-Iyaka village (open well).

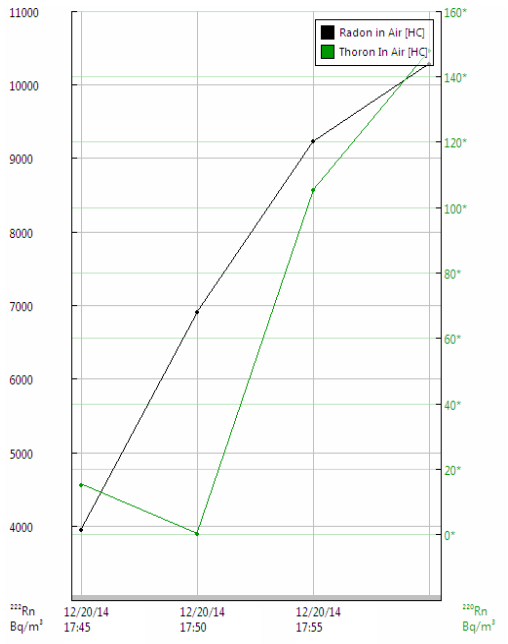


Fig 35: ^{222}**Rn** and ^{220}**Rn** concentration graph of Mika town (borehole).

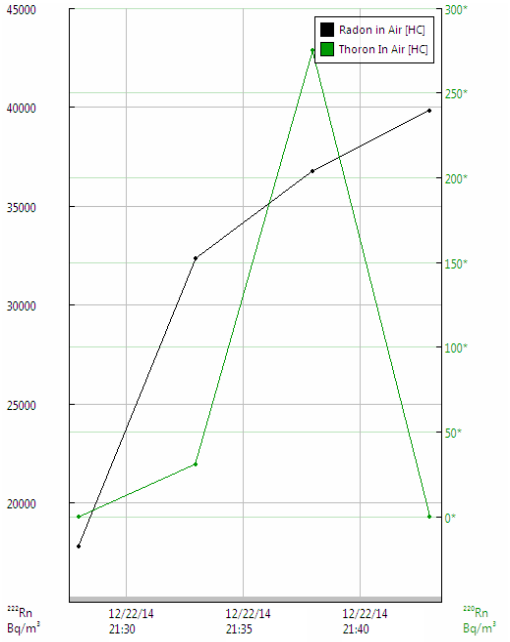


Fig 36: ^{222}**Rn** and ^{220}**Rn** concentration graph of Wuro-yaya community (borehole)

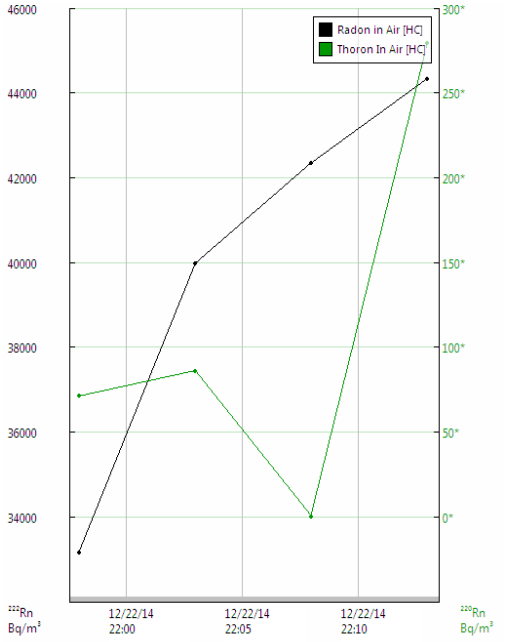


Fig 37: ^{222}**Rn** and ^{220}**Rn** concentration graph of Manzalang Village (borehole)

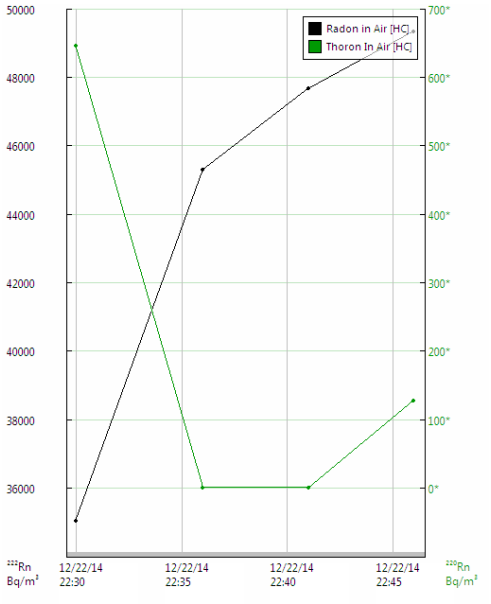


Fig 38: ^{222}**Rn** and ^{220}**Rn** concentration graph of Kwoji community

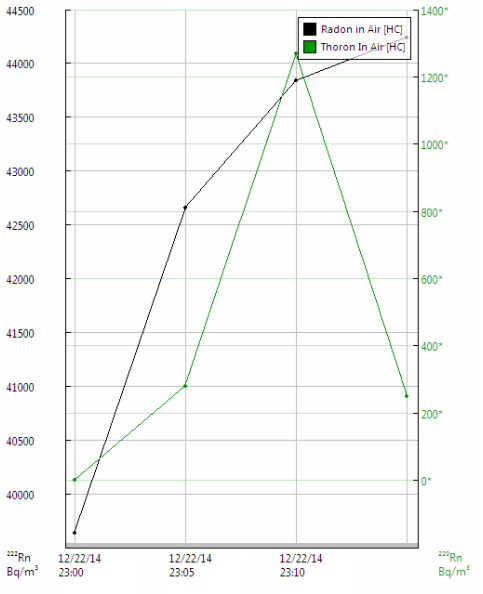


Fig 39: ^{222}**Rn** and ^{220}**Rn** concentration graph of Mararaban Yorro Community (borehole).

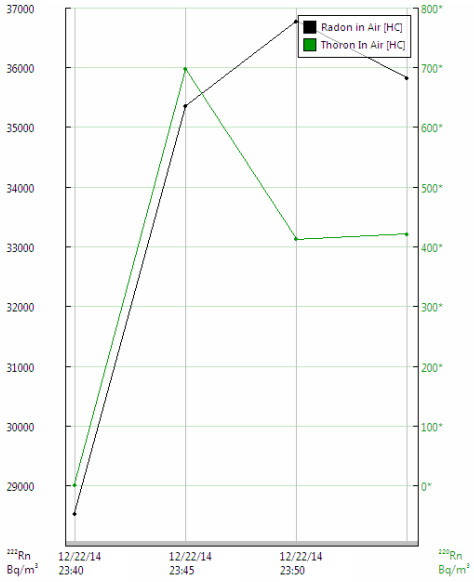


Fig 40: ^{222}**Rn** and ^{220}**Rn** concentration graph of Bakinya Village (borehole).

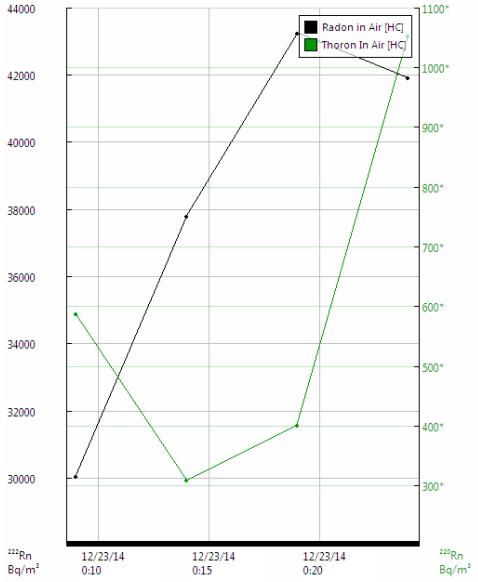


Fig 41: ^{222}**Rn** and ^{220}**Rn** concentration graph of Dilla Village (borehole).

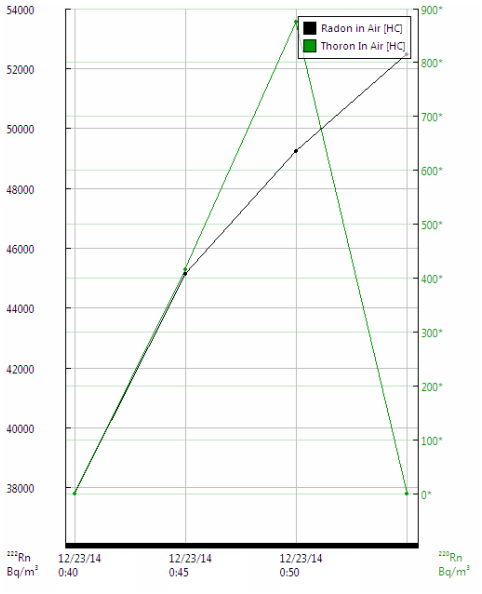


Fig 42: ^{222}**Rn** and ^{220}**Rn** concentration graph of Kpantisawa town (borehole).

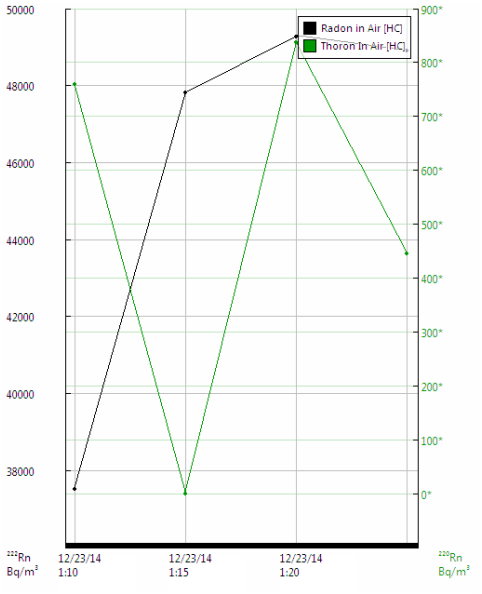


Fig 43: ^{222}**Rn** and ^{220}**Rn** concentration graph of Nyaja Village (borehole).

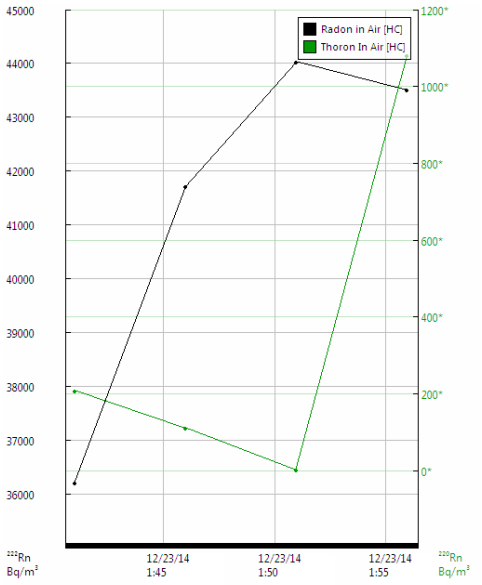


Fig 44: ^{222}**Rn** and ^{220}**Rn** concentration graph of Tapenla Village (open well).

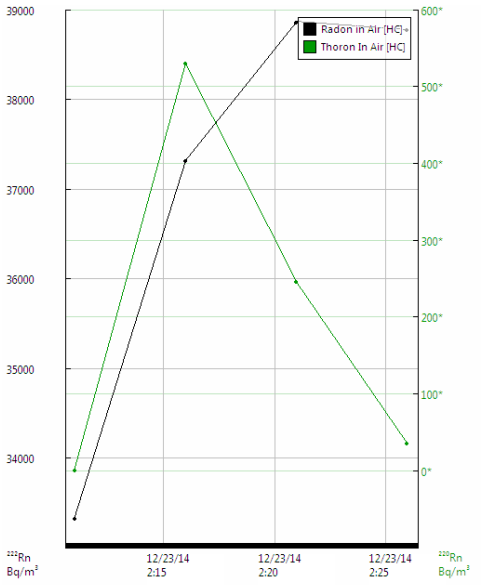


Fig 45: ^{222}**Rn** and ^{220}**Rn** concentration graph of Kassa town (borehole).

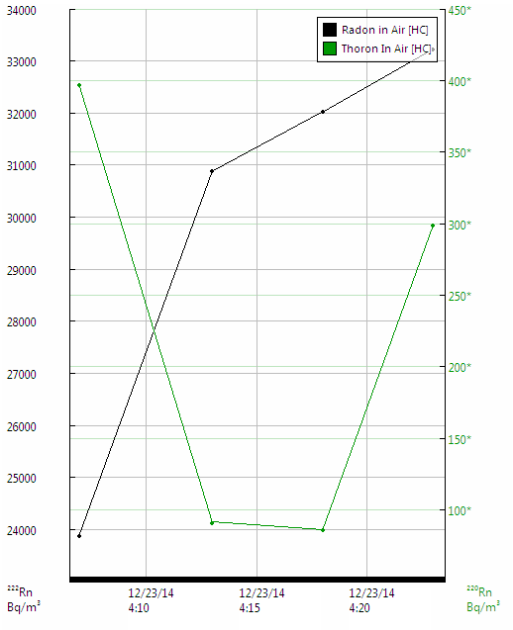


Fig 46: ^{222}**Rn** and ^{220}**Rn** concentration graph of Boduga Community (borehole).